

# The effects of storm surges on dune systems near inlets

A case-study for the Marsdiep inlet near Texel

Stan van den Broek

September 2017

Supervising committee:

Prof. dr. S.J.M.H. Hulscher

*University of Twente, Department of Water Engineering and Management*

Msc. F. G. Silva

*University of Twente, Department of Water Engineering and Management*

Prof. dr. ir. J.A. Roelvink

*UNESCO-IHE Institute for Water Education*

Dr. K. M. Wijnberg

*University of Twente, Department of Water Engineering and Management*



# Summary

During storm surges, the water level and wave height increase which results in erosion of the dunes. Extreme storm surges are capable of eroding or even breaching dunes. A lot of research has been done on the effects of storms on straight (uniform) coasts. Still, there is a gap in the accurate prediction of storm-induced coastal change on coastal dune systems near tidal inlets.

The goal of this research is to understand the behaviour of storm surge processes on a coastal dune system near a tidal inlet system. Thus, we aim at understanding how storm characteristics influence on coastal dune erosion and sedimentation on systems near tidal inlets.

XBeach, a numerical model which is developed for simulating extreme storm surges in complex situations like a tidal inlet system, is used to make a simulation of various storm surges in the Marsdiep inlet (NL). On the north side of the inlet, a large sandflat ('the Hors') is located. The choice to use this particular inlet is made because of the availability of the necessary data which was essential to run and qualitatively validate the model.

Results show that most wave energy is dissipated before reaching the dunes, thus leading to a decrease in the radiation stress. The reduction results in an increase of the water level on the west side of the sandflat. The water level gradient, created by the wave-set up, results in a constant flow across the Hors from west to east.

Erosion, caused by the dissipated energy, is observed on the west coastline of the sandflat. The eroded material is partly transported on top of the Hors, where it settles as the water depth increases and the flow velocity decreases. The rest of the eroded material is transported southwards where it settles behind the southern tip of the sandflat, where the current magnitude decreases significantly.

Water level gradient between both sides of the inlet had significant influence in the current magnitude and erosion values in/near the channel of the inlet. Higher water levels had almost no effect on both the hydrodynamic as morphodynamical processes in the inlet as they were found to be dominated by (indirectly) wave breaking on the west side of the sand flat.

These results could be used in management strategies to create a more stable or even expanding barrier island. could be used as interpretation of the hydrodynamical and morphodynamical behaviour in tidal inlets during storm surges. However, as all tidal inlets have different topographic and climate characteristics, more research is necessary to test the influence of these variables on the hydrodynamic (and morphodynamical) behaviour on the dune systems.

# Foreword

Writing a thesis is an important component of the final part of the master study Civil Engineering and Management at University of Twente. The goal of this study is to learn how to independently conduct a research and present and discuss the method and results. This report is the result of this research. The subject of this research is: ‘the effects of storm surges on dune-systems near inlets’, with special attention payed to the dune system north of the Marsdiep inlet (Texel, NL).

I worked on this report for the past half year and I have to say my knowledge, dedication and faith was tested more than once during the process. But as an old Dutch saying goes: ‘I struggle and emerge’ (‘Ik worstel en kom boven’), I eventually made it.

However, without the help of my supervisors, I would probably still be struggling. I would like to thank my daily supervisor Filipe Galiforni Silva for his positivity, availability for questions and discussion and inspiration for my research. I want to thank Kathelijne Wijnberg for her commitment, critical view and the time she made available for this study. I want to thank Dano Roelvink for his feedback and time to help me out with XBeach when needed. Finally, I want to thank Suzanne Hulscher for her feedback and advice.

Further on, I want to thank Theo Gerkema from NIOZ for the flow-data through Marsdiep and the SURFsara organisation for making the HPC-cloudcomputer available for this research, although I could not get XBeach running on the cloudcomputer.

Finally, I want to thank you for reading this report, have fun.

Stan van den Broek,

Enschede

September 2017

# Content

|   |    |
|---|----|
| Summary.....  | 3  |
| Foreword.....   | 4  |
| 1 Introduction .....  | 7  |
| 1.1 Motivation .....  | 7  |
| 1.2 Objective.....  | 7  |
| 1.3 Approach .....  | 7  |
| 1.4 Outline .....   | 8  |
| 2 Theoretical background.....                               | 9  |
| 2.1 Tidal inlet systems .....                               | 9  |
| 2.2 Storm surges (extra-tropical storms) .....              | 10 |
| 2.3 Beach-dune dynamics.....                                | 11 |
| 2.3.1 Hydrodynamics.....                                    | 11 |
| 2.3.2 Morphological processes (erosion/sedimentation) ..... | 12 |
| 3 Study area.....   | 13 |
| 3.1 The Wadden Sea .....                                    | 13 |
| 3.2 The Hors.....   | 13 |
| 3.3 Marsdiep / Molengat .....                               | 15 |
| 4 Methodology.....  | 16 |
| 4.1 XBeach .....  | 16 |
| 4.1.1 Hydrodynamic processes .....                          | 16 |
| 4.1.2 Morphodynamical processes .....                       | 17 |
| 4.2 Input parameters.....                                   | 17 |
| 4.2.1 Domain.....   | 17 |
| 4.3 Input parameters.....                                   | 19 |
| 4.3.1 Water level data .....                                | 19 |
| 4.3.2 Wave data .....                                       | 20 |
| 4.3.3 Wind data .....                                       | 20 |
| 4.3.4 Grain sizes .....                                     | 20 |
| 4.4 Validation method .....                                 | 21 |
| 4.4.1 Field measurements .....                              | 21 |
| 4.4.2 TESO-data .....                                       | 22 |
| 4.5 Sensitivity analysis.....                               | 23 |
| 5 Validation .....  | 26 |
| 5.1 TESO data.....  | 26 |
| 5.2 Dune measurements.....                                  | 27 |
| 5.2.1 The western dune field .....                          | 27 |

|  |    |
|--|----|
| 5.2.2 The middle dunes .....                                 | 28 |
| 6 Results .....  | 30 |
| 6.1 Storm 0 .....  | 30 |
| 6.2 Sensitivity analysis .....                               | 43 |
| 6.2.1 Storm 1 – Overall water level increase of 0.3m.....    | 43 |
| 6.2.2 Storm 2 – Increased water level gradient of 0.3m ..... | 45 |
| 6.2.3 Storm 3 & 4 – Adapted wind speed .....                 | 47 |
| 6.2.4 Storm 5 & 6 – Adapted wind direction.....              | 49 |
| 7 Discussion.....  | 51 |
| 7.1 Hydrodynamics .....                                      | 51 |
| 7.2 Morphodynamics.....                                      | 52 |
| 8 Conclusion .....   | 54 |
| References.....  | 56 |
| Appendix 1 – Validation report                               |    |
| Appendix 2 – Basic calculations                              |    |
| Appendix 3 – Storm surge analysis                            |    |

# Chapter 1

## Introduction

### 1.1 Motivation

Coastal dunes are natural wind-driven accumulations of sand that emerge in the coastal zone and act as natural protection system against flooding and coastline erosional phases. During storm surges, the increased water level and wave force can result in dune erosion. Extreme storm surges are capable of eroding or even breaching dunes (Houser, Hapke, & Hamilton, 2008).

A lot of research has been done on the effects of storms on straight (uniform) coasts. Still, there is a gap in the accurate prediction of storm-induced coastal change on strongly curved coastlines, areas close to inlets and other situations with a large longshore transport gradient (Anthony, 2013; Vellinga, 1986). Due to this uncertainty, it is possible that the actual erosion profile after a storm surge differs from those expected on straight coastlines.

Therefore, understanding the hydrodynamical behaviour and corresponding morphological dynamics in tidal inlet systems during storm surges give more insight in the actual strength of the dune systems nearby and results could be used in management strategies to create a more stable or even expanding barrier island.

### 1.2 Objective

The goal of this research is to understand the behaviour of storm surge processes on a coastal dune system near a tidal inlet system. Thus, we aim at understanding how storm characteristics influence on coastal dune erosion and sedimentation on systems near tidal inlets.

To narrow down the scope of the research, the choice has been made to investigate the hydrodynamic behaviour and morphological dynamics during various storm surges in one single inlet. Three research question have been defined:

- 1. What is the hydrodynamic behaviour of a storm surge on a sandflat/dune system near an inlet?*
- 2. How do different storm characteristics influence the hydrodynamic processes on the sand flat?*
- 3. Which parameter(s) is/are dominant in the process of dune erosion close to inlets during storm surges?*

### 1.3 Approach

One way to get a better understanding of the hydrodynamical behavior of dune systems near tidal inlets is by measuring water levels, wave-characteristics and wind-characteristics on various points in and around the inlet to measure hydrodynamic behavior during different storm surges. However, these ideal measurements are not available and therefore an alternative method has to be found. The best alternative is to use a numerical model. By making a simulation of a storm surge in an inlet, all hydrodynamic and morphodynamical processes on the entire inlet could be analyzed for various storm surges. However, to support reliability of the results from the numerical model, the model has to be validated. For the Marsdiep inlet, all necessary data necessary to simulate a storm surge, plus validation data, is available in the area. Therefore, this inlet is used in this case study.

## 1.4 Outline

Chapter 2 gives more background information about tidal inlets, storm surges and the hydrodynamic and morphodynamical processes near coastlines. Chapter 3 contains information about the study area: The Marsdiep inlet. Chapter 4 includes the method, here it becomes clear what numerical model is used and how the results from this model would answer the research questions. Chapter 5 contains the validation of the model. Here, results from the simulated storm surge are compared with actual hydro- and morphodynamic measurements in order to determine the reliability of the model and to distinguish deviations in the model. Chapter 6 contains the results of the simulations done with the model and Chapter 7 discusses these results. Chapter 8 summarizes and concludes the research by summarizing the research and answering the research question.

## Chapter 2

# Theoretical background

### 2.1 Tidal inlet systems

A tidal inlet system is part of a coastal system that connects the open sea with a tidal basin. A single tidal inlet can occur, but often a chain of barrier-islands is seen where all tidal inlets are connected in one system (e.g. the Wadden Sea)(de Swart & Zimmerman, 2009). The system is balanced by two forces: the wave motion, which tends to close the channels; and a tidal current, which keeps the channels open. The lagoon/closed sea behind the inlet system often holds a lot of sediment in this process, making the tidal basin shallower over time (van de Kreeke, 1990). Figure 1 shows a tidal inlet with barrier islands on both sides of the inlet.

Tidal wave (at the seaside) ensure oscillations at the sea side of the inlet, which cause a water level difference between the two sides of the inlet (sea & basin in Figure 1). This water level gradient forces a current through the inlet channel. Sediment, transported along the coastline (littoral drift), tends to settle in inlet. However, as the tidal waves moves on, the decreased area of the channel (due to sediment settlement) ensures an increased current through the channel which is able to transport the surplus sediment out of the channel. As long as these processes balance each other out, the system is in equilibrium. However, if the processes are out of equilibrium, the topography of the inlet will change and the inlet might eventually close.

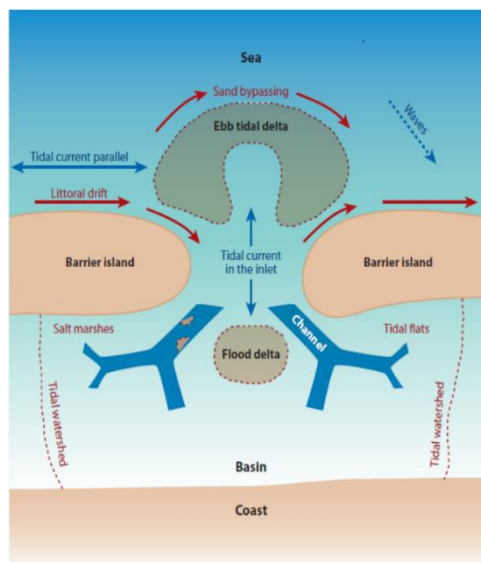


Figure 1 - Sketch of idealized tidal inlet system, showing the different geomorphologic elements and dominant processes and phenomena (de Swart & Zimmerman, 2009).

## 2.2 Storm surges (extra-tropical storms)

Storm surges are the response of the sea level to large-scale meteorological conditions. Storm surges vary per location and climate. Because this study focusses on the tidal inlet of Marsdiep, only storm surges in the North Sea area are analysed. During a storm, two main factors determine the surge level (Weisse, von Storch, Niemeier, & Knaack, 2012):

- wind fields (wind driven surge),
- the effects of the atmospheric pressure on the sea surface (pressure surge).

The wind direction and speed is determined by the atmospheric pressure difference in a certain area. During the autumn and winter, the horizontal temperature gradients are strong, creating large atmospheric pressure differences and strong winds. These wind fields can cover the North Sea and parts of the Atlantic ocean (Klein, 2015; Pugh, 1996).

Strong west winds in the North Atlantic Ocean are able to create long waves (storm surges) with a period of several hour which travel eastwards. These extra-tropical storms enter the North Sea above the north of England. Due to the Coriolis effect, the surge wave is rotated southward. As the surge moves on southwards, the sea gets shallower and narrower, which increase the wave-height (Pugh, 1996).

The Royal Netherlands Metrological Institute (KNMI) states that strong North-Western storms, as described above, have an increasing effect on the water levels. The course of the depression determines the direction, strength and duration of the storm, the speed in which it passes and the strength of the pressure drop. A slowly moving depression in south-eastern direction of the North Sea, where the air pressure quickly drops, creates the highest water levels near the Dutch coast (KNMI, 2017).

The so called inverse barometric effect implies that when the atmospheric pressure on the sea surface rises, the height of the sea surface is depressed and vice versa. For every mbar the air pressure lowers, the water will rise 1 cm. The North sea Storm of 1953 had a pressure centre of 964hPa, which resulted in a water level rise of 0.5m (Met Office, 2013).

The incoming winds in the North Sea usually rotate clockwise, which changes the initial wind direction from the south-to-west quadrant, towards the west-to-north quadrant during the storm surge (Lipari & Vledder, 2009).

The incoming short wind waves on the Dutch coast are mainly formed by the wind in the North sea, for which the wind speed and direction determine the (short) wave-height which is reached near the shoreline, although the shape of the seabed can influence the wave-height as well.

Deep-water waves that have the greatest wavelengths and longest periods travel fastest, and thus are first to arrive in regions distant from the storm which generated them. Away from the storm surge, the waves are shorter and therefore slower. When the fast traveling waves 'overtake' the shorter waves, they interfere with each other. Where the crests of the two wave trains coincide (they are 'in phase'), the wave amplitudes are added. Where the two waves are 'out of phase', such that the crests of one wave train coincide with the troughs of the other, the amplitudes cancel out (Figure 2)(The Open University, 1999a).

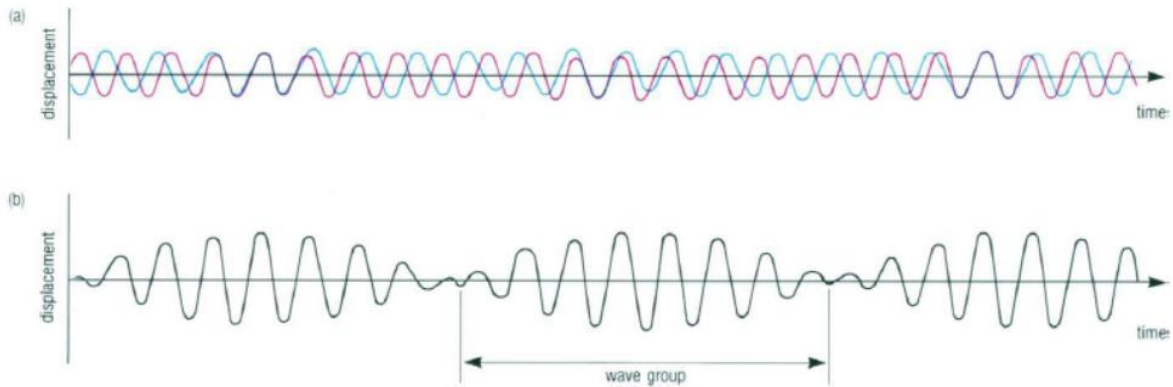


Figure 2 – (a) The merging of two wave trains (shown in red and blue) of slightly different wavelength (but the same amplitudes), to form wave groups (b)(The Open University, 1999a)

When the wave groups come closer to the coastline, the waves are affected by the bed level. Larger waves are affected in deeper water depth and tend to break earlier. In this process of wave breaking, momentum stored in the wave (radiation stress) dissipates. The sudden decrease in radiation stress causes a horizontal radiation stress gradient which results in an increase of the water level. Due to the different wave height in a wave group, the decrease in wave height (and therefore the water level increase) is strongest in the centre of the wave group where the wave amplitudes are highest. This way, long (infragravity) waves arise with a length in order of the wave groups (Herbers, Elgar, & Guza, 1995; Hoonhout, 2015).

## 2.3 Beach-dune dynamics

Beach-dune dynamics can be separated into two subjects, the hydrodynamics, which represent the waves and currents; and the morphological processes, which are a result of the hydrodynamic processes.

### 2.3.1 Hydrodynamics

In shallow water, the troughs of the wind waves undertake more influence due to the resistance of the bed and will be slowed down (The Open University, 1999a). However, the crest of the wave encounters less effects from the bottom and will retain more velocity. Eventually the upper part of the wave catches up with the bottom part and the wave breaks. In this process, the energy initially received from the wind is dissipated. Near a coastline, the strong decreasing wave height results in a strong mean water gradient: wave set up. The increase of the water level in the surf zone (the area near the coastline from the first point where waves break to the beach) depends on wave-period, bed slope and wave-height. According to Bowen, Inman, & Simmons (1968), a wave set up of 0.3m just after the waves break is a realistic value (assumed water depth at wave breaking  $h_{br} = 2.5\text{m}$  and breaker coefficient  $\gamma = 0.6$  [-]). Wave breaking is a complex process, which has multiple forms. The occurring form depends mostly on bathymetry (shallowness/steepness) and wave conditions (length/height) and results in different locations of breaking and differences in wave dissipation (The Open University, 1999a).

A fast-incoming storm surge, combined with upcoming flood, can quickly increase the water level near the coastline. The increased water level causes a gradient between both sides of the tidal inlet, which results in water flow. The higher the gradient, the higher the currents (Britannica Online Encyclopedia, 2008).

### 2.3.2 Morphological processes (erosion/sedimentation)

Beaches are accumulations of loose sand or pebbles. When the uplifting forces on the grain are higher than the resistance force, a particle will move (Figure 3).

The uplifting forces can be generated by multiple forces. As waves break in the foreshore, much of the energy is dissipated and acts as resultant force. The more energy is dissipated, the more sediment is moved (The Open University, 1999b).

Another force which is able to force sediment into motion is the flow velocity. This kind of erosion is common in rivers. The amount of sediment which is taken into transport depends on the bed level, steepness of the bed, wave height and sediment characteristics (Jansen, 1978).

Near the dunes, the shape of the erosion profile is determined by the wave height and sediment characteristics. Steetzel (1990) states that according to the findings of Vellinga (1986) the amount of erosion is determined by the maximum surge level. The formulas which are used for this theory only include cross-shore parameters and are constructed for straight coastlines.

The infragravity waves have a small amplitude and won't break near the coastline. Therefore, these waves will continue to propagate in shallower areas and are projected up the beach slope (in the swash zone), where it is found to be dominant in the morphological processes in storm conditions (Roelvink et al., 2009; The Open University, 1999b).

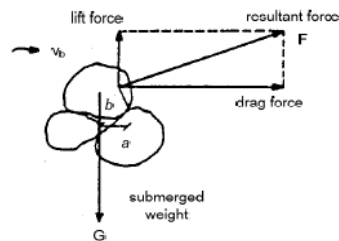


Figure 3 - Forces on grains on the bottom (Ribberink, 2011)

## Chapter 3

### Study area

#### 3.1 The Wadden Sea

The Marsdiep inlet is the first tidal inlet in the Wadden Sea, enclosed by the Dutch Main coast (south) and the island of Texel (north). The Wadden Sea is a tide- and wave dominated system which is characterized by multiple, small inlets.

The inlet itself is characterized by a large sand flat ('The Hors') at the southern side of the island of Texel and multiple ebb-tidal delta's, of which the biggest is called the Noorderhaaks as can be seen in Figure 4.

#### 3.2 The Hors

The Hors is a large sandflat at the southern side of the island of Texel. Around 1749, an ebb tidal delta grew on to Texel and became known as the Hors. During the 20<sup>th</sup> century, the sandbank Onrust merged with the Hors, both ebb tidal delta's are formed in the process of tidal motion through Marsdiep and slowly shift northwards towards Texel (Ecomare, 2017).



Figure 4 - Location of study area with detailed overview of study area (Source: google earth)

Figure 6 gives an overview of the Hors in 2012 and Figure 5 shows the Hors in 2016. Various lighter areas are visible in both figures. These areas contain dry sand whereas the darker areas are wet. The west coast is located higher (1.5m+NAP) which explains the dry sand. Rush wheatgrass grows on the sandflat, behind which the moving sand particles get stuck and form small dunes. This phenomenon is by the white stripes on the center of the Hors in both Figure 5 as 6.

During a storm surge, most of these dunes are eroded, but those that resisted, grow stronger. When the dunes are big enough, they are able to hold fresh rainwater. This property makes marram grass to grow on the dune. This grass catches a lot more sand and speeds up the process (Ecomare, 2017). However, the dune vegetation on both pictures is similar, which gives the impression that the dune growth over the years is minimal.

The bed level on the Hors is around 1.5m+NAP whereas the highest amplitude of a spring tide in 2016 in Den Helder was 0.9m+NAP (Rijkswaterstaat, 2017c). Thus, under normal conditions, the Hors is dry land. During storm surges however, the Hors is inundated. The highest measured water level was during the storm of 1953 and reached 3.25m+NAP in Den Helder (Rijkswaterstaat, 2017a). Towards the north of the sandflat, larger, vegetated dunes are visible.



Figure 6 – Overview of the Hors (picture from google earth taken at 1-10-2012)



Figure 5 - Overview of the Hors (picture from google earth taken at 18-8-2016)

### 3.3 Marsdiep / Molengat

The tidal channel south of the Hors is called Marsdiep. At the sea side of the channel, the Noorderhaaks causes a bifurcation of the main channel. Schulpengat is the southern extension of Marsdiep and flows south of the sandflat, the Northern branch, Molengat, flows at the North side of the Noorderhaaks (Figure 4).

The tidal wave approaches the Dutch coast from the south, and the approaching flood wave therefore first flows into Marsdiep towards the Wadden Sea. The water has to go around the Noorderhaaks to reach Molengat. This motion takes a lot of sediment with it and therefore causes the area northern of the Hors (Part II in Figure 7) to erode (Cleveringa, 2001). The longshore current, caused by waves breaking under an oblique angle to the shoreline, pushes the Noorderhaaks slowly towards the Hors.

The outline of the Hors has changed significantly over the last years. Wijnberg et al. (2017) explains that the changes are due to the shift of the Noorderhaaks, causing the steep channel slope of Molengat to reduce in angle. This results in erosion on the shoreline of the southwestern part of the Hors (IIIb).

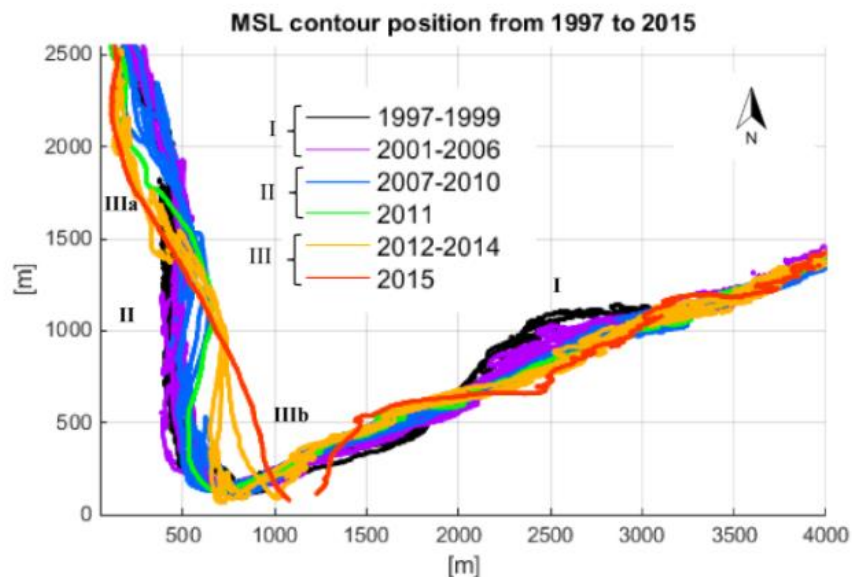


Figure 7 - Development of the outline of the Hors sandflat between 1997 and 2015 at mean sea level (0m+NAP)(Wijnberg et al., 2017)

## Chapter 4

### Methodology

As described in the approach (chapter 1.4), a numerical model is used to get a better understanding of the hydrodynamical processes on top of the Hors during a storm surge. On the scope of the present research, the model XBeach (Roelvink et. al. 2009) has been chosen. In this chapter, XBeach is introduced and it is explained how the results from this model could answer the research questions. Second, the necessary parameters which are implemented in XBeach are described. Finally, the validation of the model will be discussed.

#### 4.1 XBeach

The 2DH process-based model XBeach is able to simulate nearshore hydrodynamics of waves on a time scale of wave-groups, including surfbeat (long waves, infragravity waves) and wave-induced currents in combination with non-cohesive sediment transports, avalanching of dune fronts and morphological change on the time scale of storm events (Carrion Aretxabala, 2015; Hoonhout, 2015; Roelvink et al., 2009; Van Rooijen et al., 2014).

The model is used in earlier researches on the Dutch North sea coast Both reports state that results from the XBeach model, when properly validated, correspond well with reality. Further, XBeach is found to be able to reproduce collision and overwash regimes even in presence of a high three-dimensional flow, which makes it usable for modelling tidal inlets.

By showing the hydrodynamic processes (water levels, wave characteristics current characteristics, wind characteristics) in an overview of the inlet on different moments during the storm surge, the overall view and course of the processes in a tidal inlet system during a storm surge becomes visible. Temporal plots of several locations in/around the inlet could support the results seen from the spatial plots.

##### 4.1.1 Hydrodynamic processes

###### *Wave mode*

To calculate the hydrodynamic processes in the model, the surfbeat mode is used. This mode especially focusses on swash zone processes and is fully valid on dissipative beaches where the short waves are mostly dissipated by the time they are near the shoreline (Hoonhout, 2015). The surfbeat mode resolves the short wave varying on a wave group scale and includes long waves which are associated with these wave groups (Hoonhout, 2015).

###### *Wave directions*

The wave direction is solved at regular intervals using the stationary solver, every 72 time steps ( $\Delta 0.043$  sec), the wave direction is calculated ( $72 \cdot 0.043 = 3$  sec). The wave energy follows this wave direction. By using this method, the groupness of waves is preserved and the simulations significantly decrease in computational demand (Deltares, 2015). The implementation of the solver decreases the simulation time from 5 days to 2 days. The results show that the wave refraction on the eastside of the Hors is affected when applying this model. However, the wave heights on this part of the Hors are below 0.1m and the refraction of the waves have no significant effects on the hydrological and morphological processes on the Hors.

The order of wave steering (parameter name = order) had to be set to 1 instead of the default value of 2. This difference in parameter determines the order of wave steering, 1 = first order wave steering (short wave energy only), 2 = second order wave steering (bound long wave corresponding to short wave forcing is added) (Hoonhout, 2015). Results of simulations with

Order = 2 showed strange waves with a period of around 1 hour and an amplitude of 0.3m. These waves were most likely to be caused by the initial slushing effect of the model, due to the shape and characteristics of the model

To reduce the initial slushing even further, an initial set-up of the water level is implemented to prevent sudden changes in water level at the start of the simulation, creating the slush waves. The initial set-up of the water level takes about two hours and starts with a constant water level of 0.92m+NAP on both front- and backside of the model. Then, every half hour, the water level (mostly on the frontside) is slightly increased. After two hours, the water levels and gradient on front- and backside of the model match the levels of the storm surge of 11-1-2017.

By changing the order of wave steering to 1, in combination with adding an initial set-up of the water level gradient in the model, the 'slushwave' is smaller and not strengthened by the long waves in the model.

#### 4.1.2 Morphodynamical processes

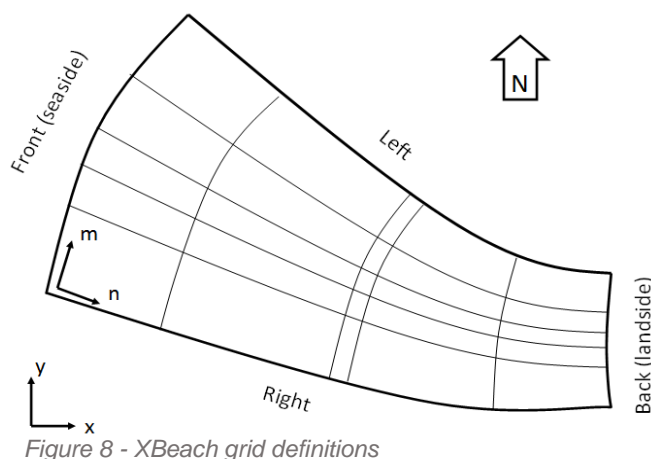
The Van Tiel-Van Rijn method is used to calculate the erosion near the coast which is caused by the flow velocity. The sediment transport on every cell-edge is calculated (with the advection-diffusion equation) and a difference in transport on the cell boundaries results in erosion or sedimentation in the grid cell (Bolle, Mercelis, Roelvink, Haerens, & Trouw, 2011; Hoonhout, 2015).

#### 4.2 Input parameters

First, bathymetry data (and topographic data) and a grid is necessary to simulate the inlet. Second, storm parameters (e.g. water levels, wave characteristics and wind characteristics) are necessary for the model to reproduce the storm surge. The used parameters and data which is used during the simulation of the storm surge is explained in this section.

##### 4.2.1 Domain

A curvilinear grid is used for the simulations. The main advantage of a curvilinear grid over a orthogonal grid is the possibility of curving the grid. This feature makes it possible to simulate the area of interest only (exclude half of the barrier island where nothing happens) and increase the grid resolution only within the area of interest. Therefore, the use of a curvilinear grid results in the saving of computation time.



Similar with an orthogonal grid, the curvilinear grid has four sides: the front (the seaside), two lateral boundaries (north- and south side (left & right in Figure 8)) and the back (tidal basin- and landside) (see Figure 8).

The front boundary follows a line perpendicular to the incoming current- and wave direction on a depth of minimal -20 m+NAP. This depth is necessary to develop realistic waves on/near the front boundary. Due to the shape of the seaside boundary and the bathymetry of the sea, the depth on the seaside varies between -20m+NAP and -30m+NAP.

The back boundary is located in Marsdiep, around 2 km away from the area of interest (and validation data). After testing different grids, it was found that this length was necessary to prevent any influence of the boundary conditions to not disturb processes on the Hors. The lateral sides in the model have a no flux boundary conditions (walls). Alternatives, which all came down to open side boundaries where flows could enter and leave, led to strange currents and water levels throughout the entire model. In an iteration processes, the lateral boundaries to be parallel to the flow, the effect of the boundaries on the result is minimized (Hoonhout, 2015; Steijn, van Banning, & Roelvink, 1998).

The bathymetry file is made using two datasets: one related to the bathymetry acquired by Rijkswaterstaat (so called Vaklodingen) and another related to the topography available through AHN. The latest Rijkswaterstaat measurements during this study originate from 2012 and contains measurements every 20 meters 2012. The AHN dataset originates from 2015 and contains measurements every 1-2 meters (Figure 9).

Between 0 m+NAP and approximately 3m+NAP, both datasets overlap. Because the topography of the hors (at 0 m+NAP) has changed between 2012 and 2015, the transition between the datasets has not been chosen on a single height, but on the locations where the bathymetric heights of the two datasets are similar. The height difference is less than 0.05m, which is lower than the measurement error of the Rijkswaterstaat dataset(Wijnberg et al., 2017). This way, the transition between the dataset is seamless and will not affect the hydrodynamic processes.

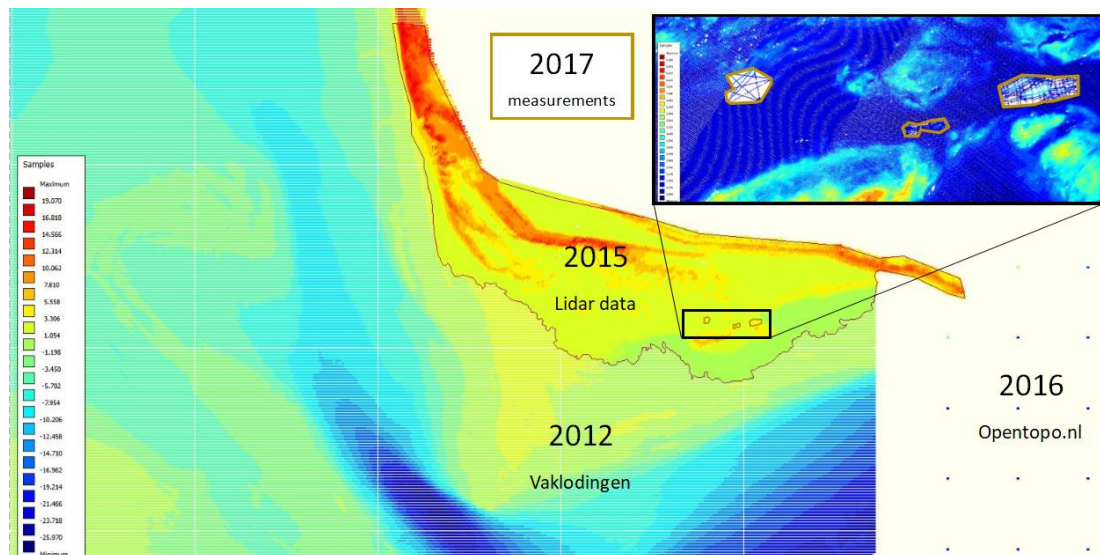


Figure 9 – Overview of bathymetry data of LIDAR(2015) and Vaklodigen (2017) on the Hors and surroundings. (Used scale in overview Hors.; blue = 28.7 m - NAP, red = 19.1m + NAP. Used scale in enlarged figure: blue = 0.8m + NAP, red = 9.5m+NAP)

### 4.3 Input parameters

#### 4.3.1 Water level data

During the simulations, two water levels time-series on both the front- and backside of the model are defined. Water level measurements from surrounding measurement stations are (linearly) interpolated to match the middle of the front- and backside of the model. For the sea side, the Texel-Noordzee and Q1 measurement stations determine the water level on the sea-boundary. At the backside, the water levels of the Den Helder and the Oudeschild measurement stations are used (50-50%). Figure 10 shows the location of the measurement stations. The water levels on both boundaries are measured every hour.

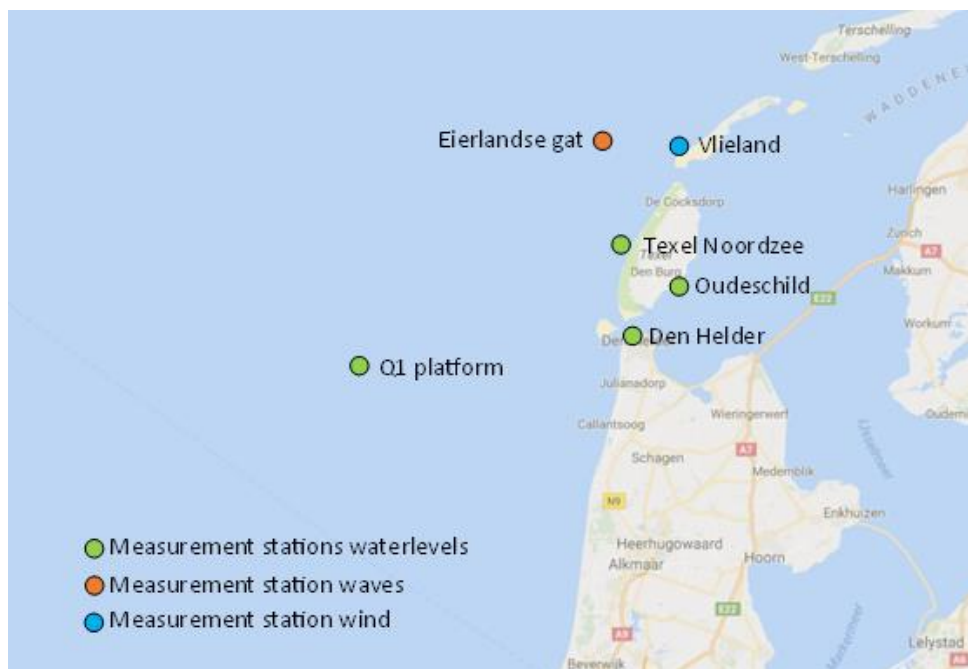


Figure 10 - Location of used measurement stations

#### 4.3.2 Wave data

Used input wave data includes hourly data of the significant wave height, wave period and main incoming wave angle in an energy spectrum of 30-500mhz. This data is acquired from the Rijkswaterstaat site (Rijkswaterstaat, 2017b). The station most nearby is 'Eierlandse gat', which is located at the north-east of the island of Texel (see Figure 10). The distance from the measurement station to the coastline is similar as the sea-boundary of the used model. The wave height differs per waterdepth and therefore it is assumed that the wave heights in 'Eierlandse gat' are representative for the simulated area.

#### 4.3.3 Wind data

Wind input parameters consists of wind speed and direction which can be changed over time. Data of the measurement station of Vlieland (again acquired from Rijkswaterstaat) is used in the model. For a limited time-series, wind data on the Hors is available. A standard deviation of the differences in wind direction and speed between 1996-1999 with wind speeds above 14m/s resulted in a mean difference in wind direction of 3°, with a standard deviation of 10°. The difference in wind speed is averaged 1.3m/s with a standard deviation of 1.5m/s. It is assumed that this difference won't affect the results of the simulations. The wind direction is measured on the last 10 minutes of the last hour and the wind speed is the hourly mean average (Koninklijk Nederlands Meteorologisch Instituut, 2017).

#### 4.3.4 Grain sizes

Grain size is based on field measurements at the Hors in 2015. The following grain sizes are used in the simulations:

D50 = 0.000220 m  
D90 = 0.000330 m

#### 4.4 Validation method

By checking the results of the simulation with actual measurements, the conformation with reality could be made. Available data in/near tidal inlet systems is scarce, however there is one inlet where all necessary input data for the numerical model and two validation datasets are available: The Marsdiep inlet, Texel (NL). Both datasets are described below.

##### 4.4.1 Field measurements

The first dataset consists of measurements on dunes located north of the Marsdiep inlet. The topography of three dune(field)s have been measured on 11-1, 12-1 and 18-1-2017. The location of the measured dunes on the Hors are shown in Figure 11 and Figure 12.



Figure 11 - Overview Hors with location of measured dunes

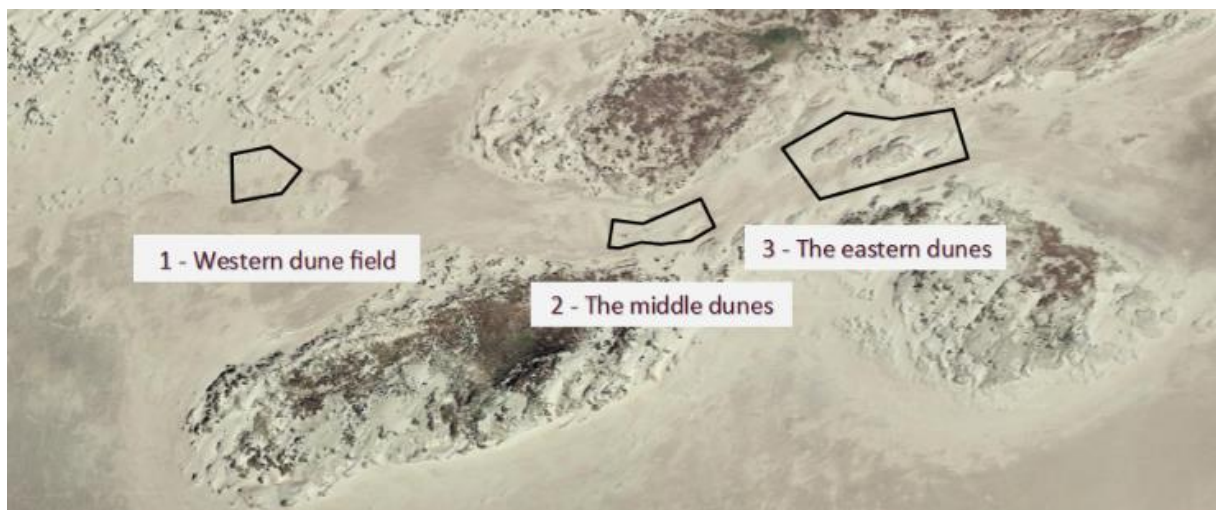


Figure 12 - The three measured dune(field)s on the Hors (located in square of Figure 11)

##### *Western dune field*

The western dune field is located in an area with a number of little dunes. The dunes are measured from five tops of dunes towards each other (between 2-3m+NAP), creating a pentagon. The five angles in the measurement are tops of small dunes.

### *The middle dunes*

The middle dune is located in between large dunes on both north and south side. Water flows under relatively high velocity through this funneling valley. Two dunes are located in the area of 'the middle dunes'. The left dune, is around 1.8m + NAP and the top of the right dune is around 2.8m + NAP.

### *The eastern dunes*

The middle dune and the eastern dunes are located in the similar valley. However, the eastern dunes are a lot bigger and are vegetated (see Figure 12), which means they can be considered stable. The height of the north-west located dune is around 3.5m+NAP and the south-eastern dune reaches 5m+NAP. The narrow passage between the dunes has a height around 1.5m+NAP.

By use of triangular interpolation, the measurements (x,y,z-data) are translated onto the grid, generating a bed level. By subtracting the bed level of 11-1 from 12-1, erosion/sedimentation patterns become visible. The erosion/sedimentation is the result of the hydrodynamical behaviour, so from the erosion values and patterns an indication of the correctness of the hydrodynamical processes can be made:

- The highest outline of the erosion on the dunes indicate the maximum water level + wave height. Because it is hypothesized that the wave height in this part of the Hors is below 0.3m, the highest erosion point (m+NAP) should be in line with the maximum water level.

- One of the 'middle dunes' is completely drowned during the storm surge. Waves are expected to be fully dissipated on this location (in the valley). Therefore, erosion and sedimentation are assumed to be dominantly caused by the (maximum) flow velocity near the dunes. By comparing the simulated dune erosion with the measured erosion, the flow velocity can be qualitatively validated.

- In the measured erosion/sedimentation profiles, a clear sedimentation trail is visible downstream of the dune. The height and length of the sedimentation trail depends on both the current magnitude and direction. Thus, after comparison of the sedimentation trail, the currents in Marsdiep are validated.

### 4.4.2 TESO-data

The second dataset consists of current measurements of Marsdiep. These measurements are acquired using acoustic Doppler current profilers (ADCPs) on board of the ferry which shuttles between Den Helder and Texel every hour (run by TESO). The equipment measures the flow's current and direction. The data of large parts of the year of 2009 is made available by the Royal Netherlands Institute for Sea Research (NIOZ)(Sassi, Gerkema, Duran-matute, & Nauw, 2016).

The ferry measures the currents in Marsdiep every 2 seconds. Due to the movement of the ship, the measurement location changes every measurement. To find currents on specific locations, ID-points are used. These ID-points are located on a fixed location and show all measured currents on that location. There are in total 109 ID-points measured by NIOZ, for this study, 14 of those ID-points are used (location number 1 t/m 14 in Figure 13).

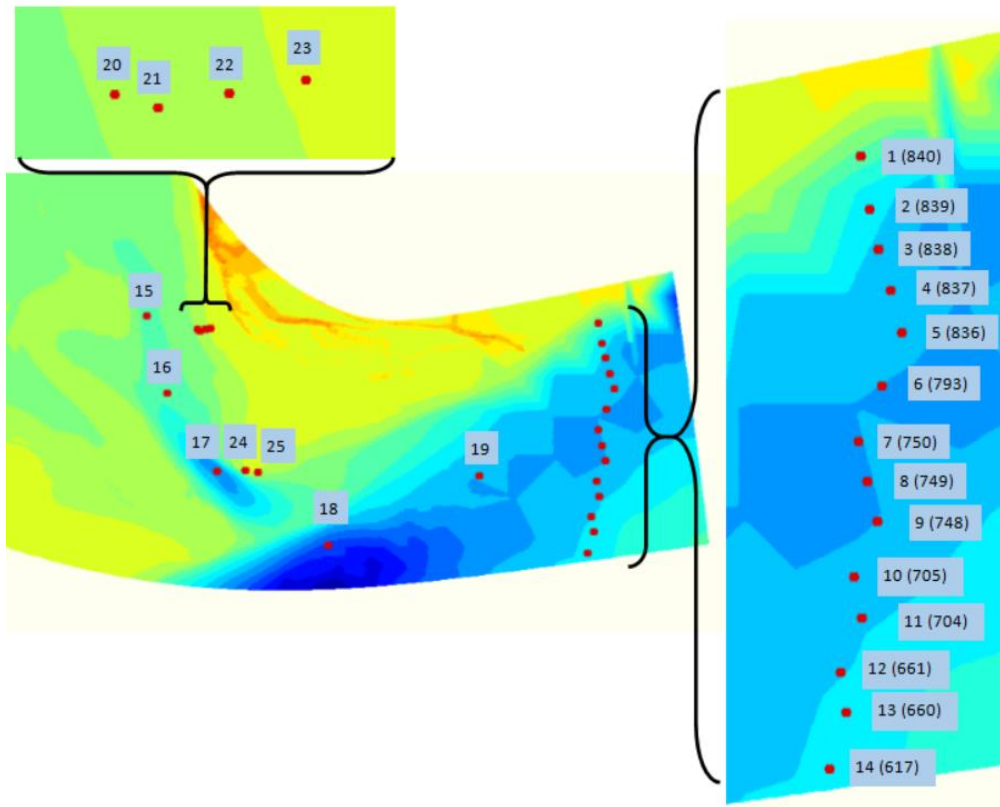


Figure 13 – Individual locations which are used to generate results, point 1-14 are ID-points of TESO-data

The use of the validation data is limited, for two reasons: the ferry to sail at night, causing data gaps in the dataset and the ferry won't sail during a storm surge (when the water levels increase over 2m+NAP).

The only storm surge within the period occurred on 4-10-2009. During this storm, a water level of 1.84m +NAP was measured in Den Helder. However, the peak of the storm occurred around 7.00am., while the first ferry crossing is at 7.30am. Due to the large gap in data, it is chosen not to use this storm directly as validation data.

It is assumed that the currents in Marsdiep fully depend on the gradient between the sea- and land side of the inlet. Difference in tides (spring-tide) generate different water level gradients between the inner- and outer side of the inlet and therefore stronger currents.

With the TESO-current data and water level measurements of 2009, an analysis was done to find the mean flow velocity and standard deviation relative to the water level gradients between the inner- and outer side of the inlet for every id-point. The results give an indication of the expected current magnitudes in Marsdiep during a storm surge (based on the water level gradient). More information about this storm surge analysis can be found in Appendix III.

Results from the storm surge analysis are compared with the simulated currents in Marsdiep for the storm surge of 11-1-2017.

#### 4.5 Sensitivity analysis

The model is validated for one single storm surge for one single inlet. To understand how the behaviour of hydrodynamics differ in other storm surges, a sensitivity analysis has been done. The validated storm surge of 11-1-2017 will be adjusted to test the effect of different parameters. With knowledge of the effect of parameters, the hydrodynamic behaviour during storm surges in other inlets can be hypothesized.

In the validation phase, it has been found that a single simulation of 6 hours takes 48 hours to run. This duration limits the amount of simulation and therefore the simulations are carefully chosen to test five hypotheses. One or two simulations are designed to test each hypothesis, these adapted versions of the storm surge of 11-1-2017 are called Storm 1-6.

#### (wind)waves

It is believed that short (wind)waves which are formed in the North Sea have little effect on the hydrodynamic and morphodynamic processes on the Hors during a storm surge. The water depth on the Hors, when flooded, has never been above 2 meters (assumed 3.25m+NAP at 1953 – 1.5m+NAP bed level Hors). Some simple wave calculations according to the method of Battjes (1974) caused all incoming waves to break in front, or the beginning of the Hors. However, after wave breaking, the waves don't cancel out entirely. It is possible that the remaining short waves remain or even increase in height on the Hors due to high wind velocities. These waves could be important in the erosion process. From this hypothesis, it has been chosen that the wave characteristics won't be changed during the simulations.

#### Water level

A second hypothesis regards the water level on the sandflat. To test the influence on the maximum water level on the hydrodynamic and morphodynamic processes on the hors, an increase of the water level is proposed. After analysing the earlier mentioned dataset with all the storm data between 1981 – 2015, multiple storm surges matched the storm characteristics of the 2017 storm surge, all with different water levels.

Due to the incoming tide from the south in combination with the storm surge coming from the north, it is a matter of chance where these waves meet and create the highest water level. A springtide at Den Helder can reach a height of 0.9m+NAP where the calculated tide level during the 2017 storm surge reached only 0.6m+NAP. Therefore **Storm 1** contains an increase of 0.3m is chosen on top of the measured water levels of 11-1-2017. The new maximum water level which is reached during this storm (in measurement point Den Helder) is 2.05m+NAP which occurs once every year (Rijkswaterstaat, 2017a).

#### Water level gradient

A third hypothesis that should be tested is the speed of the incoming storm surge. Faster incoming storm surges are associated with heavier storm surges (KNMI, 2017). When the water level in the North Sea rises quickly, a relatively high gradient between both sides of the inlet is created which will result in stronger currents in the inlet. Higher currents are associated with higher erosion and sediment transport, which could lead to stronger erosion on the west part of the Hors and more sedimentation on the east part of the Hors (where the water depth increases and sediment transport decreases). From this hypothesis, it has been decided that in **Storm 2**, the water level on the front-side will be linearly increased with 0.3m to measure the effects of water level gradients on the outer- and inner side of the inlet. This increase causes a maximum gradient of 0.55m between front- and back of the model. In 2009, the largest occurring gradient between the front- and back side reached 0.43m. The value of 0.55m might be a little extreme, the increase of the water level 0.3m on the seaside can be compared with the results of **Storm 1**.

#### Wind speed

A fourth hypothesis affects the wind speed. It is believed that wind speed has only a minor influence on the wave heights on the Hors. From the storm surge analysis, storm with a similar water level and wind direction occur with wind velocities between 12-24 m/s. Using the method of Bretschneider, a quick calculation shows that a wind speed of 12m/s could develop new waves of about 0.11m (over 1500m, with a uniform depth of 0.5m) (ENW, 2007). A wind speed of 24m/s increases the wave height to 0.16m. This difference of 0.05m would not significantly

change the hydrodynamic or morphological processes on the Hors. However, the absence of wind could cancel out all waves on the Hors and would therefore be an influence on the system. Besides that, the calculation of Bretschneider is meant for a uniform underground, where the Hors is more irregular. It is possible that the wind reacts differently in XBeach than this basic calculation implies. The Bretschneider calculations can be found in Appendix II – Basic calculations. Due to the uncertainty of this hypothesis, two simulations will be done regarding the wind velocity. A version of the 11-1-2017 storm surge with an increased wind velocity of 24m/s (instead of 17m/s) I simulated in **Storm 3** and a simulation of the 11-1 storm surge with the absence of all wind parameters is simulated in **Storm 4**. These simulations provide the necessary information to test the hypothesis of the influence of wind in a tidal inlet system.

#### Wind direction

The final hypothesis concerns the wind direction. It is believed that a wind from the north blows the dunes towards the south and would therefore decrease erosion on the dune field north of the Hors. A wind current from the west however would give more erosion on the dunes on the Hors because it enstrengthens the waves and blows them more towards the dunes.

From the storm surge analysis, similar storm surges to the validation storm surge (water levels max +/- 20cm difference, wind velocities max +/- 2 m/s difference and wave directions max +/- 10° difference) are filtered from the large dataset. The remaining storm surges have wind directions which range between 270° and 340°. **Storm 5** is simulated with the minimal wind directions (270°), and **Storm 6** is simulated with a wind coming from 340°.

Table 1 shows the characteristics of the validated storm surge of 11-1-2017 (Storm 0) and the six adapted storm surges (Storm 1-6) that are simulated during the sensitivity analysis. The changed parameters are written in bold.

Table 1 - Characteristics of the different storm surges (on moment of maximum water level)

| Storm nr. | Adapted storm parameter            | Peak water level    | Wind direction | Wind speed     | Wave height        | Waveperiod | Wave direction |
|-----------|------------------------------------|---------------------|----------------|----------------|--------------------|------------|----------------|
|           |                                    | Den Helder [cm+NAP] | Vlieland [°]   | Vlieland [m/s] | Eierlandse gat [m] |            |                |
| 0         | -                                  | 1.75                | 290            | 17             | 5.5                | 7.5        | 309            |
| 1         | Overall water level increase +0.3m | <b>2.05</b>         | 290            | 17             | 5.5                | 7.5        | 309            |
| 2         | Increased water level gradient     | <b>~ 2.05</b>       | 290            | 17             | 5.5                | 7.5        | 309            |
| 3         | Wind speed +7m/s                   | 1.75                | 290            | <b>24</b>      | 5.5                | 7.5        | 309            |
| 4         | No wind                            | 1.75                | -              | -              | 5.5                | 7.5        | 309            |
| 5         | Wind direction 270 °               | 1.75                | <b>270</b>     | 17             | 5.5                | 7.5        | 309            |
| 6         | Wind direction 340 °               | 1.75                | <b>340</b>     | 17             | 5.5                | 7.5        | 309            |

# Chapter 5

## Validation

### 5.1 TESO data

Figure 14 shows the expected currents magnitudes during the storm surge (blue line), which based on the analysis of the TESO-data, and the simulated current magnitude and the simulated current magnitudes (orange line).

Results show an overall underestimation of the current magnitude of with a maximum of approximately 0.6m/s during the first peak (at 3 hours) into the storm surge. The shape of the timeline of the simulated currents is rather different than the expected timeline. In the expected current speed, a wave pattern is visible with peaks on the moments where the water level gradient (between inner- and outer side of the inlet) the highest. The current in the simulation however shows only one peak during the storm surge. After 6 hours into the storm surge, the water level gradient becomes negative, and the current would be expected to increase again. However, this is not visible in the simulation. When looked at a point in the middle of Molengat, the current wave is better visible, although still a delay is visible of about two hours.

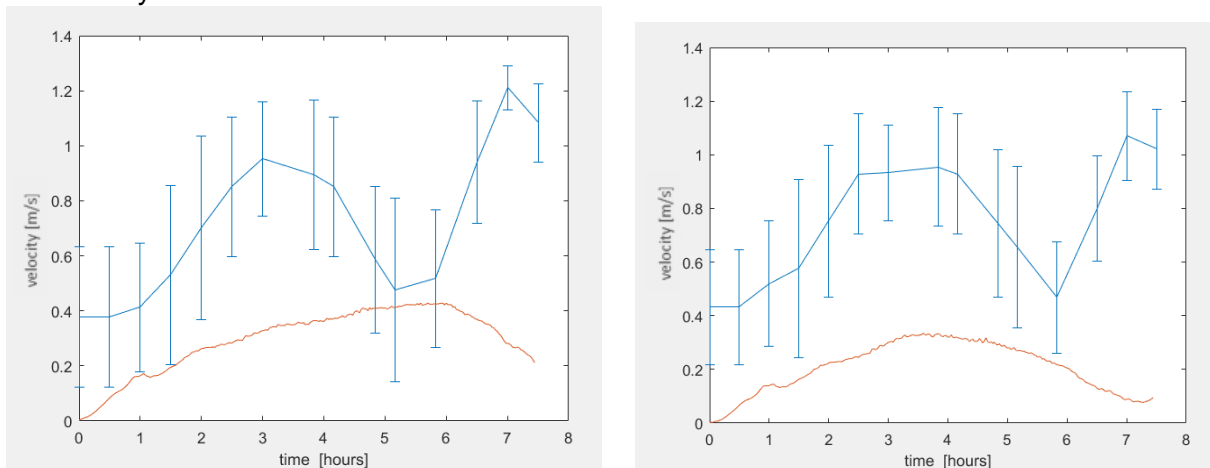


Figure 14 – Left: Simulated currents (red) are compared with reference data (blue) in the center of Marsdiep (id-point 796). right: Simulated (red) and reference currents (blue) are compared on a point located south side of Marsdiep (id-point 705).

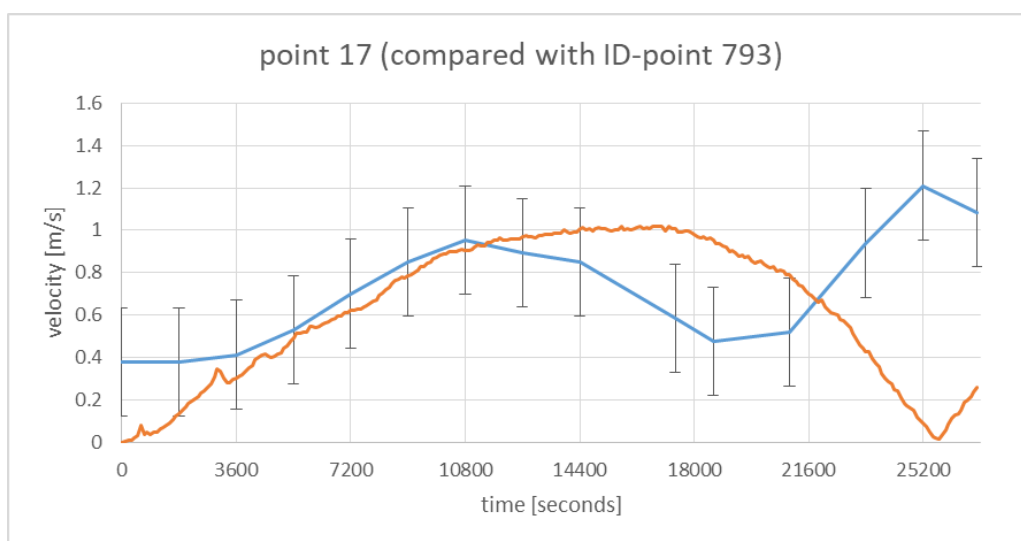


Figure 15 - Currents in Molengat (point 17 on Figure 13) compared with the expected currents on point 6 (ID-point 793)

## 5.2 Dune measurements

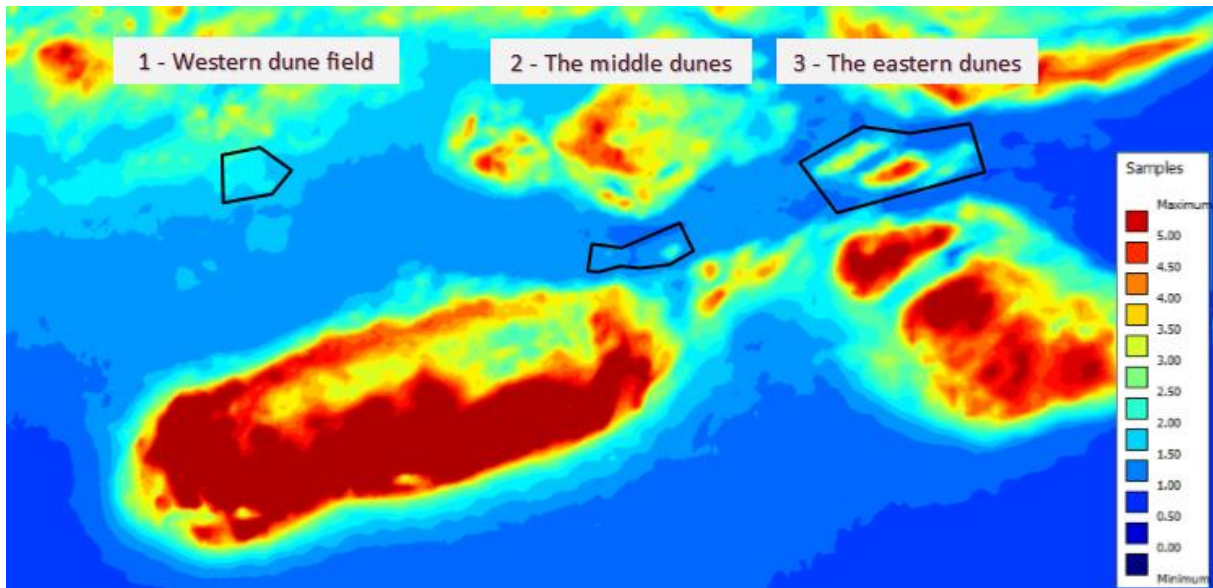


Figure 16 - Overview of bathymetry of three measured dune(field)s on the Hors (located in square of Figure 11) (blue = 0m+NAP, red = 5m +NAP)

This chapter contains the comparison of the erosion/accretion of the 'western dune field' and 'the middle dunes' of the simulation with the measured values. The 'eastern dunes' are disregarded, due to large amount of noise, the measurements are become unreliable.

### 5.2.1 The western dune field

Figure 17 and Figure 18 show both the simulated and measured dune erosion of the western dune field during the storm surge of 11-1-2017. The first thing to notice is the lack of erosion in the simulation, where the bed level is over 1.9m+NAP. The small dune in the south-west of the measured area (556.65, 111.75), shows a similar erosion pattern with the measurements. The measured value is lower, however, the erosion on the south-west side of this dune is similar in both results.

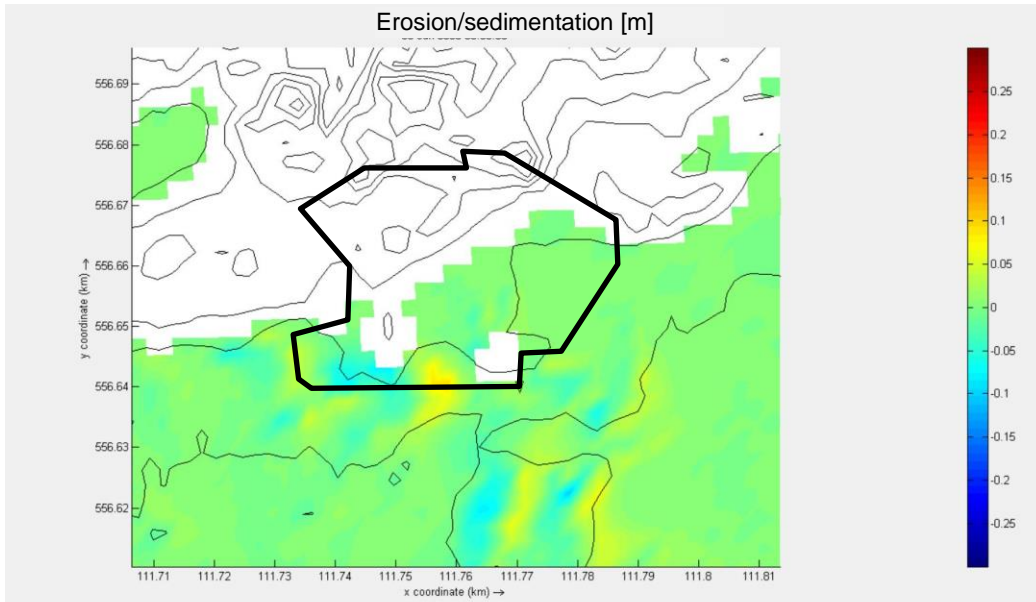


Figure 17 - Simulated erosion/sedimentation of 'the western dunes'

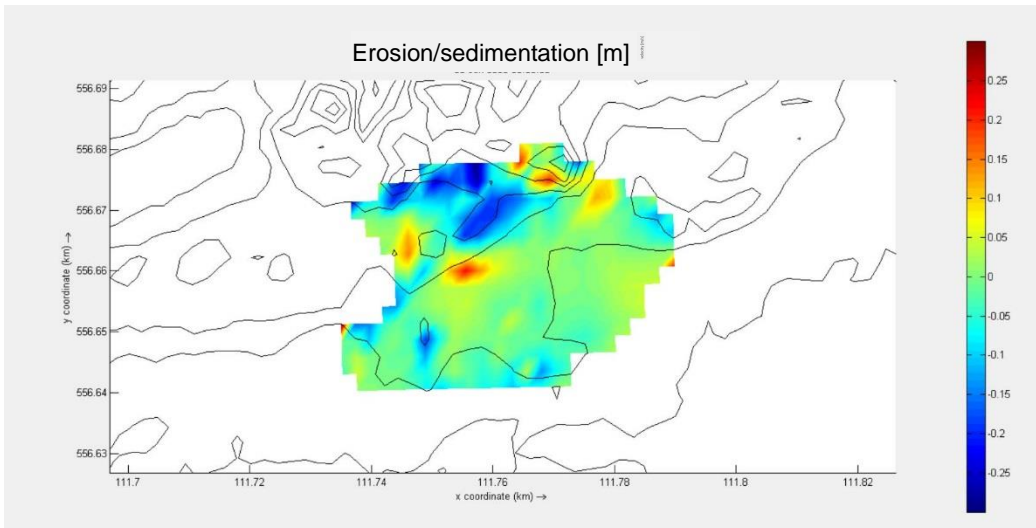


Figure 18 - Measured erosion/sedimentation between 11-1-2017 and 12-1-2017

### 5.2.2 The middle dunes

The erosion sedimentation in the simulation (Figure 20) is found to be visibly comparable with the measurements (in both erosion/sedimentation levels as patterns (Figure 19)). For the left dune, which has a peak of 1.8m+NAP, the erosion is about 0.05m overestimated, whereas the erosion pattern on top of the dune, with a sedimentation around (0.05m) behind it is shown in both figures. For the right dune, the top is not eroded in the simulation, where erosion occurred in the measurements. Apart from this, both erosion on the north-west side of 0.2m and the sedimentation of 0.07m on the east side of the dune is observed in both the simulated results as in the reference data.

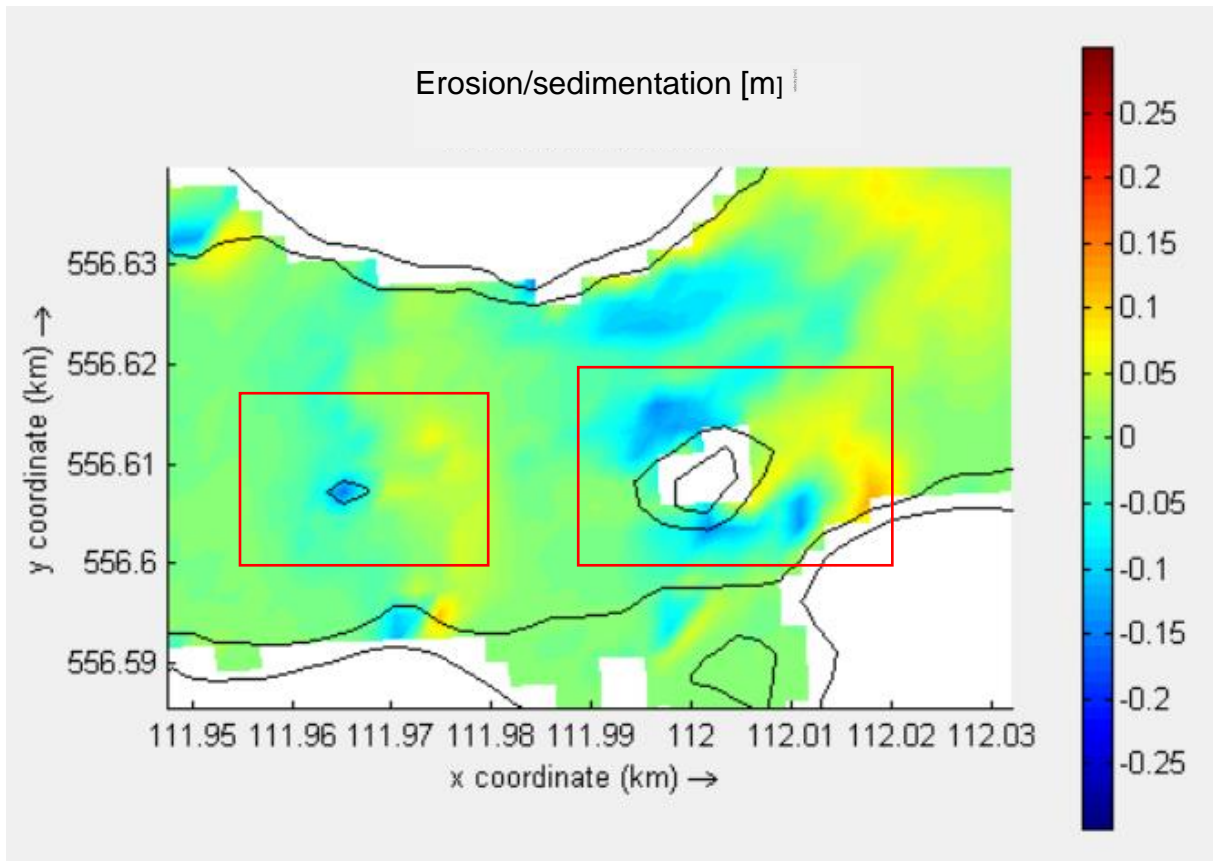


Figure 20 - Simulated erosion/sedimentation of the storm surge of 11-1-2017

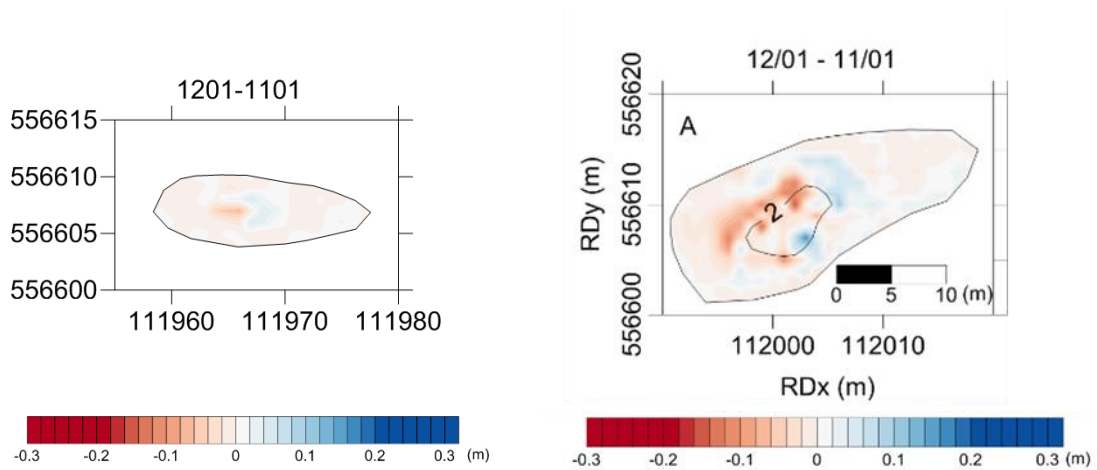


Figure 19 - Measured dune erosion/sedimentation of the middle dunes

# Chapter 6

## Results

### 6.1 Storm 0

The storm surge of 11-1-2017 causes an increase of the water level to a maximum height of 1.86m+NAP (measured on front-side of the model) with waves from the north-west ( $280^{\circ}$ - $310^{\circ}$ ) and significant wave height of approx. 4-5m. The wave height decreases as the waves come closer to the coastline, as can be seen in Figure 21. Figure 22 shows the water level and current-vector on the peak of the storm surge. A water level increase of 0.15m on the western part of the Hors is visible compared with the surrounding water levels. During the peak of the storm surge, the water level gradient between the front- and back side of the model is approximately 0.00m. Figure 23 shows that the waves in Molengat come from the North-east ( $310^{\circ}$ ) but rotate southwards as they enter the Hors ( $280^{\circ}$ - $300^{\circ}$ ) due to the refraction. On the north-east side of the Hors, wave angles even come from the south-east ( $<260^{\circ}$ ).

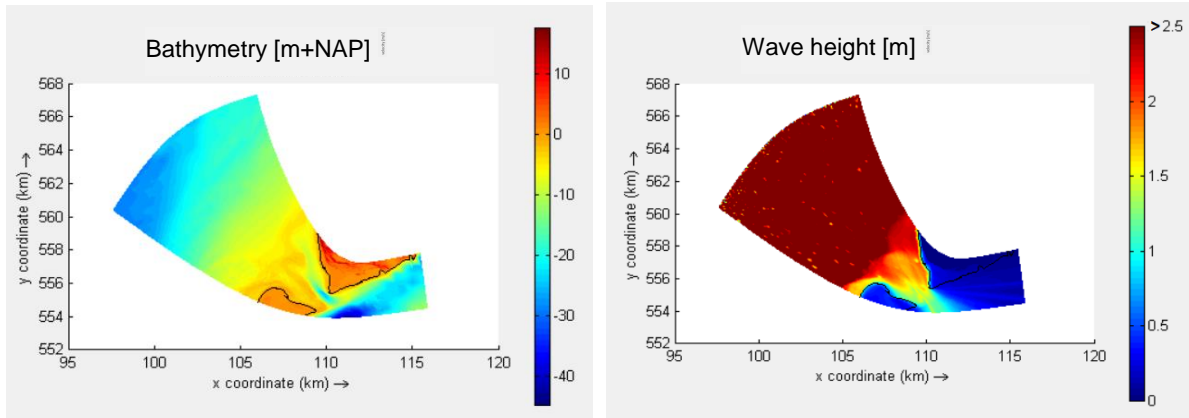


Figure 21 - A: Overview of the bed level in the simulated area [m+NAP] – B: Waveheight on peak of the storm surge (5.5hr into storm surge), max. shown waveheight = 2.5m). Contour line on 0m+NAP

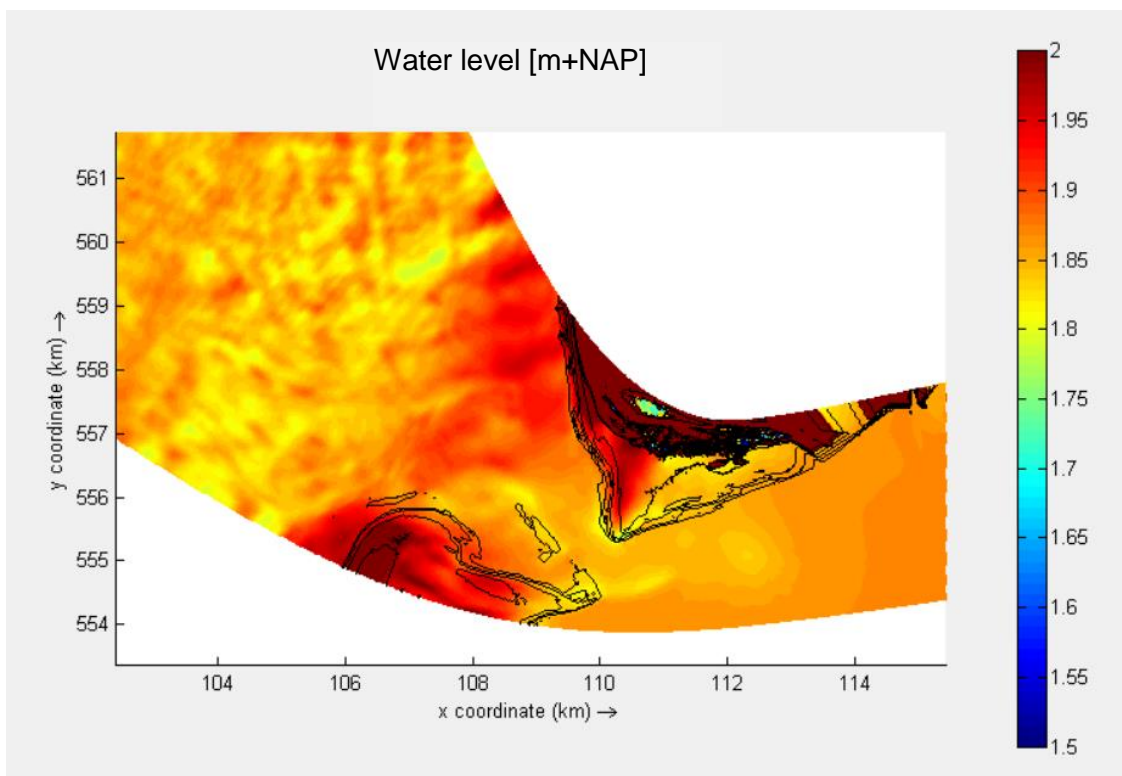


Figure 22 – Water levels on the Hors during the peak of the storm surge of 11-1 ( $t = 5.5hr$ )

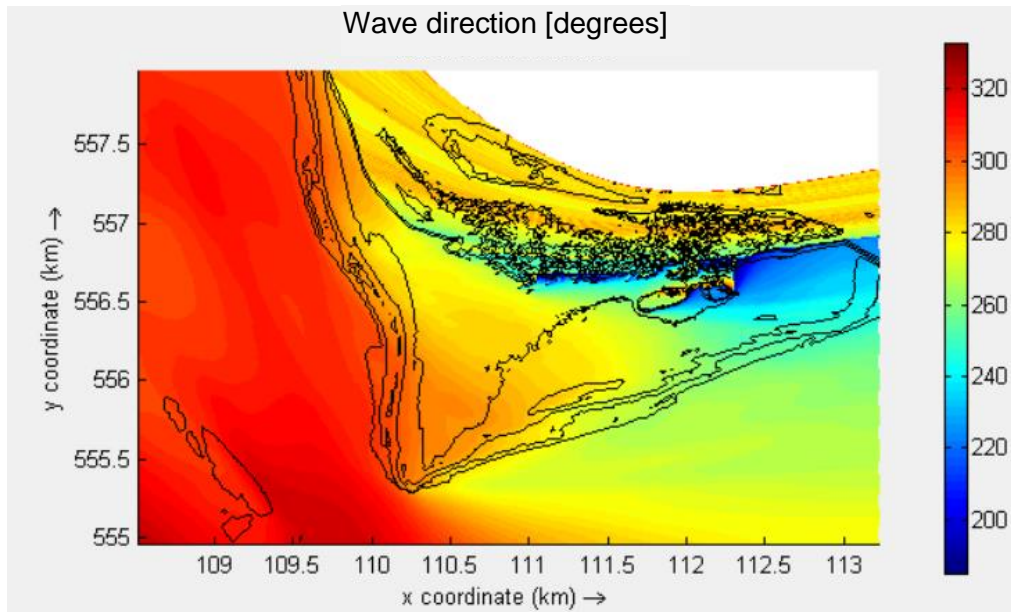


Figure 23 - Wave angle during the peak of the storm surge ( $t = 200$ , 5.5hr into storm surge)

Figure 25 shows the course of the wave height over the cross-section. In this figure, three phases can be distinguished. At the first phase ① around 300 meters into the cross-section, an increase in the wave height of 0.15m is visible. After the peak at ① the wave height decreases. Two 'waves' of decreasing wave heights are observed, which show similarity with the shape in decreasing depth of the two sand bars. The third phase ③ occurs on top of the Hors (from 1000 meters), where the wave height linearly decreases from 0.3m towards 0.2m.

Figure 26 shows the water level and bed level of the cross-section during the peak of the storm surge. The increase of the water level on the west side of the Hors, which is earlier observed in Figure 22, is visible in this figure as well (around 800 meters). After this water level peak, the water level decreases. Despite the decreasing water level, the water depth increases due to a faster decreasing bed level.

Figure 27 shows the current magnitude and the current direction on the cross-section during the peak of the storm surge. Two large flow velocity peaks are identified at 600 and 800 meters into the cross-section, on the locations where the wave height decrease is maximal. The first peak is a flow towards the south ( $330^\circ$ ) whereas the second peak flows more towards the south-east ( $310^\circ$ ).

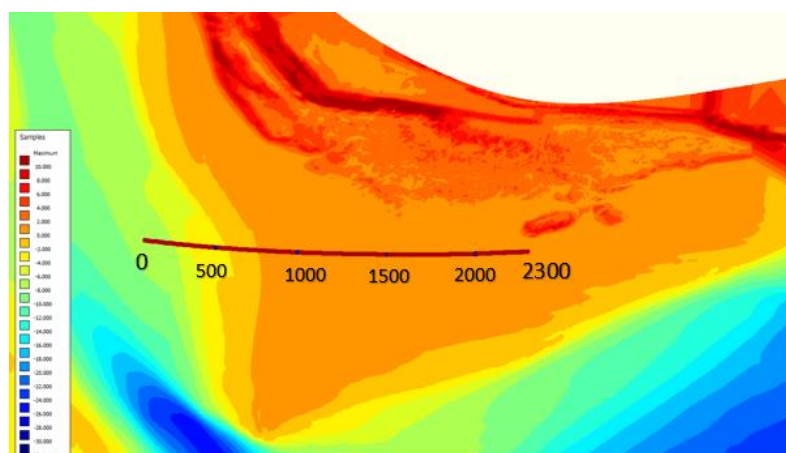


Figure 24 - Overview Hors with location cross-

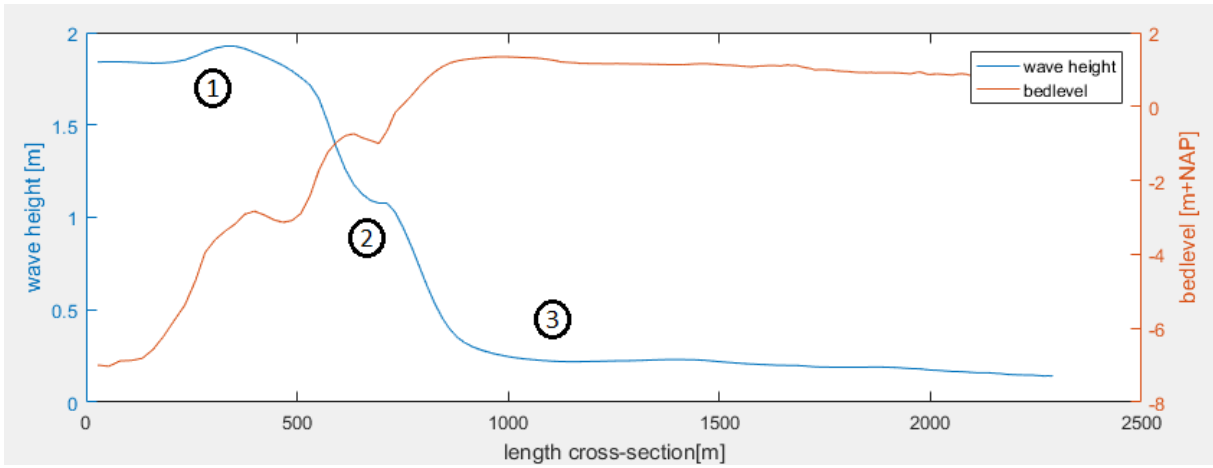


Figure 25 - Wave height and bed level on the cross-section of Figure 24 during the peak of the storm surge (5.5hr)

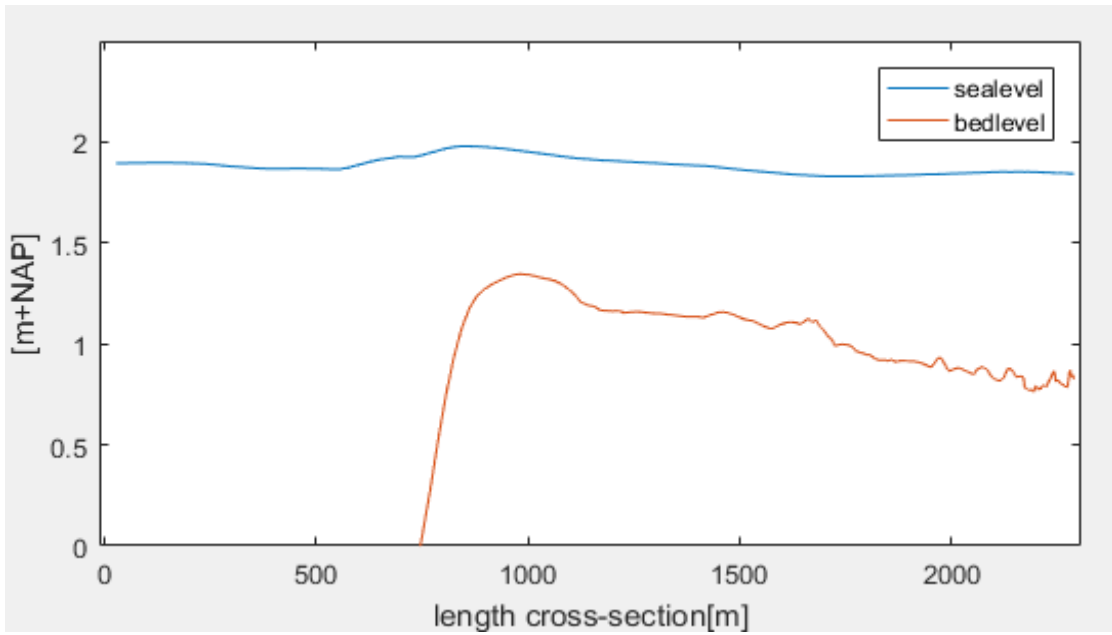


Figure 26 – Bed level and water level on the cross-section of Figure 24 during the peak of the storm surge (5.5hr)

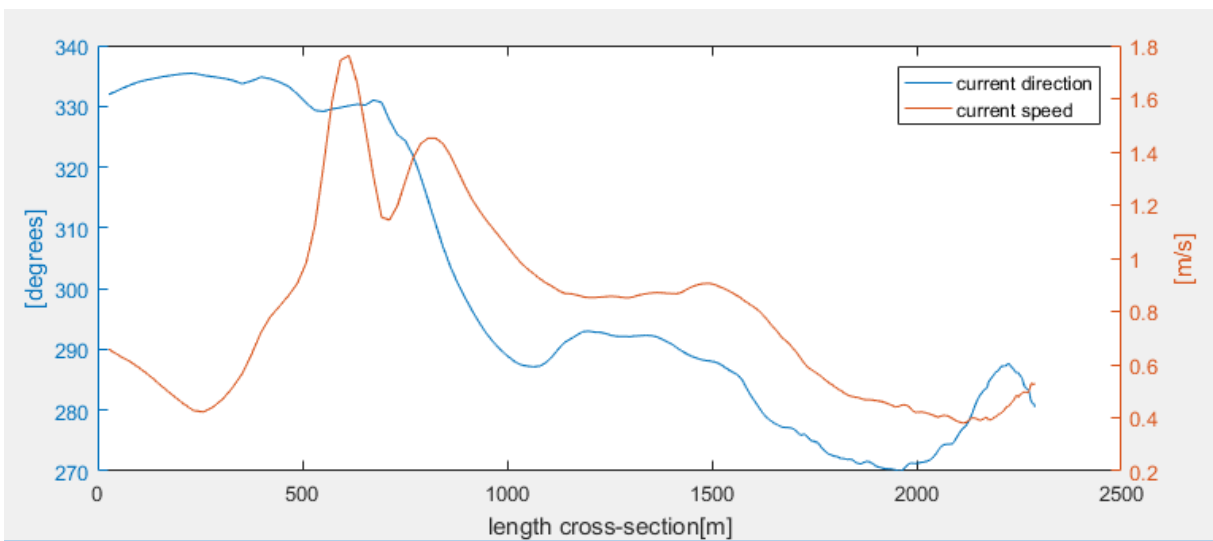


Figure 27 – Current height and direction on the cross-section of Figure 24 during the peak of the storm surge (5.5hr)

Figure 28, Figure 29 and Figure 30 show the flow velocity and direction on three different moments of the storm surge. Figure 28 shows the storm surge at 2.75 hr. into the storm surge. The first two hours of the simulation are used for spin-up of the model, so the actual storm surge has just started 45 minutes. The water level gradient between front- and backside of the model is on this moment 0.2m and the water level near the Hors is approximately 1.3m + NAP, which means the water depth on top of the Hors varies between 0 – 0.2m.

Figure 29 shows the current magnitude and direction at the peak of the storm surge (5.5hr into storm surge). Compared with Figure 28, the flow velocity on top of the Hors has increased, whereas the currents in Marsdiep have remained similar. The water level gradient between front- and backside of the model is on this moment 0.08 meter and the water level in Marsdiep is approximately 1.85m + NAP. The flow direction has not changed from 2.75 hours, except for the water direction on the north-east side of the Hors. In this region, currents point towards the east (270°) instead of North-east (230°) which is observed at the start of the storm surge. Also, a vortex is visible in Marsdiep, south-west of the Hors.

Figure 30 shows the current magnitude and direction at the final phase of the storm surge (7.3 hours into storm surge). On this moment, the water level gradient is negative (-0.40m) and the water level in Marsdiep reaches 1.5m+NAP. The current direction in Marsdiep has reversed and flows with a magnitude of maximal 0.5m/s towards the front (north-west side) of the model. The flow magnitude has decreased but the flow direction on the Hors is comparable with the observed ones in Figure 29.

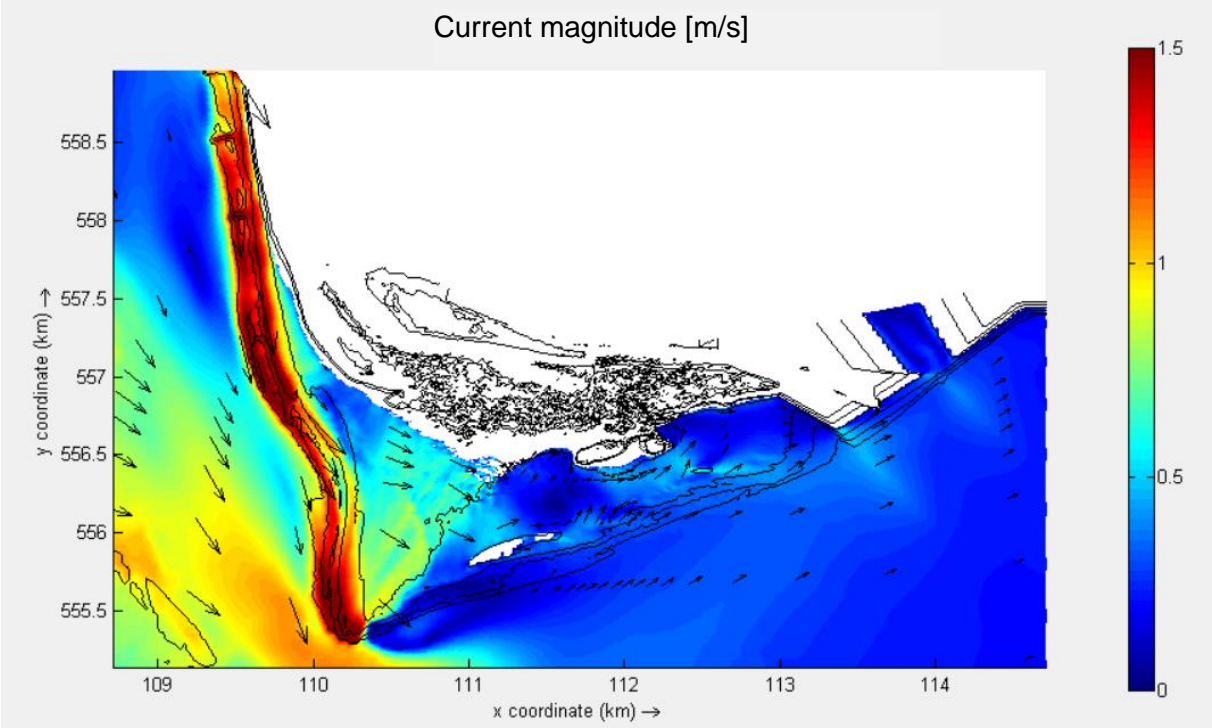


Figure 28 - Currents on the Hors at the start of the storm surge (t = 100, 2.45hr into storm surge) (where the water level gradient is maximum)

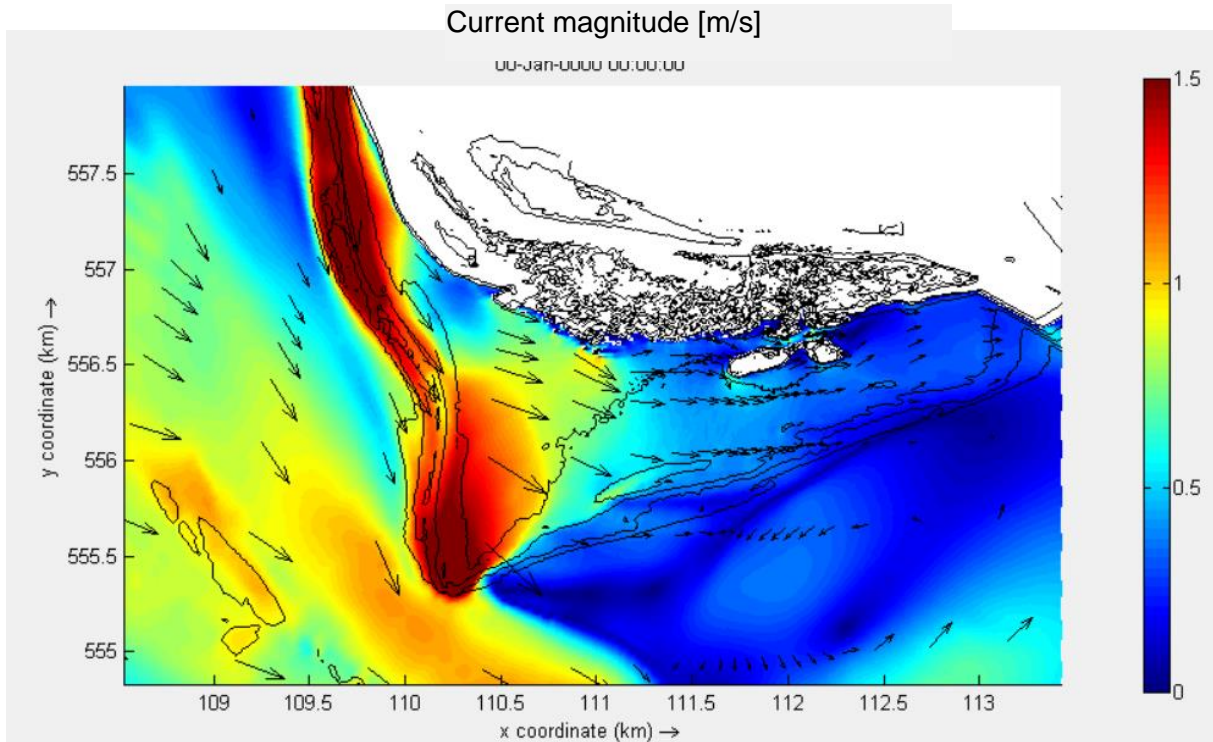


Figure 29 - Currents on the Hors during the peak water level ( $t = 200$ , 5.5hr into storm surge)

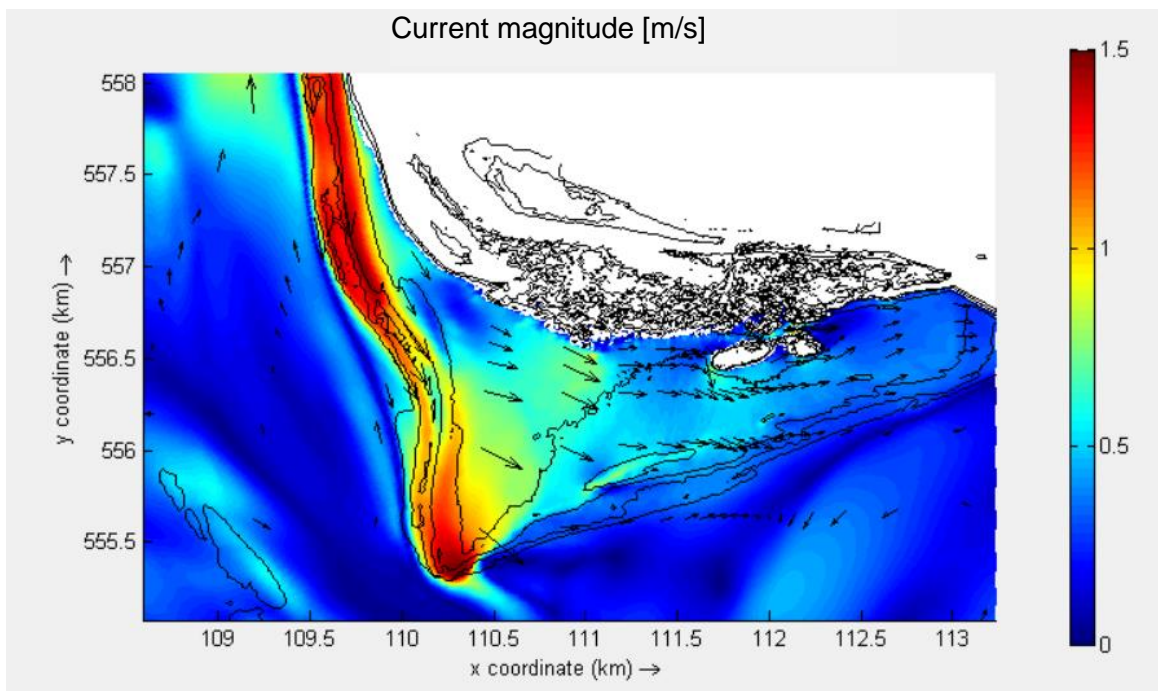


Figure 30 - Currents on the Hors at the end of the storm surge ( $t = 265$ , 7.3hr into storm surge)

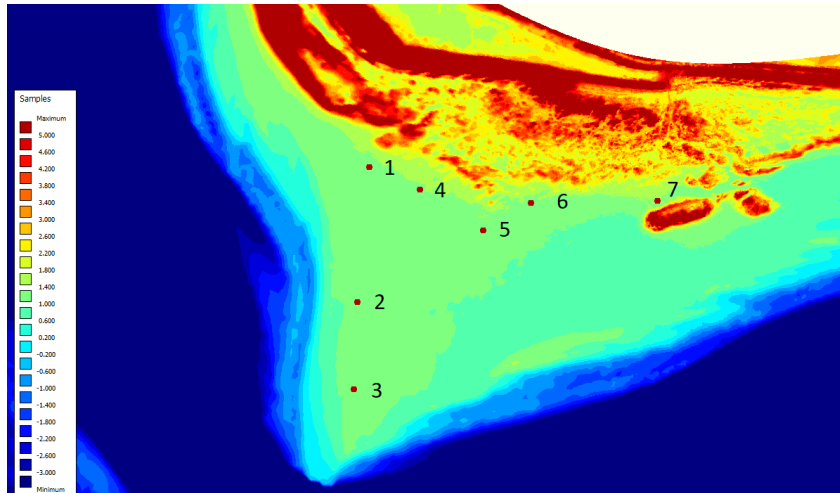


Figure 31 - Seven points on the Hors which will be further examined

To get more information about the progression of water level, wave height and flow over the Hors over time, 7 points on the Hors are selected which show the results of the hydrodynamic processes of the simulation over time (Figure 31).

Figure 32 shows increase of the water level on the west part of the Hors. Point 1, 2 and 4 are comparable, with a mutual difference of max 0.1m. The other points show decreased water levels, point 3 reaches a water level about 0.10m lower than on point 2. The points further east (point 5 and 6) show an even further decreased water level. The most eastern point (7), located in between dunes, shows however an increased water level relative to point 5 and 6 of max. 0.05m.

Figure 33 shows the wave height over time. Point 6 and 7 (located on eastside on the Hors) show the lowest overall wave heights with a maximum height of 0.05m. Point 1, 4 and 5 (located on the west/ centre of the Hors) show increasing wave heights with a varying maximum height of 0.2 – 0.25m. Points 2 and 3, located on the west side of the Hors show the highest wave heights with 0.3m.

In Figure 34 and Figure 35, the flow characteristics on the seven points are shown. The overall trend is similar as seen in Figure 28 t/m Figure 30. The highest flow velocity is seen in point 3, where the current flows towards the south (330°), point 1, 2, 4 and 5 flow towards the south-east (between 280° - 300°) where the flow velocity varies between 0.6 and 1.4 m/s. Point 6 and 7 show a flow velocity beneath 0.4m/s towards the north-east (240° - 270°). The flow direction across the Hors does not change throughout the whole storm surge, even when the water level gradient becomes negative.

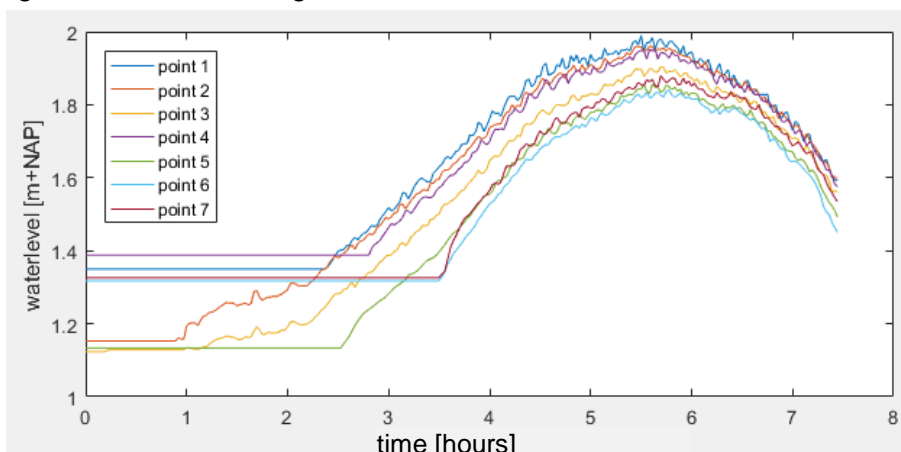


Figure 32 – water level over time on the seven points shown in Figure 31

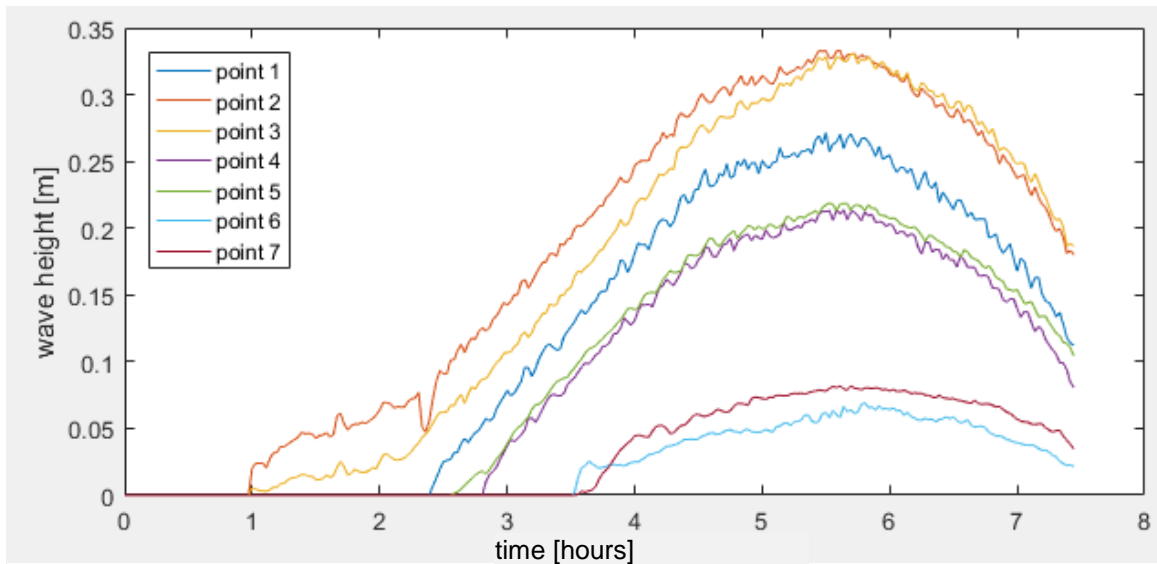


Figure 33 – significant wave height over time on the seven points shown in Figure 33

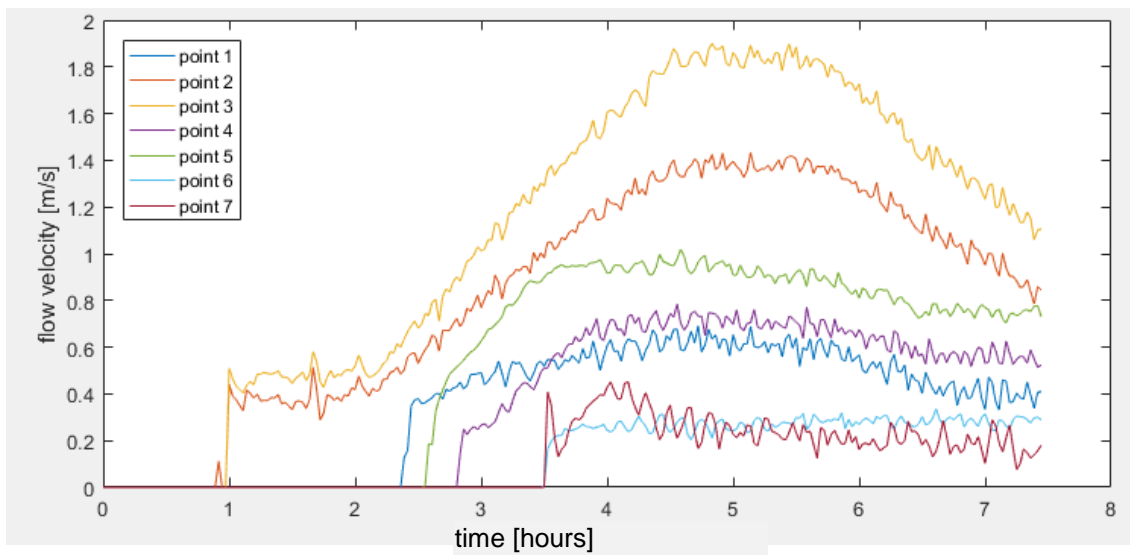


Figure 34 - flow velocity over time on the seven points shown in Figure 33

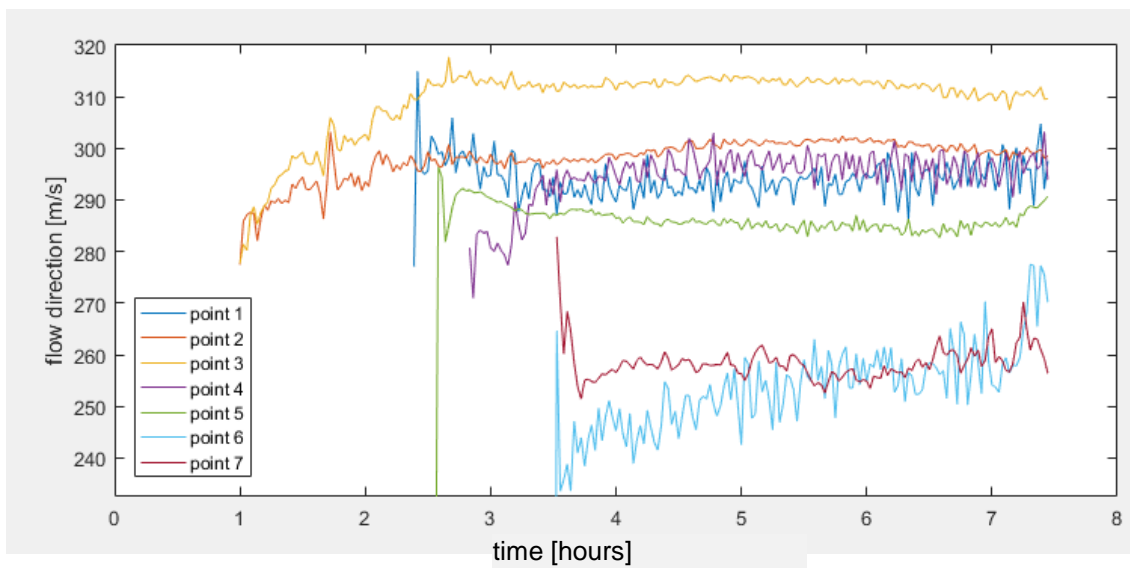


Figure 35 – current direction over time on the seven points shown in Figure 31

Figure 36 shows the simulated erosion/sedimentation after the storm surge. On the north-west coastline of the Hors, both the sandbar in front of the coast and the coastline itself are eroded up to half a meter. Beneath the two sand bars, accretion of maximal 0.5 is visible. Further south less erosion (up to 0.3m), and even less accretion (up to 0.1m) takes place. South-east of the tip of the Hors, the bed level increases maximal 1.5m. On top of the Hors, an overall sedimentation of 0.1m is visible.

The A-A' cross-section (Figure 37) show that the largest change in bed level happens during the first hour of the storm surge (the third hour of the simulation with spin-up of two hours). Throughout the storm, the erosion rate decreases per hour.

The second cross-section B-B' (Figure 38) shows a cross-section where mostly erosion occurs. The erosion of the first bar (between 0 – 100 meters), seems to be constant but the erosion rate is too low to be sure. The bed level change (erosion) of the coastline (100-200 meters) is heaviest during the peak of the storm surge (between 4<sup>th</sup> and 6<sup>th</sup> hour), where the bed level decreases max. 0.07m per hour.

In the first part of the third cross-section (C-C') (Figure 39), the erosion rate is constant throughout the storm surge (around 50 meters). Further into the cross-section (between 200-300 meters), more particles settle during the heaviest part (the 5<sup>th</sup> and 6<sup>th</sup> hour) of the storm surge, where the bed level increased over 0.5m, which is half of the total bed level increase.

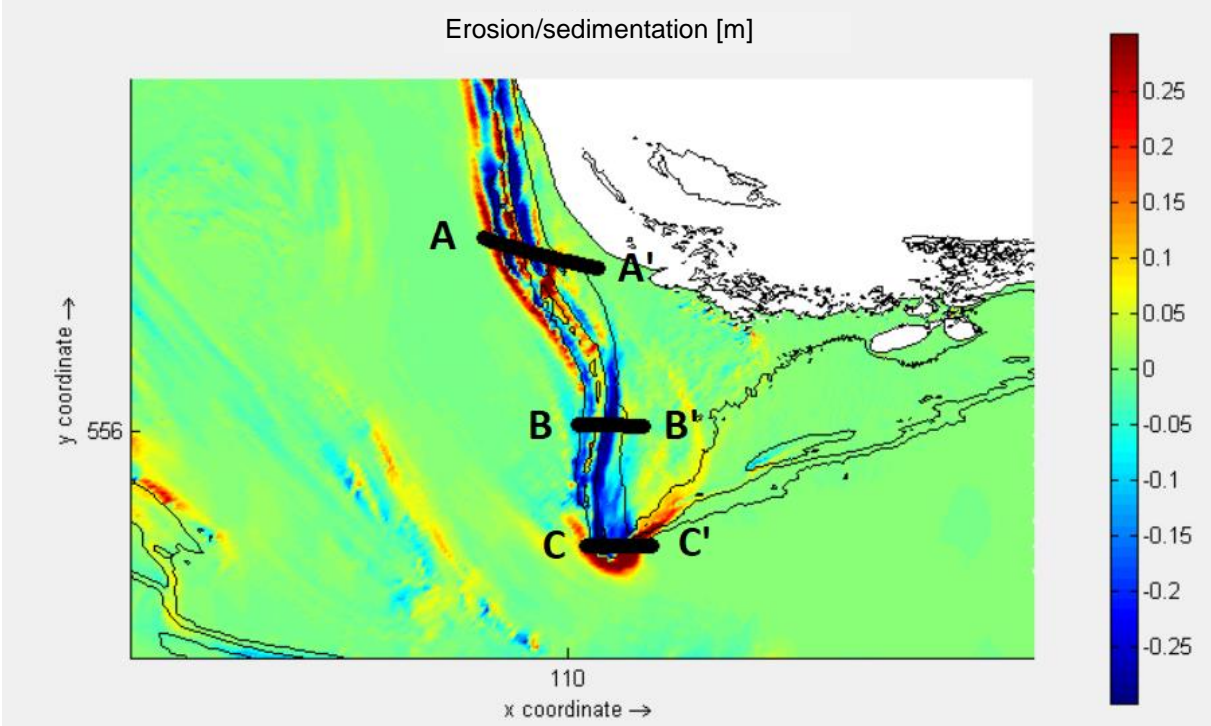


Figure 36 – Overview of the erosion profiles after the simulated storm surge of 11-1-2017, with cross-sections A-A', B-B' and C-C'(black lines)

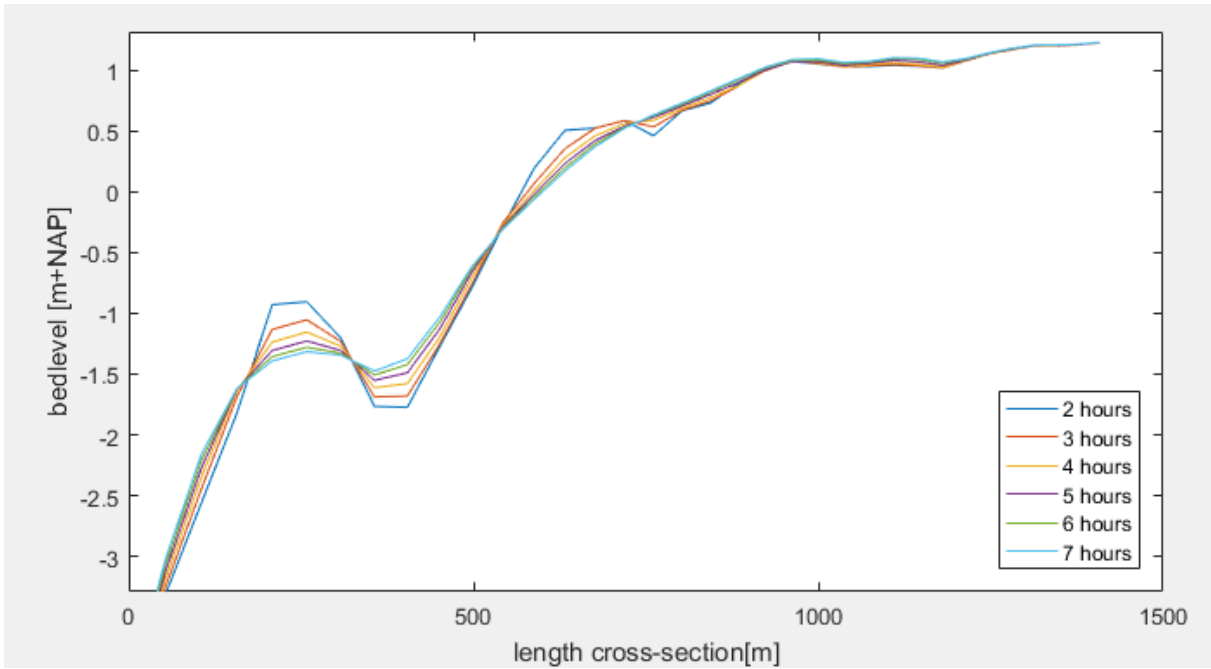


Figure 37 – bed level of cross-section A-A' ( $A = 0$ ,  $A' = 730\text{m}$ ) during the storm surge of 11-1-2017

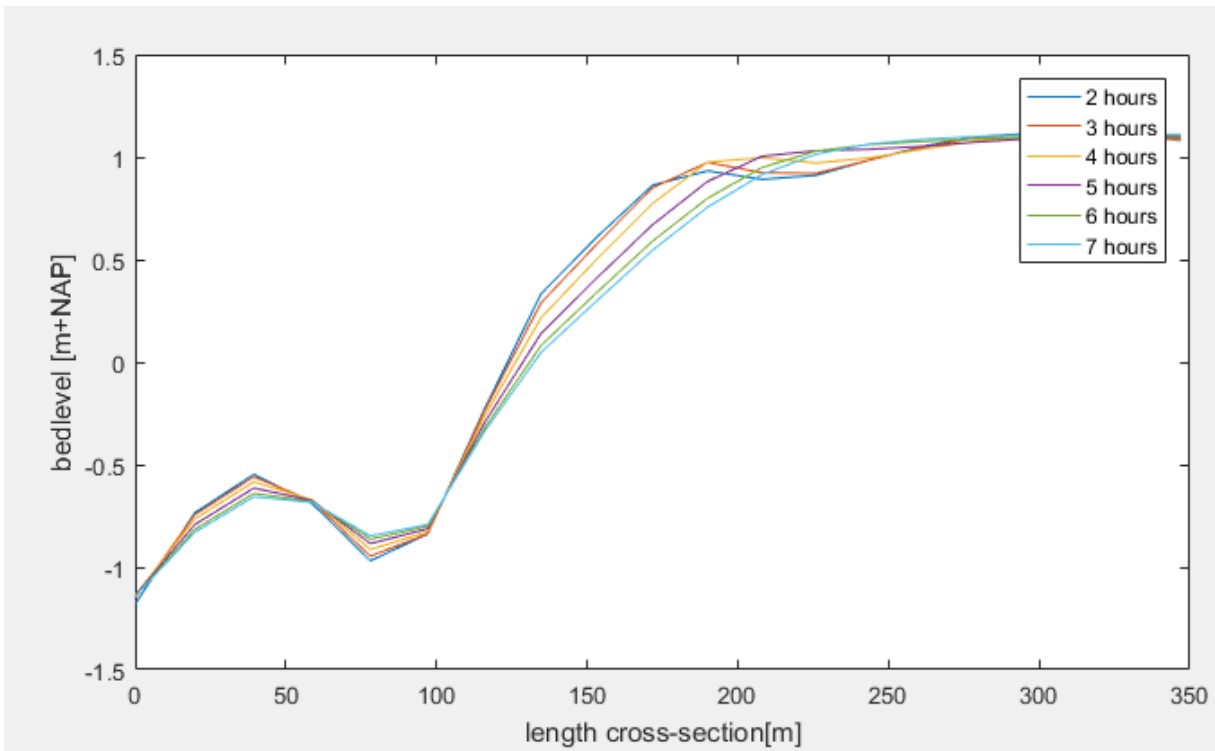


Figure 38 – bed level of cross-section B-B' ( $B = 0$ ,  $B'' = 350\text{m}$ ) during the storm surge of 11-1-2017

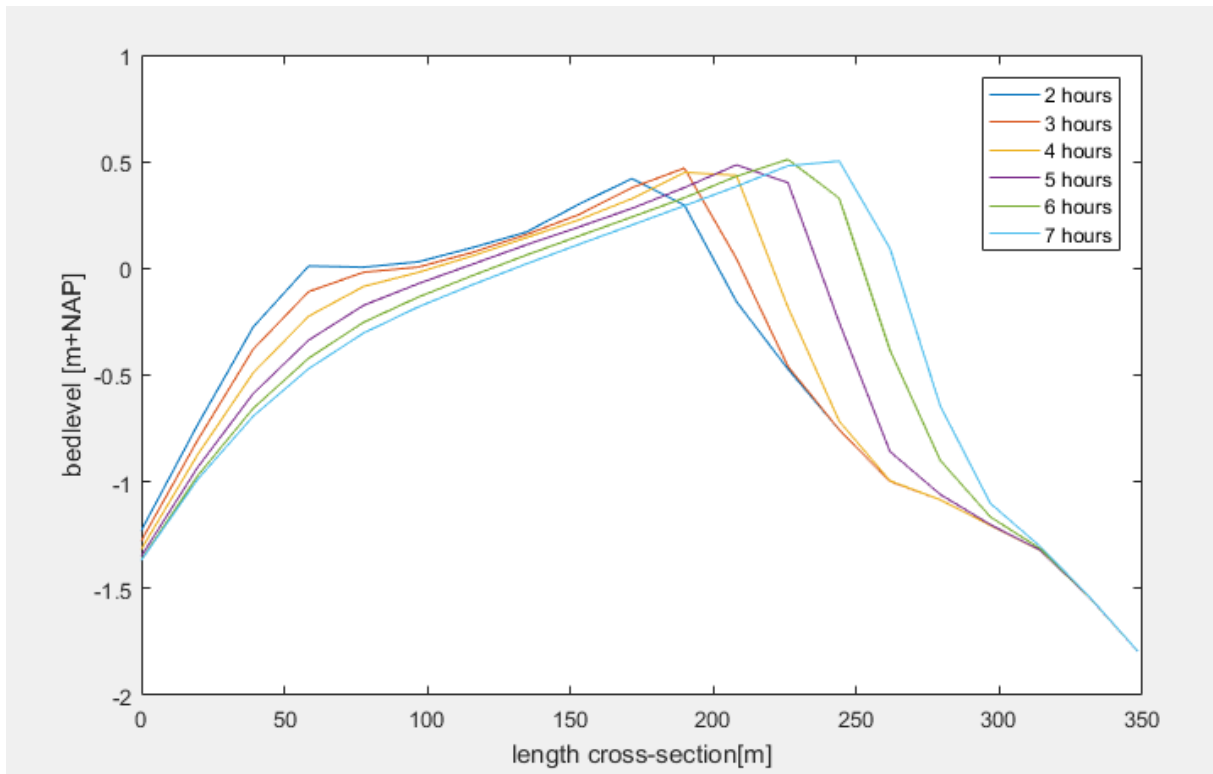


Figure 39 – bed level of cross-section C-C' (C = 0, C' = 350m) during storm surge of 11-1-2017

The erosion/accretion of the dunes on the north-west side of the sand flat are shown in Figure 42. The dunes, with tops around 2m+NAP are eroded (max. erosion of 0.3m). On the south-east side of the tops, sedimentation of max. 0.2m is visible.

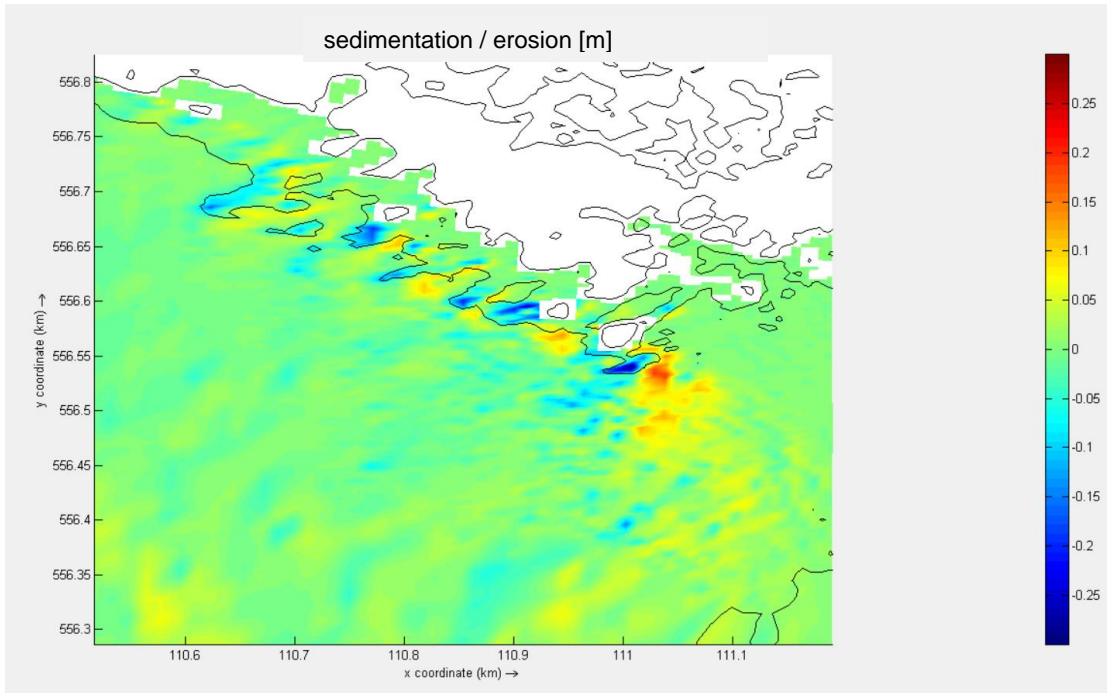


Figure 42 – Left: Close up of the erosion/ sedimentation on the North/west side of the Hors (blue is erosion of 0.3m, red = sedimentation of 0.3m). Black contour lines show bathymetry of 1.5m+NAP and 2m+NAP

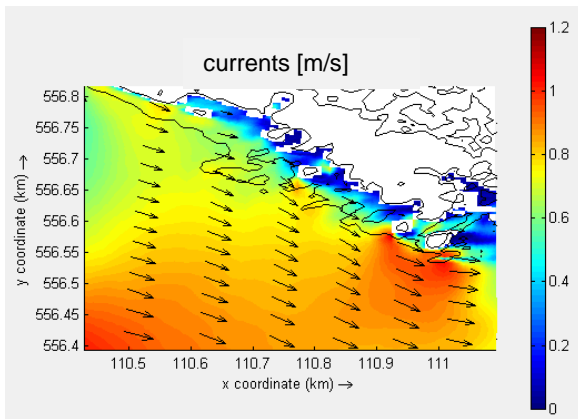


Figure 41A – Current magnitude (+direction shown by currents) on the Hors during the peak water level (5:30 hours into storm surge)

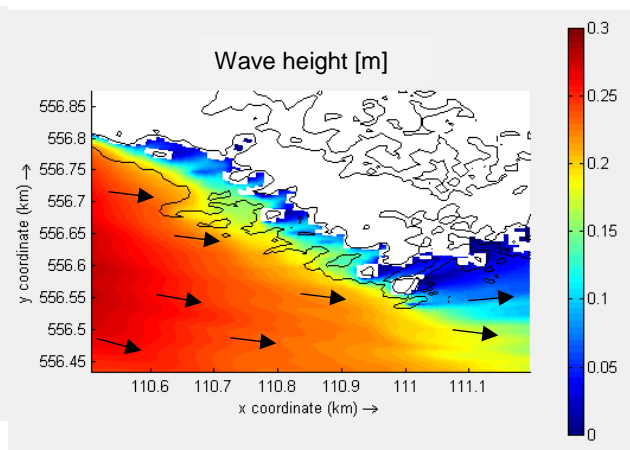


Figure 41B - Wave height (+direction shown by currents) on the Hors during the peak water level (5:30 into storm surge)

### North eastern dunes

On the North-east side of the sandflat, a large dune with a height of 4m+NAP is located (see Figure 43). This dune is vegetated, from which it is assumed that the dune is stable. On the North side of this dune, a small valley occurs where a couple smaller dunes are located. The waves in this area are mostly dissipated (waveheight < 0.2m) (Figure 44). The flow velocity in the funnel shaped valley increases to 1.5m/s, which is 0.5m/s higher than the flow velocity south of the valley. In the valley, erosion (0.3m) and sedimentation (0.3m) is visible (Figure 45).

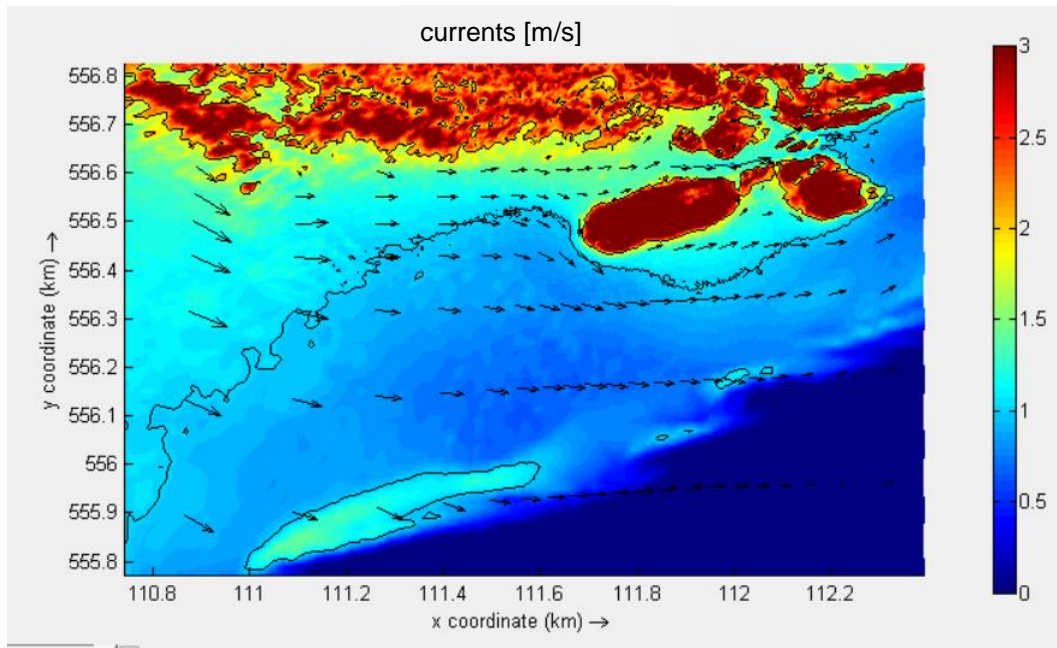


Figure 43 - Current vectors in the north-east side of the Hors during the peak of the storm surge (5.5hr into storm surge)

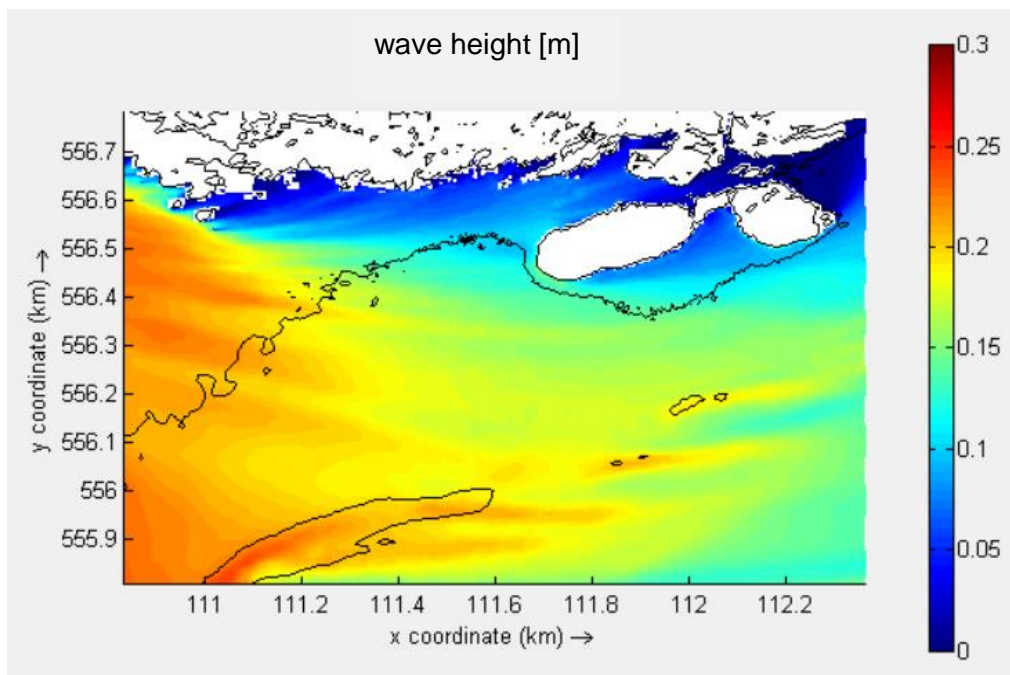


Figure 44 - Wave heights in the north-east side of the Hors during the peak of the storm surge (5.5hr into storm surge)

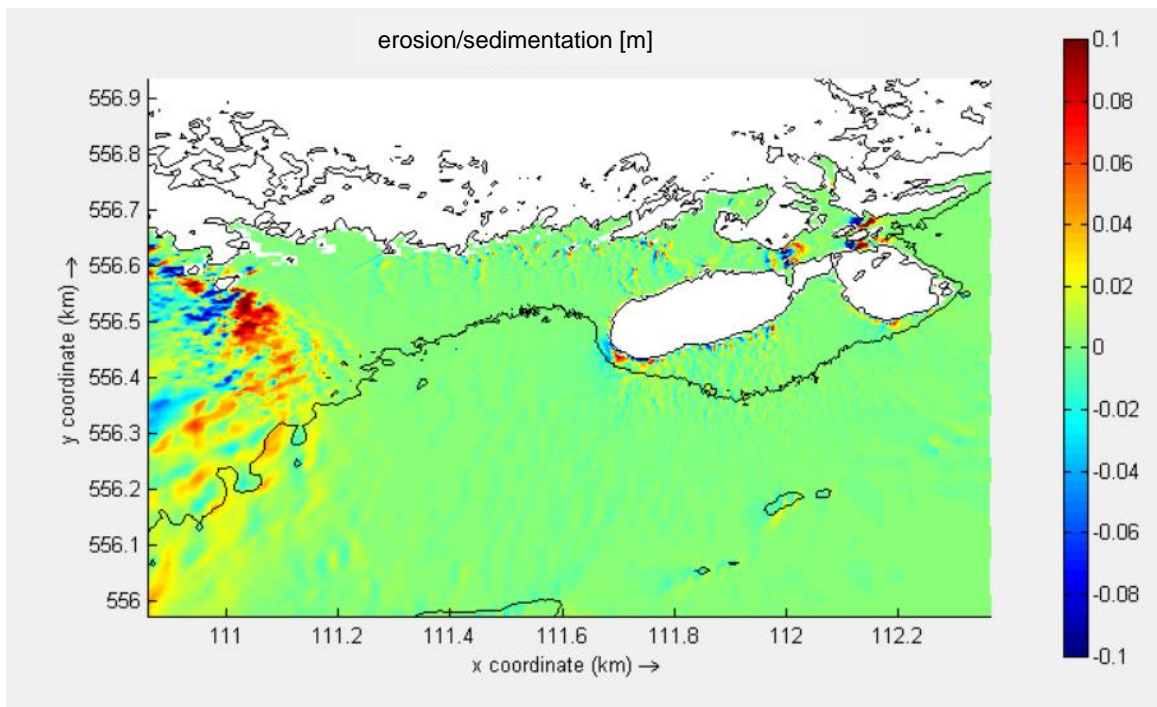


Figure 45 – Erosion/sedimentation in the north-east side of the Hors after the storm surge

## 6.2 Sensitivity analysis

### 6.2.1 Storm 1 – Overall water level increase of 0.3m

Storm 1 consists of the storm surge of 11-1-2017 with an overall increased water level of 0.3 meter.

Please note the different scales in Figure 46, where a difference of 0.3m is chosen to see the effect of the increased water levels on top of the Hors. Overall, the figures are comparable, which means that the increase of 0.3m generated at the boundaries of the model is seen back on the Hors. Only on the west side of the Hors, a lower water level increase (0.2/0.25m) is observed in Storm 1.

Figure 47 shows that the increased water level allows larger waves on top of the Hors, where in Storm 0 the wave height decreases to 0.2-0.3m, Storm one allows waves between 0.3-0.4m. The shape of the wave propagation and dissipation remains similar. The flow velocities in the tidal inlet have not changed after the increased water level (Figure 48).

Figure 49 shows an increase of erosion on the north-west part of the Hors. However, the erosion/accretion patterns on the outline of the Hors does not seem affected by the increased water level (Figure 50).

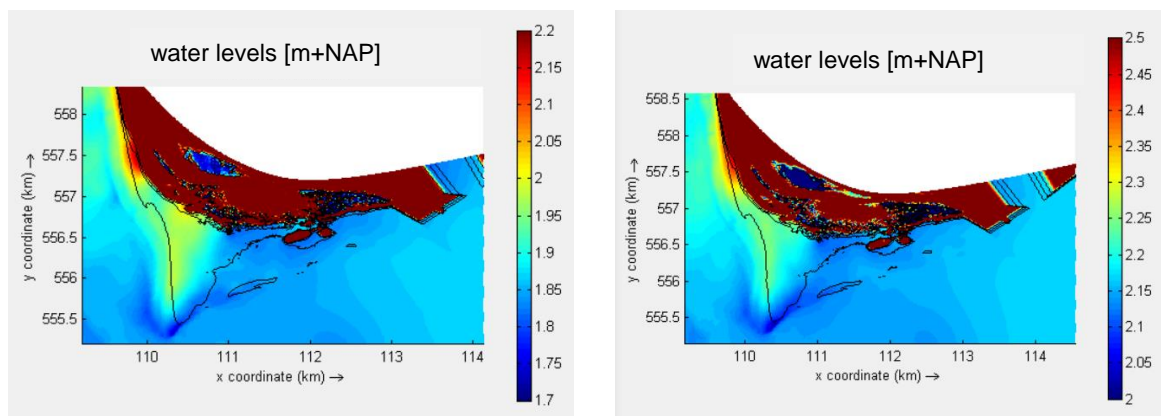


Figure 46 - Water levels during the peak of the storm surge (5:30hours into storm surge) with storm 0 (left) and storm 1 (right), note that the whole values in the left figure vary between 1.7 - 2.2m +NAP and the right figure 2 - 2.5m +NAP (0.3m higher)

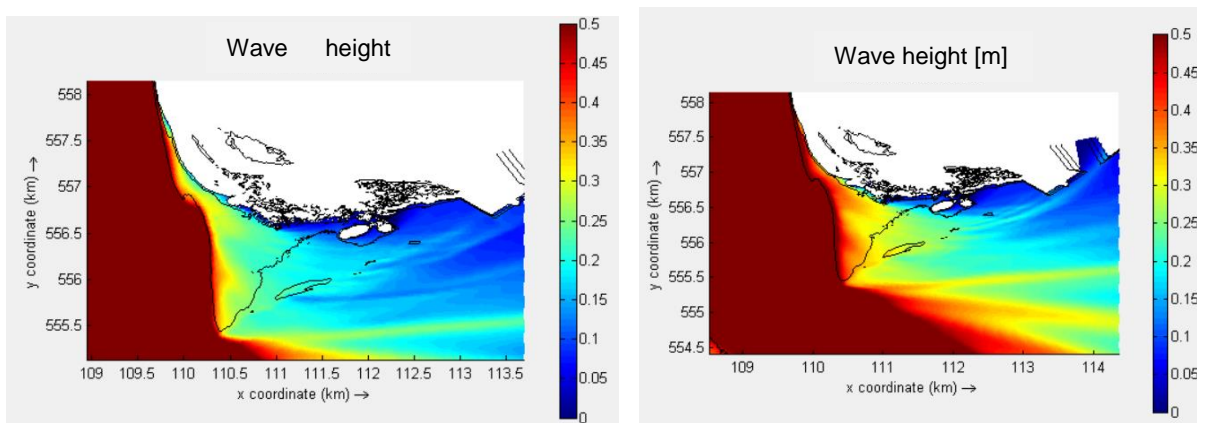


Figure 47 - Wave heights on the Hors (fixed max. shown value of 0.5m) on Storm 0 (left) and storm 1 (right)

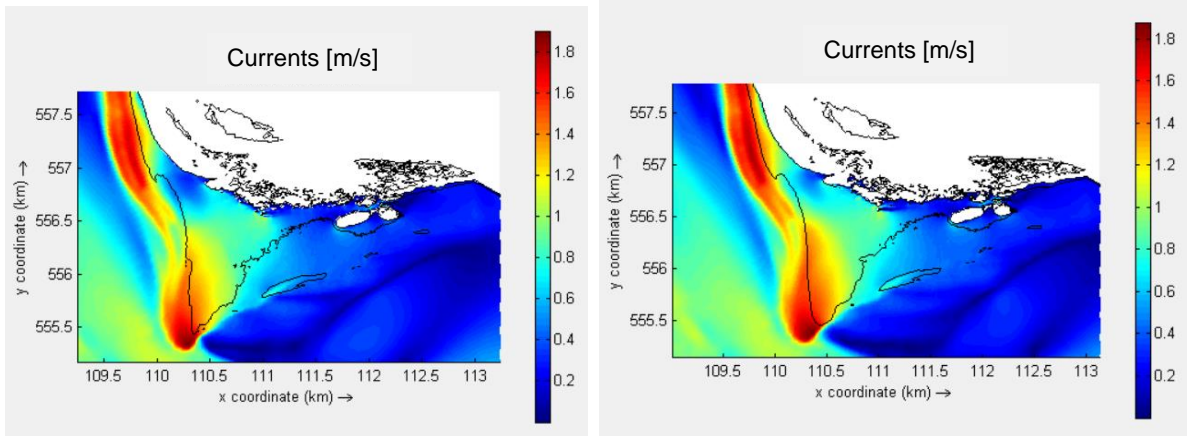


Figure 48 - Current magnitudes on the Hors on Storm 0 (left) and storm 1 (right) during the peak of the storm

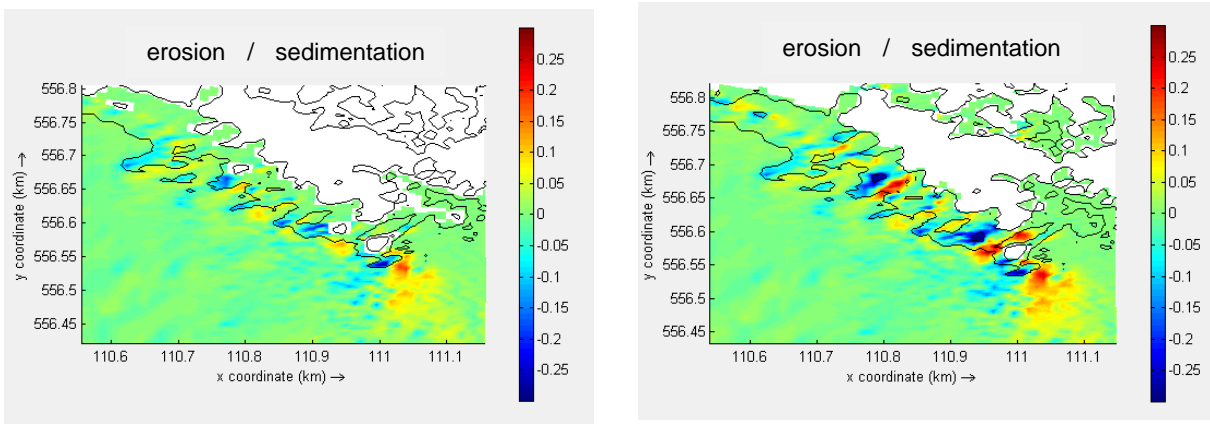


Figure 49 - Erosion profiles on the North Western dunes after Storm 0 (left) and storm 1 (right)

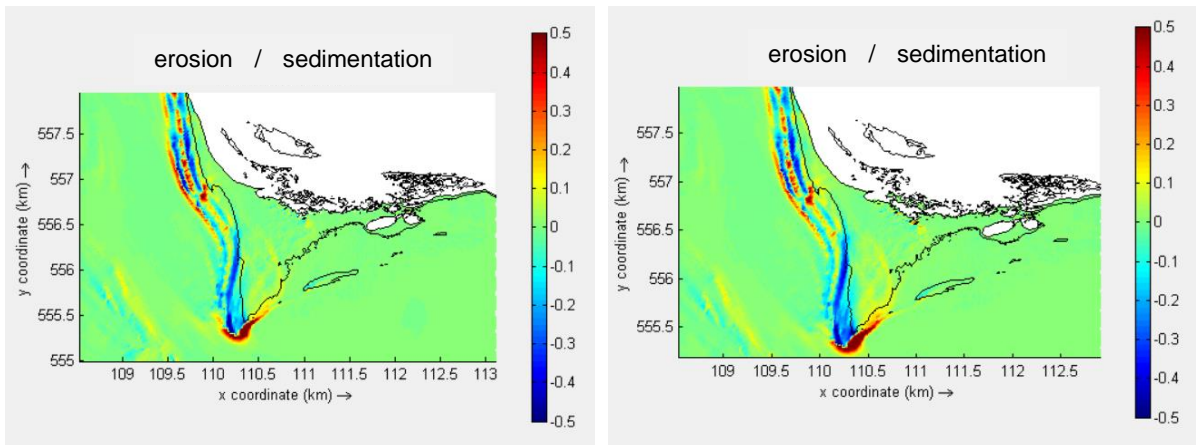


Figure 50 - Erosion profiles on the (outline of the) Hors after Storm 0 (left) and storm 1 (right)

### 6.2.2 Storm 2 – Increased water level gradient of 0.3m

Figure 51, Figure 52 and Figure 53 show the maximum water level (on 5.5hr into storm surge) of storm 0, 1 and 2. Although storm 2 has (on this point) a similar water level at the front (seaside) of the model, the water level in Marsdiep is only moderate influenced with an increase of water level of 0.1m, compared with storm 0. On the east side of the Hors, the water levels reach a level even 0.05m lower than measured in storm 0.

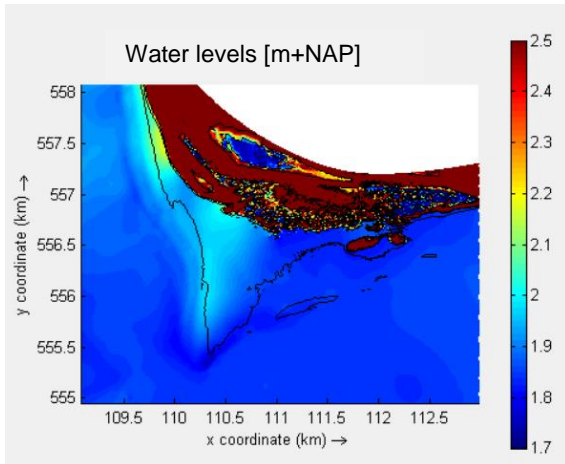


Figure 51 - Storm 0: Water level during the peak of the storm surge

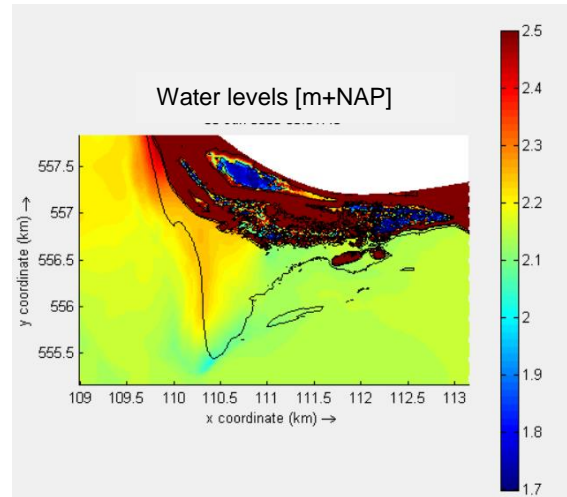


Figure 52 - Storm 1: Water level during the peak of the storm surge

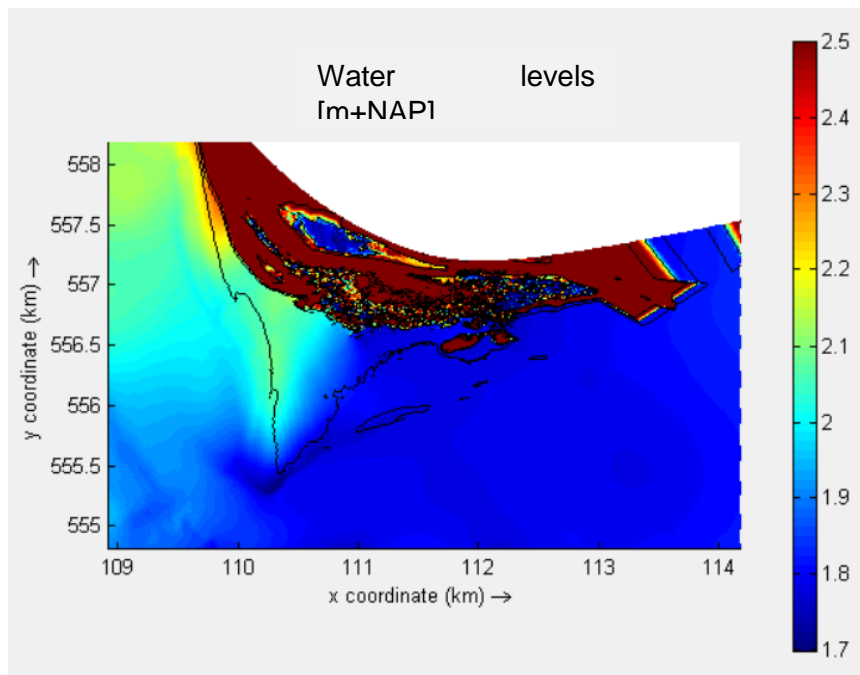


Figure 53 - Storm 2: Water level during the peak of the storm surge

In the previous section, it was shown that a larger water level did not result in larger currents in Marsdiep. Figure 54 shows that a storm surge with a doubled gradient result in a doubling of the current in Marsdiep. On the sandflat, the velocity only slightly increases with max. 0.2m/s.

Figure 55 shows the erosion of the outline of the Hors during storm 0, 1 and 2. The erosion values and - patterns of storm 0 and 1 are similar. However, the erosion patterns (especially in Marsdiep) have significantly increased. The accretion on top of the Hors however remains unchanged from the earlier simulations (storm 0 and storm 1).

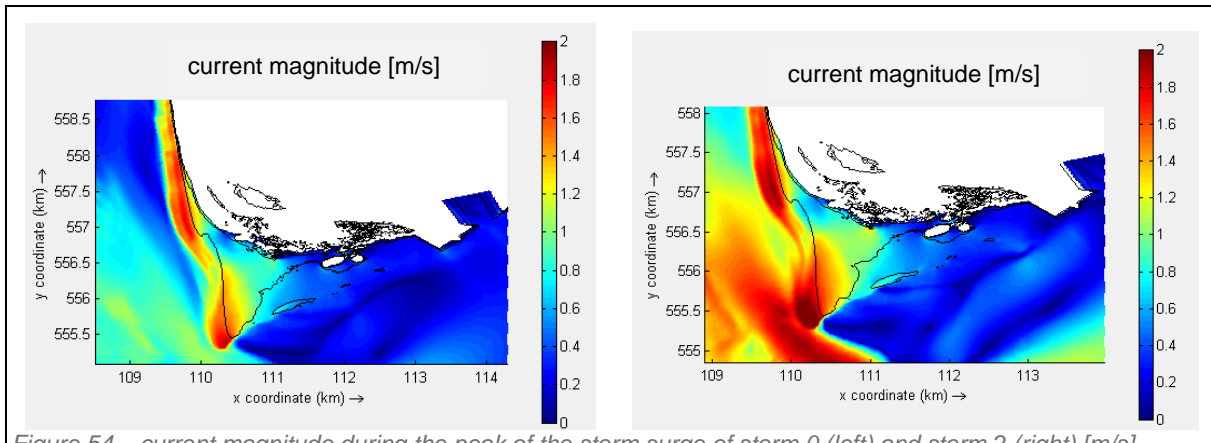


Figure 54 – current magnitude during the peak of the storm surge of storm 0 (left) and storm 2 (right) [m/s]

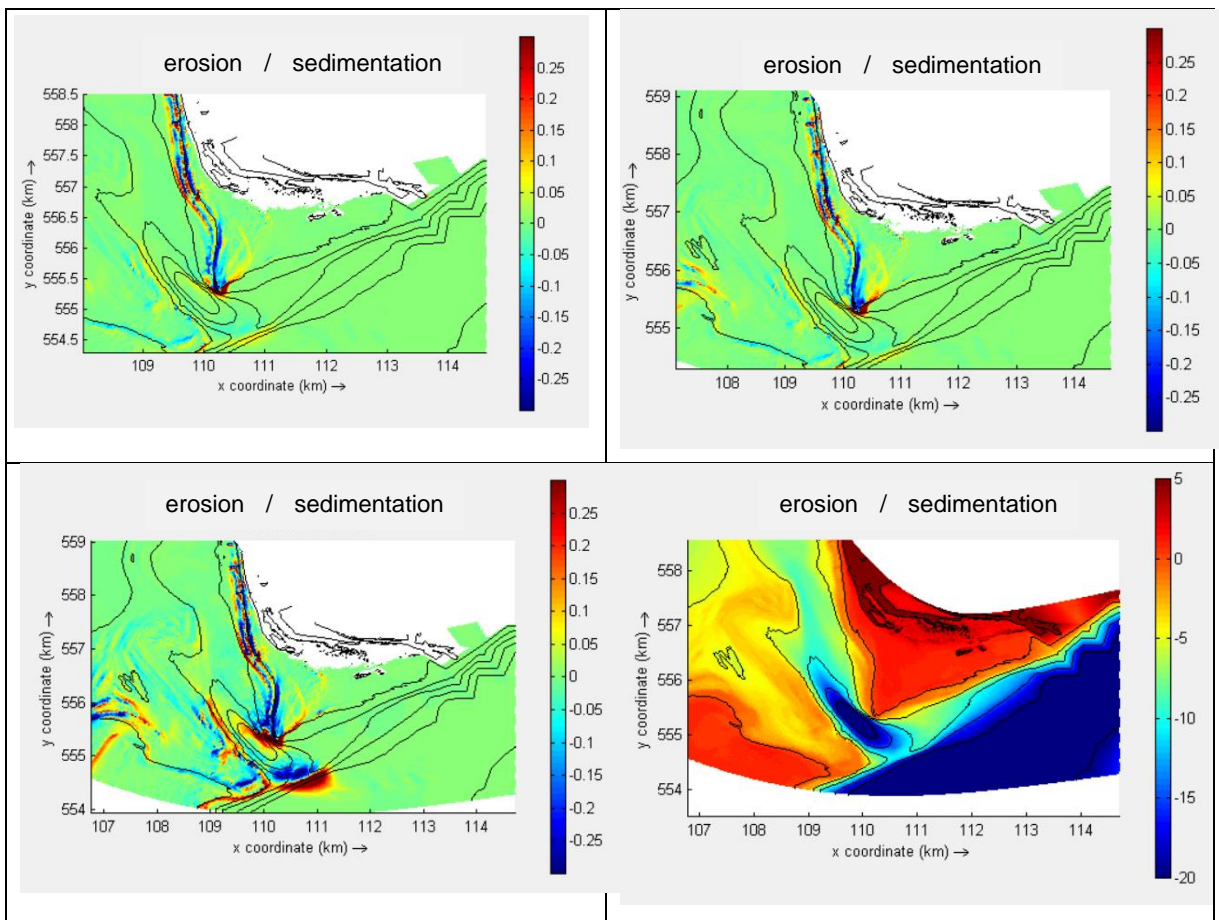


Figure 55 – erosion patterns on/near the Hors of storm 0 (upper left), storm 1 (upper right) and storm 2 (bottom left) and the bathymetry with contour lines as used in the other figures (bottom right)

### 6.2.3 Storm 3 & 4 – Adapted wind speed

The effects of the increased wind velocity of Storm 3 and the absence of wind in Storm 4 on the wave height are shown and compared with Storm 0 and Storm 1 (Figure 56), but no differences are observed. A more detailed look can be taken at individual points on top of the Hors. At the western part of the Hors (point 1 in Figure 58), an increased wind speed assures a higher wave height of max 0.01m and absence of wind decreases the wave height even less. Further towards the east side (point 5 in Figure 59), this difference disappears.

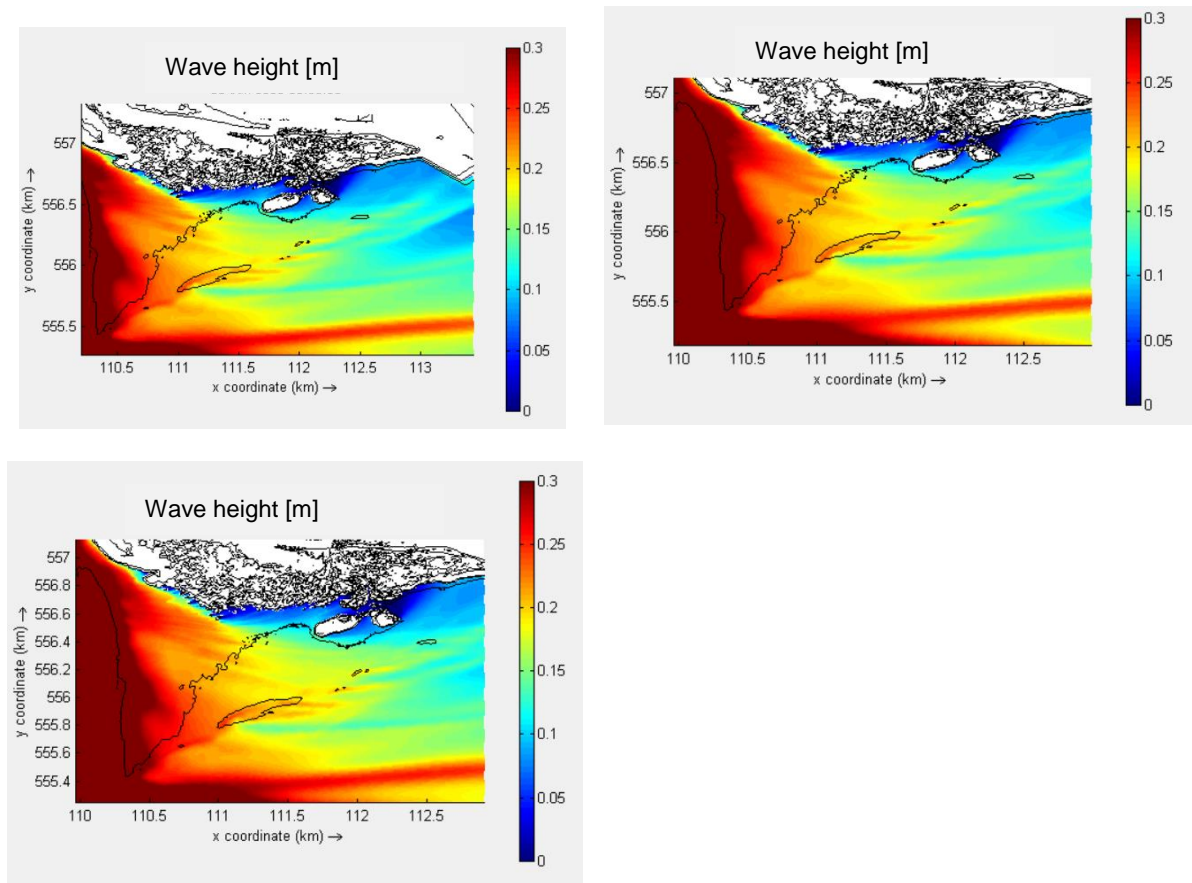


Figure 56 - Wave height during peak of the storm surge of Storm 0 (upper left), Storm 3 (upper right) and Storm 4 (bottom left)

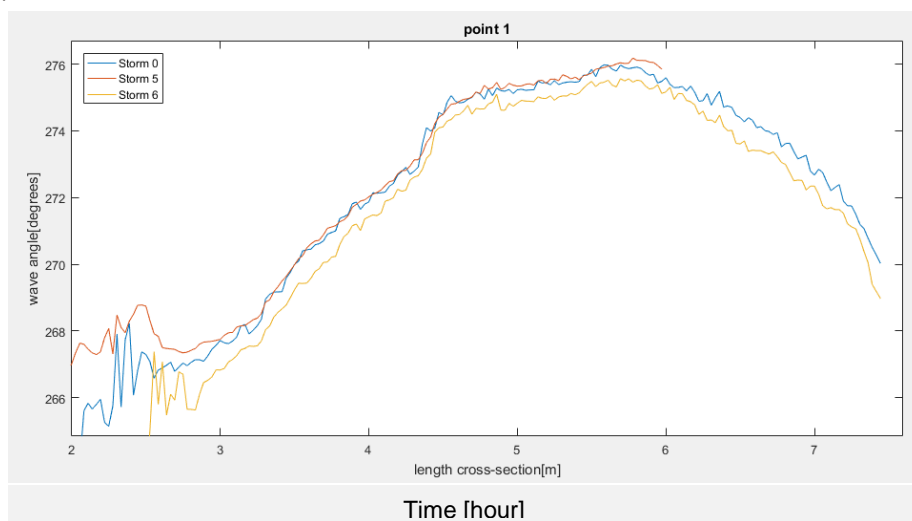


Figure 57 – wave angle on point 1 during storm surge 0, 3 and 4

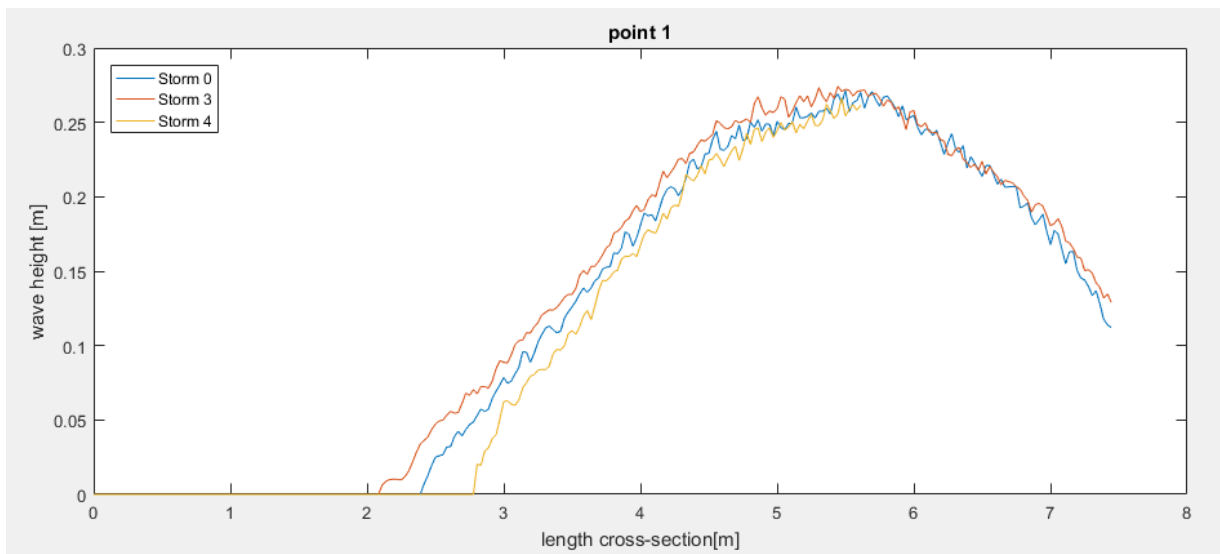


Figure 58 - Waveheight on point 1 during storm surge 0, 3 and 4

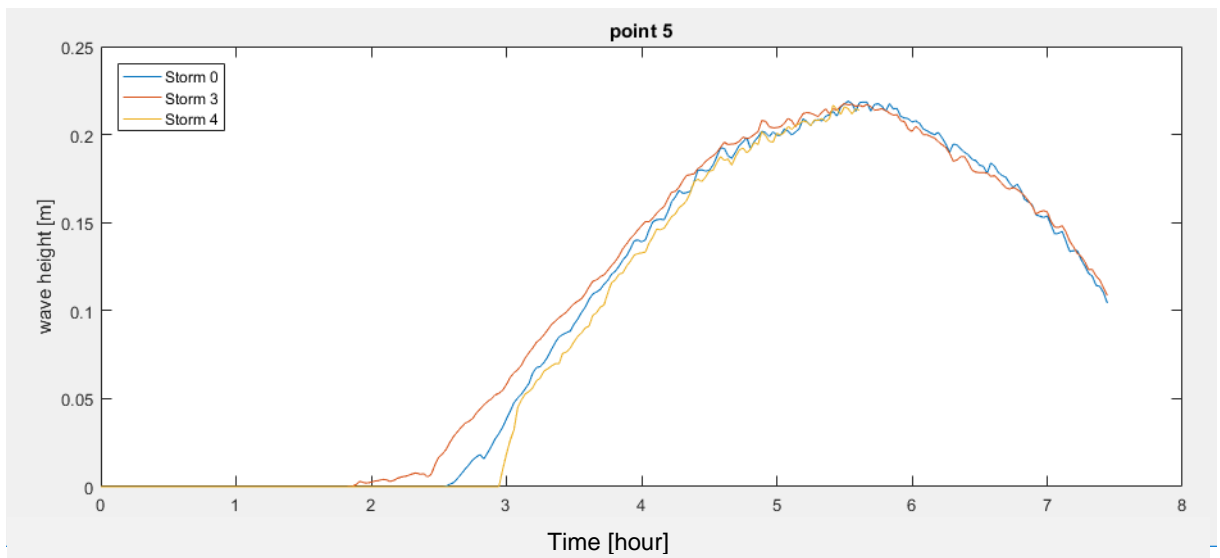
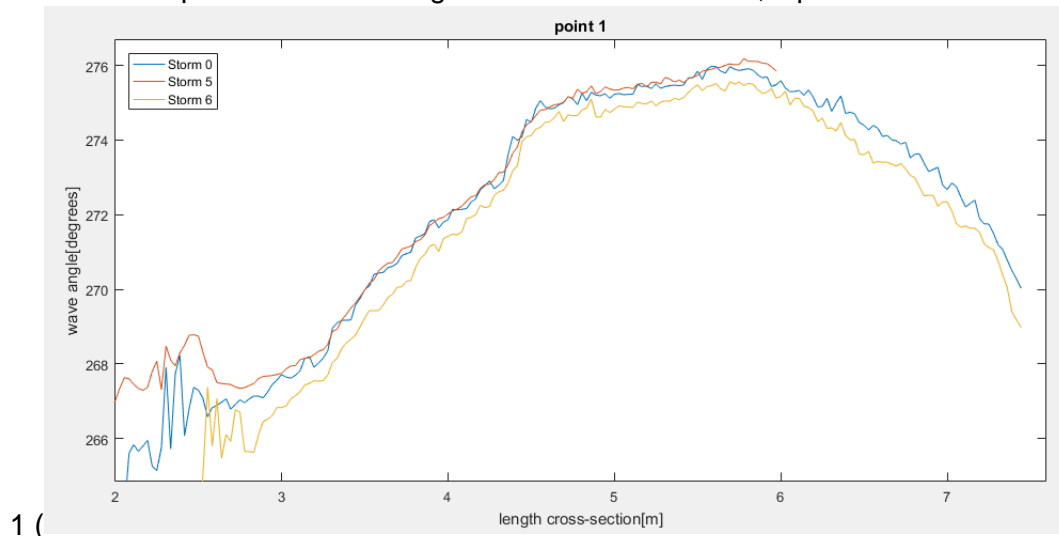


Figure 59 - Waveheight on point 5 during storm surge 0, 3 and 4

### 6.2.4 Storm 5 & 6 – Adapted wind direction

A change in wind direction results in a minimal effect in wave angle, as all sub-plots in Figure 60 show comparable results. To get a more detailed result, a plot is made from individual point



1 (

Figure 61). The results show that the wave direction of storm 6 (wind from north 340) decreases the wave angle with 1 degree compared with Storm 0. The change in wind direction from the west (storm 5) has no effect.

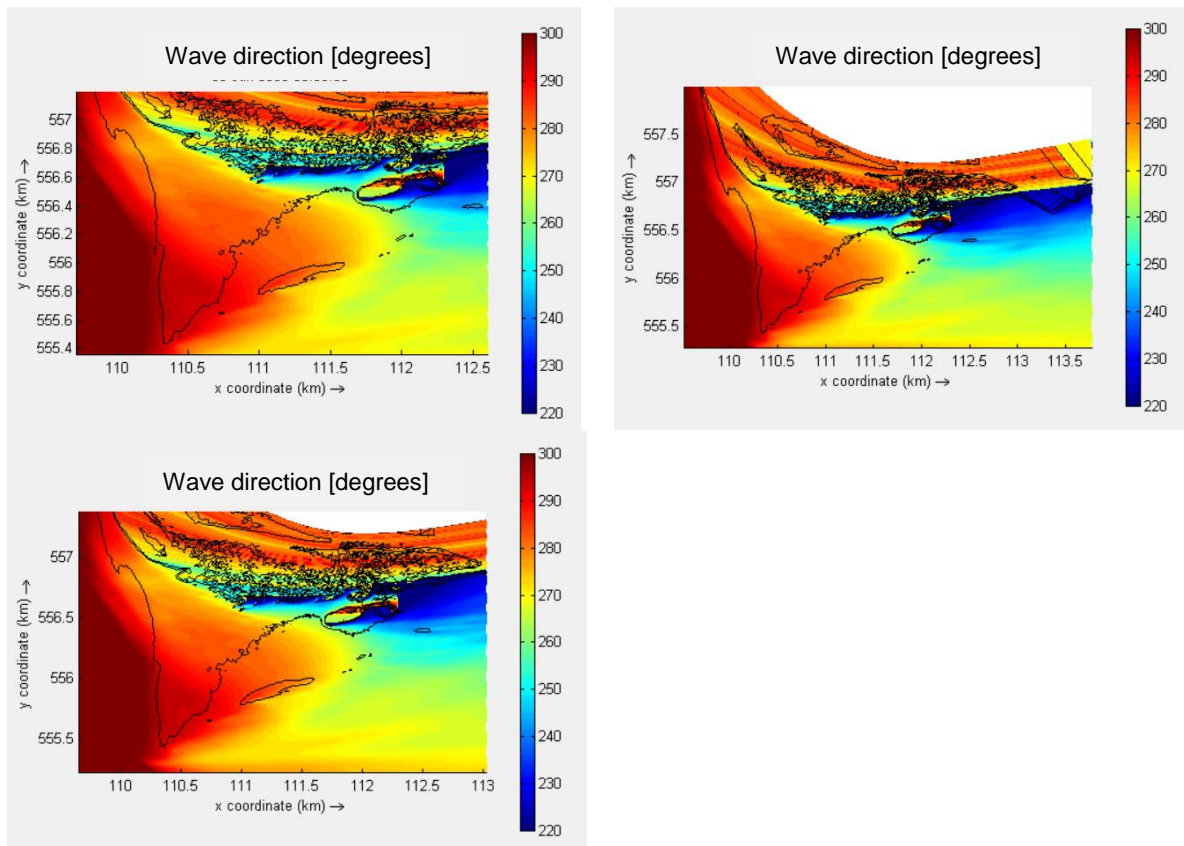


Figure 60 – Wave angles on the peak of the storm surges of Storm 0 (upper left), Storm 5 (upper right) and Storm 6 (bottom left)

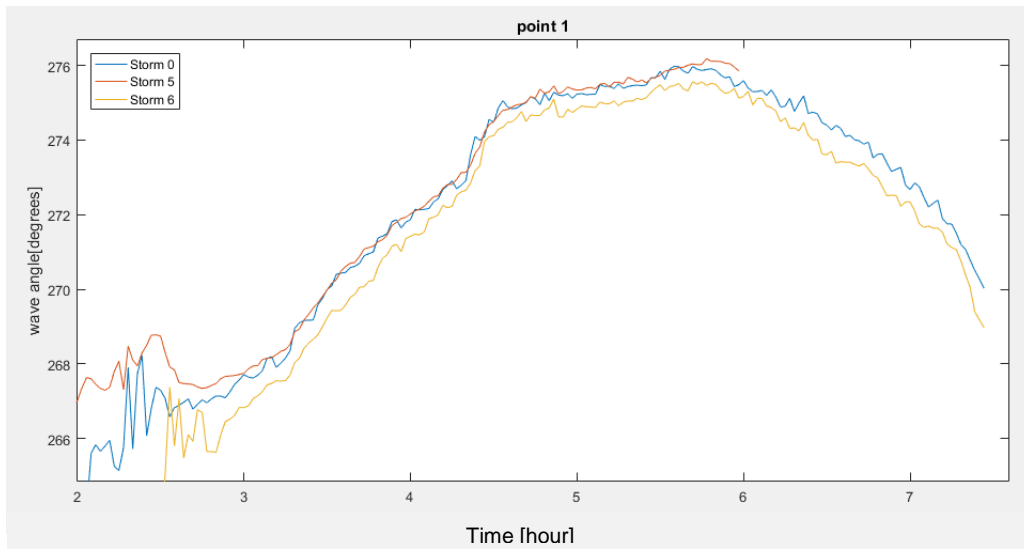


Figure 61 – wave angle on point 1 during storm 0, 5 and 6

## Chapter 7

### Discussion

This research focussed on both the hydrodynamic and morphological processes that take place on the Hors during a storm surge. This chapter analyses and discusses the found results to answer the set objective. This chapter is divided in three parts, in the first part, the hydrodynamic and morphologic processes of the simulated storm surge of 11-1-2017 are discussed. The second part focusses on the dominant processes, found in the sensitivity analysis. The third and final part discusses the applicability of the results for other tidal inlets.

#### 7.1 Hydrodynamics

In storm 0 it is seen that the wave height decreases from 4 meters in deep water, to 0.2m on top of the Hors. The incoming waves are breaking under an oblique angle towards the shoreline. The dissipated energy (due to the wave breaking) causes a reduction of the radiation stress.

The local reduction of the wave height causes a spatial gradient in the radiation stress, resulting in a water level increase (wave set-up) on the west side of the Hors and a strong southwards current west of the Hors. Similar results were found by Engelstad et al. (2017), who used XBeach to simulate a storm surge on a different tidal inlet in the Wadden Sea.

The water level increase on the west side of the Hors results in a water level gradient between the west- and east side, which causes a flow across the Hors (from west to east).

The flow in Marsdiep is, as expected, dominantly forced by the water level gradient between the front- and backside of the model (outer side inlet and inner side inlet). However, although currents on the Hors are influenced by the water level gradient, wave-induced water gradients are the dominant barotropic component for the currents onto the Hors. The hypothesis that storm surges with higher water level gradients have higher flow rates on top of the Hors were expected. However, that this process would continue even when the water level gradient becomes negative (in the final stage of the storm surge) were not included. Similar results are found by Engelstad et al. (2017) for Westgat (inlet between Terschelling and Ameland).

The flow on top of the Hors is also influenced by the water level. It is hypothesized that a higher water level has relatively lower effects from the bed friction, thus allowing the currents to go faster. The decrease in wave height depends on the water depth. For the model: a higher water level in the model results in higher waves on the Hors and therefore less wave dissipation. This concludes in a lower wave-set up and therefore in a lower water level gradient on top of the Hors, which results in lower currents across the Hors.

In this model, wind had no influence on the waves. An increase or absence of the wind made no significant differences in wave direction and magnitude on top of the Hors. Broken waves on top of the Hors remained a height of 0.2m. Due to the shallowness of the water (bottom friction), the waves are unable to grow (Bretschneider). The waves changed course on the Hors, so it can be stated that the effect of refraction has more influence than the wind speed, regardless of the wind direction.

It is possible that the wind in XBeach is underestimated. According to the XBeach manual, wind-driven currents and local wind set-up are included in the model. However, due to the limited water depth on top of the Hors (and therefore the limited wave height), it is questionable if the effect of the wind could become significant. The chosen maximum wind speed (24m/s =

9Bft) is believed to be high enough. It is believed that if this wind speed has no significant influence, higher (unrealistic) wind currents would have minimal effect as well.

At the start of the research, it was believed that the wind direction would affect the course of the wave which wasn't seen back in the simulation. It is possible that the `single_dir` function (which determines the wave direction every 3 seconds (instead of every 0.045 sec) might decrease the refraction effects of the wind to insignificant levels. As it has been shown during the validation phase, that implementation of the `single_dir` function decreases the refraction on the north-eastern side of the Hors.

It has to be noted that the results in this research are all based on one single storm. The storm characteristics are analysed and it is found that such a storm is common. However, during this research, only single storm parameters are changed in the sensitivity analysis. It is possible that a combination of different storm parameters results in a different hydrodynamic behaviour in the inlet system.

## 7.2 Morphodynamics

The hydrodynamic processes cause morphological processes. Because in different parts of the Hors, different hydrodynamic processes are dominant for the morphological changes, the Hors is separated in three parts. As can be seen in Figure 62.

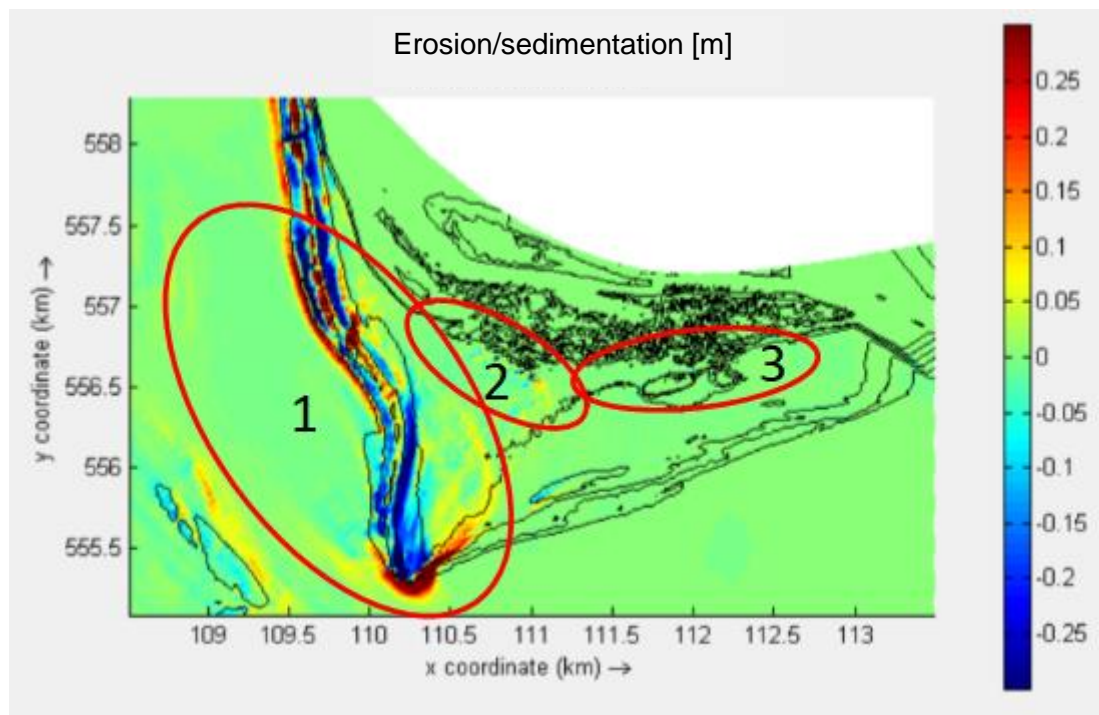


Figure 62 - Dune erosion after storm 0 with the Hors divided into three different parts

### 1- West coastline + sandflat

The breaking waves on the west side of the Hors (as explained in the last section (6.1.1)), cause turbulence on the bottom, lifting up sediment. The wave motion, in combination with the bathymetry, transports sand particles to deeper parts. Because the waves break under an oblique angle, longitudinal currents are developed and the particles are transported southwards. The shape of the Hors, in combination with the increased currents, causes the southern half of the West coastline to only erode. The sand particles are transported on top of the Hors, where the water depth increases, the flow velocity decreases and the particles sink to the bottom and sand particles are transported southwards, where the velocity (and sediment transport) even further increases. These findings confirm the hypothesis, set by

Wijnberg et al. (2017), that sand deposits on the wide sandflat above spring high tide level during a storm surge. Behind the southern tip of the sand flat, the area gets much wider and the flow velocity drops almost to 0 m/s. Here, all sediment, taken up from the west coastline of the Hors, settles.

### *2 – Dunes north-west side*

The erosion/sedimentation of the dunes on the north-west side of the Hors are dominated by the wave height, water level and current speed. The wave height in this area is still 0.3 meter (in Storm 0) and increase with higher water levels. Results show an increased erosion pattern with higher water levels, where the current magnitude remains similar from which the conclusion is drawn that the waves influence the wave height. However, the currents influence the sediment flow, the sediment taken from the top of the dunes is often transported normal to the wave direction. However, the simulation shows sedimentation in the same direction as the current on top of the Hors, which therefore influences the erosion/sedimentation patterns. The influence of these parameters on the impact of a storm on a barrier island were also found by Sallenger (2000) although he notices that the impact of the storm surge also depends on geometry, particularly in the vertical dimension.

### *3 – Dunes north-east side*

The dunes located on the north-east side of the Hors are located in a shadow zone, the waves are dissipated (wave height max. 0.05m) and the flow velocity is low (compared with the west side of the Hors), which makes the erosion on these dunes minimal. However, in the validation phase, it was found that the simulated erosion is lower than the measured sedimentation due to an underestimation of the maximum water level, and therefore the erosion patterns on the north-east side of the Hors. However, other dune measurements in the area which are believed to be dominantly eroded by the current magnitude show comparable results and simple calculations for the maximum wave height correspond with the simulated results. Other researches (Engelstad et al., 2017; Roelvink et al., 2009) found the influence of infragravity waves to be important in the morphodynamical processes in tidal inlets. The termination of parts of the properties of the infragravity waves (wave steering and wave stirring) could be the reason of the underestimation of maximum bed level of the morphological processes. Other reasons for the underestimation could be the coarseness of the grid which causes deviations in the bed level or errors in the dune measurements.

## Chapter 8

### Conclusion

This research focussed to learn the hydrodynamic behaviour on the dune systems near the inlet during storm surges. To reach this objective, three research questions are derived in section 1.2. This chapter answers these questions individually, which are repeated below for convenience. The answers to these questions are found by the use of the numerical model XBeach. In this model, the storm surge of 11-1-2017 is qualitatively validated the Marsdiep inlet area. The beach-dune system adjacent to this inlet is called 'The Hors' and is located on in the southern part of the Island of Texel.

*What is the hydrodynamic behaviour of a storm surge on a sandflat/dune system near an inlet?*

Results shown that the hydrodynamic behaviour of a storm surge on a the Hors can be divided in two aspects, waves and currents. The height of the waves depends on the water depth. In the inlet, the water depth is limited, causing the waves to break and decrease in height. Due to the shallowness of the entire inlet, the wave height in the open sea does not matter for the wave height which reaches the Hors. The dissipation of energy due to the wave breaking results in an increase of the water level (wave set-up) on top of the Hors. The waves which remain have a maximum height of 0.3m. The water level gradient on top of the Hors (created by the wave set-up) causes a constant current over the Hors. This process remains, even if the water flow through the inlet is reversed.

*How do different storm characteristics influence the hydrodynamic processes on the sand flat?*

Increase in the water level allows higher waves on/near the Hors. Simulations with varying wind conditions showed no difference in sedimentation/erosion profiles or values. An increased water level gradient between the front- and back boundary of the model (outer- and inner side of the inlet) is associated with higher currents across the Hors and results in more sedimentation on top of the Hors. Although it has to be noted that a water level gradient is used in the simulation which is 30% higher than the highest measured value in the year of 2009.

*Which parameter(s) is/are dominant in the process of dune erosion close to inlets during storm surges?*

The wave breaking on the west coastline of the Hors brings sediment into suspension. This sediment is transported partly onto the Hors and partly southwards, further into Molengat. The gradient on the Hors (created by the wave set-up) causes a constant current over the Hors which is able to transport the sediment up to the centre of the Hors, where the velocity drops and the sediment settles.

Waves are found to affect the dune erosion on the north-west side of the sand flat. Simulations with varying wind conditions showed no difference in sedimentation/erosion profiles or values as well. Increased flow velocity through the inlet, due to an increased water level gradient between the outer – and inner side of the inlet, resulted in more erosion/sedimentation in Marsdiep on top of the Hors although these differences were minor compared with the increased erosion/sedimentation in Marsdiep.

With this research, it is shown that the hydrodynamic behaviour on dune systems near tidal inlets indeed differ from straight coastlines. The information about the hydrodynamic and morphological processes on the different parts of the Hors sandflat can be used to create a stable and even growing dune-beach system near tidal inlets.

# References

- Anthony, E. J. (2013). Storms, shoreface morphodynamics, sand supply, and the accretion and erosion of coastal dune barriers in the southern North Sea. *Geomorphology*, 199, 8–21. <https://doi.org/10.1016/j.geomorph.2012.06.007>
- Battjes, J. A. (1974). *Computation of set-up, longshore currents, run-up and overtopping due to wind-generated waves*.
- Bolle, A., Mercelis, P., Roelvink, D., Haerens, P., & Trouw, K. (2011). Application and Validation of Xbeach for three different field sites. *Coastal Engineering Proceedings*, 1–13.
- Bowen, A. J., Inman, D. L., & Simmons, V. P. (1968). Wave “set-down” and set-Up. *Journal of Geophysical Research*, 73(8), 2569–2577.
- Britannica Online Encyclopedia. (2008). Hydrodynamica.
- Carrion Aretxabala, B. (2015). Morphological impact of the Sinterklaas storm at Het Zwin: Numerical modelling with XBeach, 75.
- Cleveringa, J. (2001). *Zand voor zuidwest Texel*.
- de Swart, H. E., & Zimmerman, J. T. F. (2009). Morphodynamics of tidal inlet systems. *Annual Review of Fluid Mechanics*, 41, 203–229. <https://doi.org/10.1146/annurev.fluid.010908.165159>
- Deltares. (2015). *Release notes Xbeach, version 1.22.4867, codename “Kingsday.”*
- Ecomare. (2017). De Hors. Retrieved August 5, 2017, from <https://www.ecomare.nl/verdiep/leesvoer/waddengebied/nederlandse-wadden/texel/de-hors/>
- Engelstad, A., Ruessink, B. G., Wesselman, D., Hoekstra, P., Oost, A., & van der Vegt, M. (2017). Observations of waves and currents during barrier island inundation. *Journal of Geophysical Research: Oceans*, (September). <https://doi.org/10.1002/esp.4235>
- ENW. (2007). Ontwerpbelastingen voor het rivierengebied.
- Herbers, T. H. C., Elgar, S., & Guza, R. T. (1995). Generation and propagation of infragravity waves. *Journal of Geophysical Research*, 100(C12), 24,863-24,872.
- Hoonhout, B. (2015). User manual - Xbeach pre- 1.22.4344 documentation. Retrieved July 1, 2017, from <http://xbeach.readthedocs.io/en/latest/>
- Houser, C., Hapke, C., & Hamilton, S. (2008). Controls on coastal dune morphology, shoreline erosion and barrier island response to extreme storms. *Geomorphology*, 100(3–4), 223–240. <https://doi.org/10.1016/j.geomorph.2007.12.007>
- Jansen, P. P. (ed). (1978). *Principles of River Engineering, the non-tidal alluvial river*. Delftse Uitgevers Maatschappij, ISBN 90-6562-146-6.
- Klein, J. (2015). The North Sea Storm Surge Atlas: Performance Assessment and Uncertainty Analysis, (February).
- KNMI. (2017). KNMI - Stormvloed. Retrieved January 5, 2017, from <https://www.knmi.nl/kennis-en-datacentrum/uitleg/stormvloed>
- Koninklijk Nederlands Meteorologisch Instituut. (2017). Uurgegevens van het weer in Nederland. Retrieved July 1, 2017, from <https://www.knmi.nl/nederland-nu/klimatologie/uurgegevens>

- Lipari, G., & Vledder, G. P. v. (2009). Viability study of prototype windstorm for the Wadden Sea surges. *Measurement*, (May 2009). <https://doi.org/10.1115/1.802915.ch1>
- Met Office. (2013). 1953 east coast flood - 60 years on. Retrieved from <http://www.metoffice.gov.uk/news/in-depth/1953-east-coast-flood>
- Pugh, D. T. (1996). Tides, surges and mean sea-level (reprinted with corrections). *Marine and Petroleum Geology*, 5(3), 301. [https://doi.org/10.1016/0264-8172\(88\)90013-X](https://doi.org/10.1016/0264-8172(88)90013-X)
- Ribberink, J. S. (2011). *River dynamics - II: Transport Processes and Morphology*.
- Rijkswaterstaat. (2017a). Stormvloedrapport 13 en 14 januari 2017 (SR94), 2017.
- Rijkswaterstaat. (2017b). Waterbase Historische waterkwantiteit- en waterkwaliteitsgegevens. Retrieved July 1, 2017, from <http://live.waterbase.nl/waterbase>
- Rijkswaterstaat. (2017c). Watergegevens Rijkswaterstaat. Retrieved from <http://watergegevens.rws.nl/BulkDownload/>
- Roelvink, D., Reniers, A., van Dongeren, A., van Thiel de Vries, J., McCall, R., & Lescinski, J. (2009). Modelling storm impacts on beaches, dunes and barrier islands. *Coastal Engineering*, 56(11–12), 1133–1152. <https://doi.org/10.1016/j.coastaleng.2009.08.006>
- Sallenger, A. H. (2000). Storm Impact Scale for Barrier Islands. *Journal of Coastal Research*. <https://doi.org/10.2307/4300099>
- Sassi, M. G., Gerkema, T., Duran-matute, M., & Nauw, J. J. (2016). Residual water transport in the Marsdiep tidal inlet inferred from observations and a numerical model, 21–42.
- Steetzel, H. J. (1990). Cross-Shore Transport During Storm Surges. *Coastal Engineering Proceedings*, 1(22), 1922–1934. <https://doi.org/10.9753/icce.v22>
- Steijn, R. C., van Banning, G. K. F. M., & Roelvink, J. R. (1998). *Gevoeligheidsberekeningen Eijerland en ZW-Texel Fase 2: ZW-Texel*.
- The Open University. (1999a). Chapter 1 - Waves. In *Waves, Tides and Shallow-Water Processes* (pp. 11–49). <https://doi.org/http://dx.doi.org/10.1016/B978-008036372-1/50002-7>
- The Open University. (1999b). Chapter 5 - Beaches. In *Waves, tides and shallow water processes* (pp. 125–148).
- van de Kreeke, J. (1990). Can multiple tidal inlets be stable? *Estuarine, Coastal and Shelf Science*, 30(3), 261–273. [https://doi.org/10.1016/0272-7714\(90\)90051-R](https://doi.org/10.1016/0272-7714(90)90051-R)
- Van Rooijen, A., Van Thiel de Vries, J. S. M., McCall, R. T., Van Dongeren, A. R., Roelvink, J. A., & Reniers, A. J. H. M. (2014). Modeling of wave attenuation by vegetation with XBeach. In *36th IAHR World Congress* (pp. 1–7).
- Vellinga, P. (1986). Beach and dune erosion during storm surges. *Coastal Engineering*, 6(4), 361–387. [https://doi.org/10.1016/0378-3839\(82\)90007-2](https://doi.org/10.1016/0378-3839(82)90007-2)
- Weisse, R., von Storch, H., Niemeyer, H. D., & Knaack, H. (2012). Changing North Sea storm surge climate: An increasing hazard? *Ocean and Coastal Management*, 68, 58–68. <https://doi.org/10.1016/j.ocecoaman.2011.09.005>
- Wijnberg, K., van der Spek, A., Galiforni Silva, F., Elias, E., van der Wegen, M., & Slinger, J. (2017). Connecting subtidal and subaerial sand transport pathways in the Texel inlet system. *Coastal Dynamics*.



## Appendix I – Validation report

# Validation report

Validation of the XBeach model used during the masterthesis of Stan van den Broek

This report is part of the research: ‘The effects of storm surges on dune systems near inlets’. This research the final part of the master Civil Engineering and Management of Stan van den Broek. The report analyses the XBeach model as used during the research and discusses its validity in order to support the results which are generated within this research.

## Contents

|  |    |
|--|----|
| Chapter 1 - Introduction.....                    | 3  |
| Chapter 2 – XBeach (settings + input data) ..... | 4  |
| 2.1 Input data.....                              | 4  |
| 2.1.1 Basic model settings.....                  | 4  |
| 2.1.2 Storm settings (optional settings).....    | 6  |
| 2.2. Parameter settings / processes.....         | 8  |
| Chapter 3 – Reference data .....                 | 11 |
| 3.1 TESO current data .....                      | 11 |
| 3.2 Dune (erosion) measurements.....             | 13 |
| 3.2.1 Western dune field.....                    | 15 |
| 3.2.2 The middle dunes .....                     | 17 |
| 3.2.3 The eastern dunes.....                     | 18 |
| Chapter 4 – Results.....                         | 20 |
| 4.1 Main results .....                           | 21 |
| 4.2 TESO current data .....                      | 22 |
| 4.3 Dune erosion .....                           | 26 |
| 4.2.1 Overall erosion patterns.....              | 26 |
| 4.2.2 Western dune field.....                    | 28 |
| 4.2.3 The middle dunes .....                     | 27 |
| 4.2.4 The eastern dunes.....                     | 28 |
| Chapter 5 – Discussion .....                     | 29 |
| Chapter 6 – Conclusion .....                     | 30 |
| Literature.....                                  | 31 |
| Appendix 1 – Xblog .....                         | 32 |

## Chapter 1 - Introduction

To gather information about the limitations, deviations, and reliability of a numerical model, results from the model are compared with actual measurements.

For the validation of the model as it is used in the , two datasets of measured data are available which to validate the storm surge of 11-1-2017: current characteristics (speed + direction) in Marsdiep and measured dune erosion of three dunes on the Hors itself during the storm surge of January 2017. Besides this data, water levels near the boundaries of the model are compared with the imposed water levels to check the similarity.

In Chapter 2, XBeach is introduced and the used model settings are explained. Chapter 3 focusses on the hydrodynamic validation with the dataset of TESO. In Chapter 4, the measured erosion patterns are compared with the simulated patterns. In Chapter 5, all results are discussed and the validity of the model will be explained.

## Chapter 2 – XBeach (settings + input data)

XBeach is an extended model which is able to model extreme beach behaviour like hurricane impacts and storm surges. The model includes wave breaking, surf and swash zone processes, dune erosion, overwashing and breaching (Roelvink et al., 2009).

The model is used in earlier researches on the Dutch North sea coast (Nederhoff, Elias, & Vermaas, 2016) (Carrion Aretxabala, 2015). Both reports state that results from the XBeach model corresponds well with reality and is able to reproduce collision and overwash regimes even in presence of a highly three-dimensional flow, which makes it usable for modelling tidal inlets.

XBeach is an extended model with a large range of possibilities. For both the hydrodynamic processes as the morphodynamic processes, multiple methods are possible to implement. For all parameters, a default value is available. This value will be used when no value is by the user. The default values are chosen after calculation and validation which fit best. However, some situations require different settings. In order to find the settings which give the most representative results, the most simple version of the model is executed and strange or deviating results are processed in the parameter files. After various of these validation rounds, the final model settings are presented in this validation report.

XBeach is continuously in development and therefore parameters and implementable methods might differ per version. During this research, XBeach version 1.22.4937 is used.

### 2.1 Input data

The most basic model settings, which are required to run the model are a grid- and bathymetry file and wave characteristics. To get a realistic representation of a storm surge on the Hors, a couple more parameter(files) needs to be defined, including: waterlevels (tide/storm surge), wind parameters, changing wave characteristics and grain sizes. Finally, the parameters which are chosen to optimize the results are explained.

#### 2.1.1 Basic model settings

##### *Grid*

The used grid is constructed in the program RGFGGrid (v. 4.20.00.34496) which is part of the Delft3D (Hydro-morphodynamics & Water quality) program (v. 4.01.00). This program is able to construct curvilinear grids. An simplified drawing of such a grid, with the names of the boundaries, is shown in Figure 1.

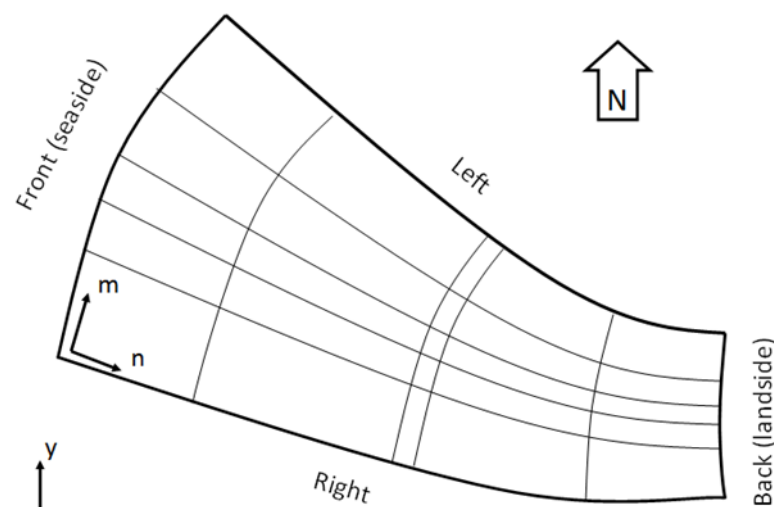


Figure 1 - XBeach grid definitions

## Appendix 1 – Validation report

During the design of the grid a couple of requirements had to be met, these requirements are defined in Table 1 (Deltares, 2014).

Table 1 – grid requirements (Deltares, 2014)

|  |                   |
|--|-------------------|
| max grid size at seaside                           | 50m x 50m         |
| max (local) grid size to see erosion patterns      | 3 m x 3 m         |
| max size difference between two adjacent gridcells | 1.2 [-]           |
| orthogonality in inner model area                  | 0.02 – 0.04       |
| smoothness (max. value)                            | 1.2               |
| Aspect ratio *                                     | between 1 – 2 [-] |

\* aspect ratio must be in the range unless the flow is predominantly along one of the grid lines.

The location of the sea boundary is chosen on a line where the water depth is around 30 metres. The minimal water depth has to be large enough to generate a realistic propagation of the waves into the model. The minimal water depth could be lower for the storm surge, however during future simulations, higher waves might be applied and therefore, a larger water depth is required. The land boundary is chosen in Marsdiep around 2 km away from the Hors to make sure that the boundary conditions won't affect the processes on the Hors.

### Bathymetry

The bathymetry file is constructed in QUICKIN (v. 4.20.00.34503). This program is, like RGFRID, a program within Delft3D. Two bathymetry files are used during this research. Both bathymetries are constructed with two dataset, the first one is Lidar data From Rijkswaterstaat, so called Vaklodingen. This dataset, available via an open source webpage from Deltares, contains depth values every 20 meter in the North- and Wadden Sea. At the start of this research, the latest Vaklodingen dataset available was measured in 2012. Near the end of this research, a new Vaklodingen dataset became available with measurements of 2017. The second dataset which is used to construct the bathymetry is LIDAR data from Actueel Hoogtebestand Nederland (AHN) and originates from 2015. This dataset contains measurements of the Hors. The bathymetry on the Hors is from a much more detailed quality, with height points every 1-2 meters.

For the first bathymetry, the Vaklodingen measurements from 2012 and AHN measurements of 2015 are used. For the second bathymetry, the Vaklodingen measurements of 2017 are used with the AHN LIDAR measurements of 2015. The Vaklodingen dataset of 2012 overlaps the 2015 LIDAR data. Due to differences in the outer shape of the Hors, the 2015 LIDAR data is implemented on the Hors itself, where the bed level differences between the two datasets was less than 0.05m (Figure 2).

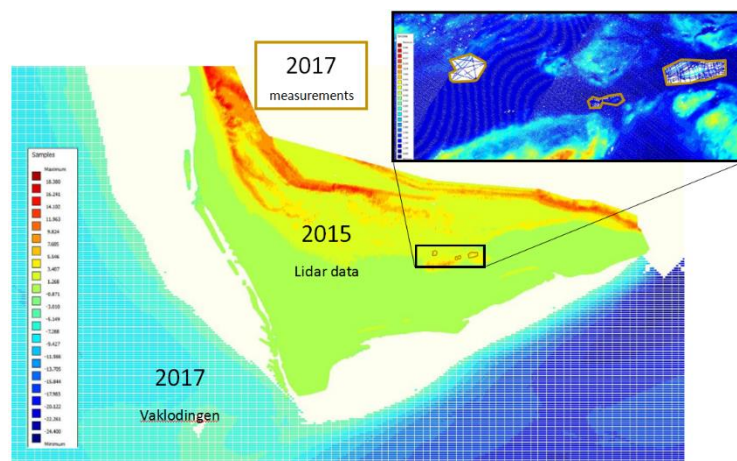


Figure 2 - Sources of bathymetry 2017

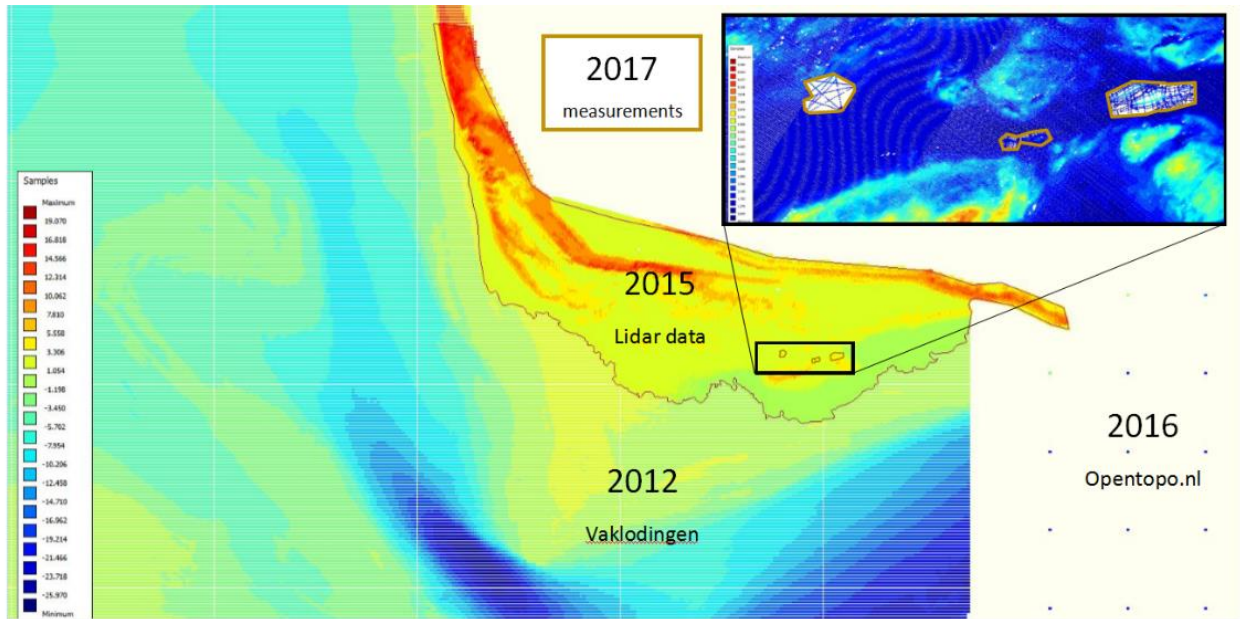


Figure 3 - Bathymetry data of LIDAR(2015) and Vaklodingen (2012)

The bathymetry on the Hors is from a much more detailed quality, with sample points every 1-2 meters. This dataset is also LIDAR data from Actueel Hoogtebestand Nederland (AHN) and originates from 2015. The boundaries of this detailed dataset are chosen in a way that the two datasets smoothly merge. This comes to a height around 1.5m +NAP.

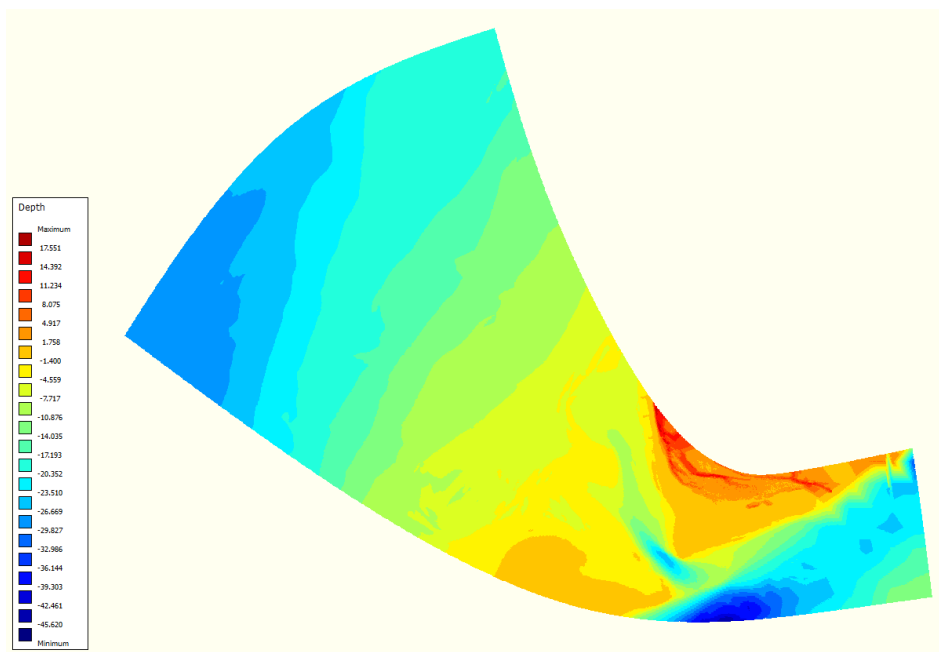


Figure 4A - Bathymetry 2012 Blue = -45m, red = 17.5m +

## 2.1.2 Storm settings (optional settings)

### Waterlevel data

During the simulations, two waterlevels are defined which change over time. The first waterlevel is at the seaward boundary and the second waterlevel is located at the landward boundary. The difference between these boundaries is mainly responsible for the flow between the sea- and landside. Because there are no measurement-station exact on the sea- and landboundaries. Values from surrounding measurement stations have to be (linear)

## Appendix 1 – Validation report

interpolated. For the sea side, this is done with the Texel-Noordzee and Q1 measurement stations, where the Texel-Noordzee determined for almost 75% the waterlevel and Q1 for around 25%. At the landside, the waterlevels of the Den Helder station and the Oudeschild station are equally averaged to get the correct waterlevel at the landboundary. Figure 5 shows this situation. The waterlevels on both boundaries change every hour.

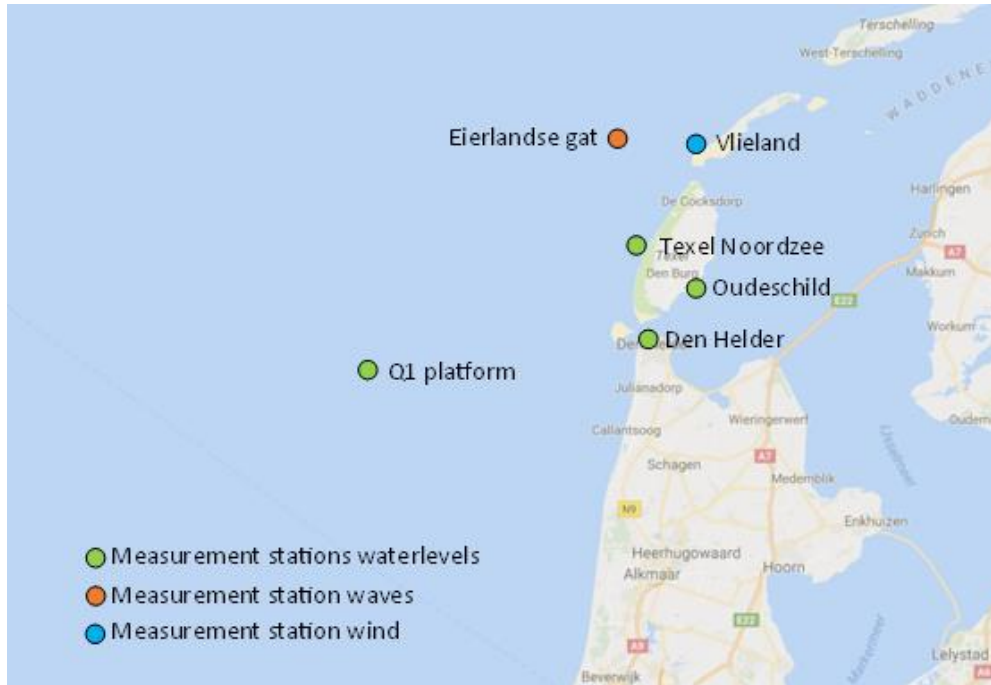


Figure 5 Location of used measurement stations

After testing, the system remained more stable when the difference between the two waterlevels on the boundaries (gradient) was slowly introduced. The first 2 hours are setup, from that point, every half hour a new water level is defined. During the peak waterlevels more values are defined to decrease the spontaneous change in gradient. XBeach linearly interpolates the waterlevel between the defined waterlevels which results in the waterlevels shown in Figure 6.

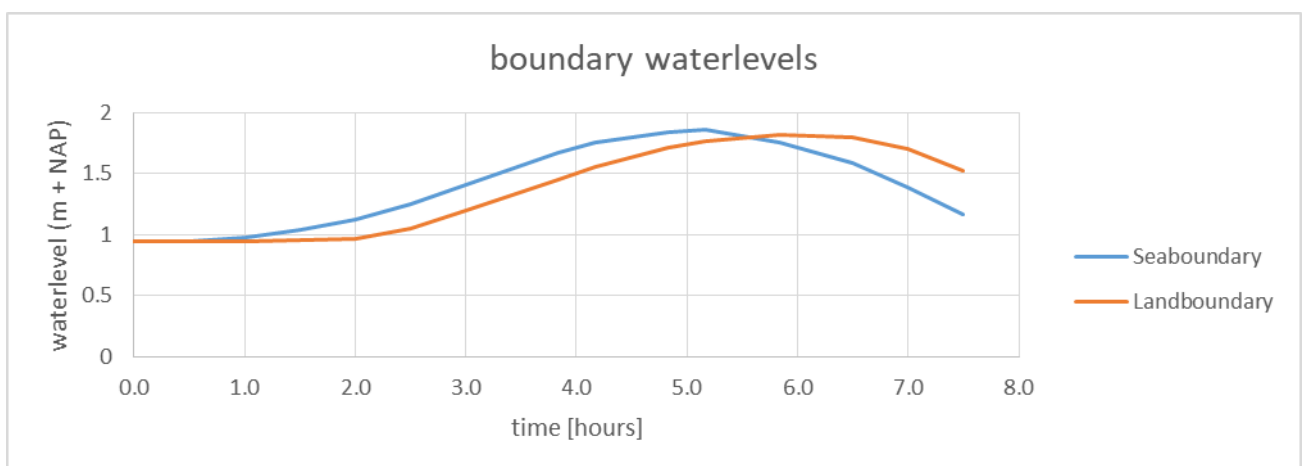


Figure 6 – Imposed boundary waterlevels on both the sea boundary and land boundary during the storm surge of 11-1-2017

#### *Wave data*

Wave data of several measurement stations near the Dutch coast, including hourly data of the significant wave height, wave period and main incoming wave angle in an energyspectrum of 30-500mhz, is acquired from the rijkswaterstaat site (Rijkswaterstaat, 2017). The most nearby station is 'Eierlandse gat', which is located at the north-east of the island of Texel. Besides the location, the distance to the coast is similar to the sea-boundary of the used model. The wave height differs per waterdepth and therefore it is assumed that the wave heights in 'Eierlandse gat' are representative for the simulated area.

#### *Wind data*

Hourly wind speeds and directions from the measurement station of Vlieland are chosen. For a limited time series(1996 – 2014), wind data on the Hors is available. A standard deviation of the differences in wind direction and speed between 1996-1999 with wind speeds above 14m/s resulted in a mean difference in winddirection of 3°, with a standard deviation of 10°. The difference in windspeed is averaged 1.3m/s with a standard deviation of 1.5m/s. It is assumed that this difference won't affect the results of the simulations. Therefore the Vlieland measurement station is chosen as wind input station as input source for the 2017 storm surge. The wind direction is measured on the last 10 minutes of the last hour and the wind speed is the hourly mean average (Koninklijk Nederlands Meteorologisch Instituut, 2017).

#### *Grain sizes*

XBeach asks for a D50 (50% of the particles has a smaller diameter) and D90 (90% of the particles has a smaller diameter) to determine the range of sediment size. The sediment width (D50-D90) of 3 samples on the Hors, field measurements Filipe (only top 5cm sediment) are used to determine the D50 and D90 values, the used values are:

D50 = 0.000220 m  
D90 = 0.000330 m

## 2.2. Parameter settings / processes

#### *Wave mode*

To calculate the hydrodynamic processes in the model, the surfbeat mode is used. This mode especially focusses on swash zone processes and is fully valid on dissipative beaches where the short waves are mostly dissipated by the time they are near the shoreline (Hoonhout, 2015). The surfbeat mode resolves the short wave varying on a wave group scale and includes long waves which are associated with these wave groups (Hoonhout, 2015)

The short wave action is calculated with the wave action balance equation, this equation includes the effects of wave growth and dissipation due to wind generation, bottom dissipation and wave breaking (in deep and shallow water) (Holthuijsen, Booij, & Herbers, 1989). The equation solves the variation of the wave height on the scale of wave groups, this way, both short- and long waves are accounted for (Hoonhout, 2015). Figure 7 shows this principle.

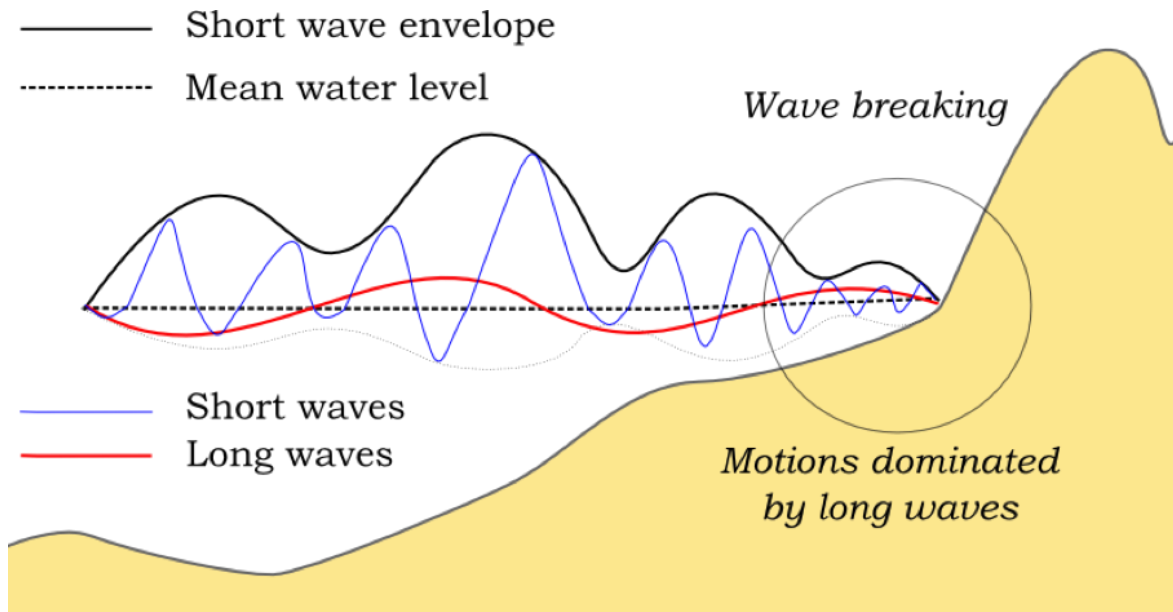


Figure 7 - Principle sketch of the relevant wave processes (Hoonhout, 2015)

Short wave dissipation is accounted for by two processes: wave breaking and bottom friction. Dissipation by wave breaking is calculated by counting the amount of breaking waves, multiplied by the dissipation per breaking event (keyword: break = roelvink2). If the wave height exceeds its maximum height, which is calculated with the water depth, a breaker index and a fraction of the wave height itself. The XBeach manual explains that instationary surf beat mode can be activated using the keyword: wavemodel = surfbeat, however in my version of XBeach (version 1.22.4937) this keyword is not recognised. When using a jonswap wave spectra (keyword: instat = jons\_table), XBeach computes the short waves as wave energy, but the long (infragravity) waves will be fully solved.

#### *Flow boundary conditions*

Currents in XBeach are formed by a waterlevel difference between the fixed waterlevels on both the Front (seaside) of the model and the back (landside) of the model, see Figure 1. Due to the shape and size of the grid and bathymetry, the left and right boundaries of the model are closed (see Figure 4) and will be considered walls. Alternatives, which all came down to open side boundaries where flows could enter and leave led to strange currents and waterlevels throughout the entire model. By designing the left- and right boundary to be parallel to the flow, the effect of the boundaries on the result is minimized. s

#### *Wave directions*

The wave direction is solved at regular intervals using the stationary solver. The wave energy follows this wave direction. By using this method, the groupiness of waves preserved (as good as possible) and the simulations significantly decreases in computational demand. The results show that the wave refraction on the eastern side of the Hors is affected when applying this model, however it shows no significant changes in the flow pattern, wave height or erosion profiles on the Hors itself. To increase the simulation speed (with a factor 2(!)), the single\_dir method is used (single\_dir = 1) (Deltares, 2015).

The order of wave steering (keyword: order) had to be set to 1 instead of the default value of 2. This difference in parameter determines the order of wave steering, 1 = first order wave steering (short wave energy only), 2 = second order wave steering (bound long wave corresponding to short wave forcing is added)(Hoonhout, 2015).

## Appendix 1 – Validation report

At order 2, strange waves with a period of around 1 hour were seen in the results. These waves were most likely to be caused by the initial slushing effect of the model, due to the shape and characteristics of the model. By changing the order of wave steering to 1, in combination with adding an initial set-up of the waterlevel differences in the model, the 'slushwave' is smaller and not strengthened by the waves in the model.

### *Morphodynamic processes*

As said in the introduction (1.1.3 – Beach dune dynamics), erosion on/near the coast can be caused by multiple processes. During this research, the Van Tiel-Van Rijn method (keyword: form = vanthiel\_vanrijn) is used to calculate the erosion near the coast which is caused by the water velocity. The sediment transport on every cell-edge is calculated (with the advection-diffusion) and a difference in transport on the cell boundaries results in erosion or sedimentation in the grid cell.

Wave breaking leads to turbulence of the water near the bed. This factor ( $k_b$ ) is included in the orbital velocity which is used in the advection-diffusion equation (Bolle, Mercelis, Roelvink, Haerens, & Trouw, 2011; Hoonhout, 2015).

## Chapter 3 – Reference data

To make a realistic representation of Marsdiep and its surroundings, the model needs to be validated. By checking the results of certain parameters with real measurements, the conformation with reality can be made and if needed, the model can be adapted to give better results. Two datasets of measured parameters are available nearby, both are analysed in the next two sections.

### 3.1 TESO current data

Beneath the ferry which shuttles between Den Helder and Texel every hour, measurement equipment is attached. This equipment measures among others the flow's current and direction. The TESO data of the whole year of 2009 is made available by the Royal Netherlands Institute for Sea Research (NIOZ). The validation purpose of this data is limited, considering the ferry only sail when the waterlevel is beneath 2m+NAP. The highest measured waterlevel where the corresponding waterlevel is known occurred on 4-10-2009. During this storm, a waterlevel of 1.84m +NAP was measured in Den Helder. This waterlevel is high enough to flood the Hors and therefore creating a similar situation as the 2017 storm, by simulating the storm of 2009, similar flow velocities and directions should be found.

The ferry measures the currents in Marsdiep every 2 seconds. Due to the movement of the ship, the measurement location changes every measurement. To find currents on specific locations, ID-points are used. These ID-points are located on a fixed location and show all measured currents on that location. There are in total 109 ID-points measured by NIOZ, for this study, 14 of those ID-points are used (location number 1 t/m 14 in Figure 8).

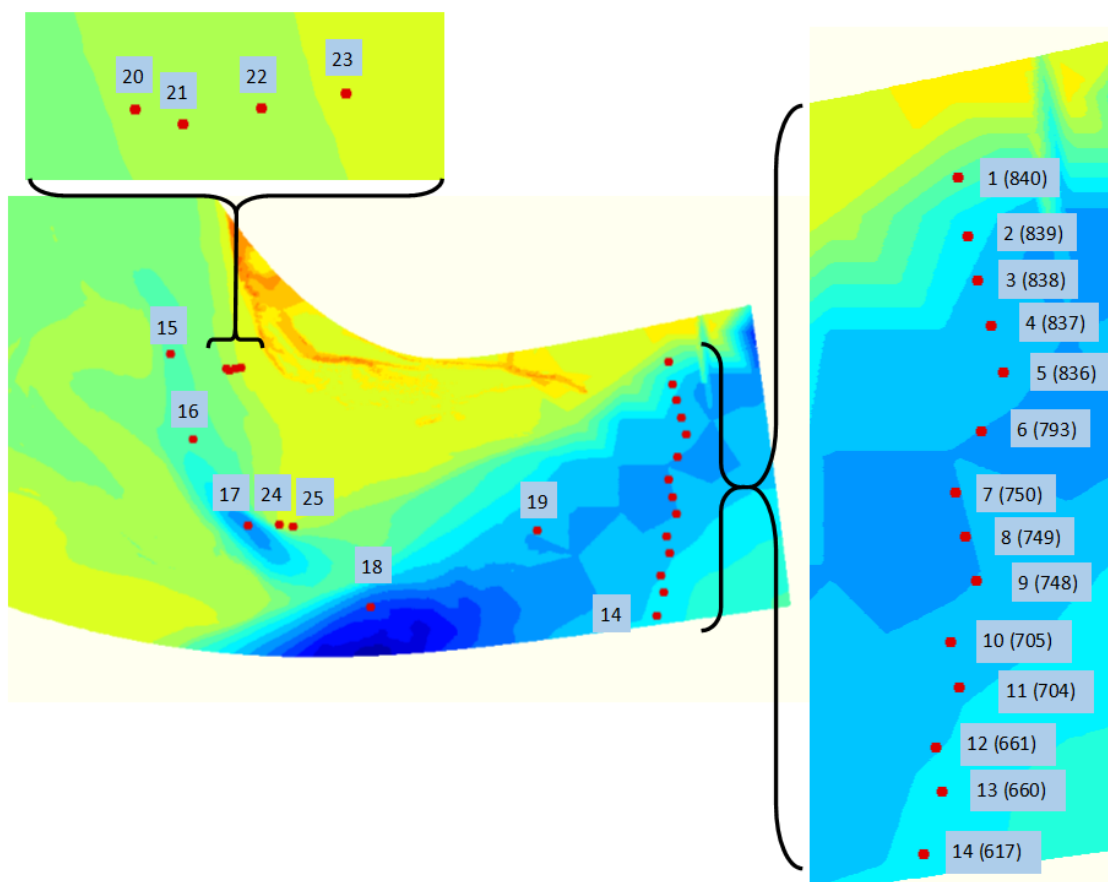


Figure 8 - points (coordinates) defined to give results. At point 1 t/m 14 TESO - idpoints are added

## Appendix 1 – Validation report

The highest currents are expected at 1/4<sup>th</sup> and 3/4<sup>th</sup> of the storm surge, when the waterlevel difference between both sides of the inlet are maximal. However, the peak of the storm surge of 4-10-2009 is at 7.00 am, whereas the first crossing is at 7.30 am. Therefore, there is no data available of the expected maximum currents in Marsdiep during the concerned storm surge. However, if assumed the (infragravity) waves have no influence on the flow velocity in Marsdiep, the water level difference between both sides of the inlet determines the flow velocity in Marsdiep. A larger gradient, results in more flow.

With data of waterlevels of the measurement stations of Q1, Texel Noordzee, Den Helder and Oudeschild, the waterlevels as they are modelled are calculated for the whole year of 2009. This way, the currents are linked with the waterlevel difference between the sea- and land. From this dataset, the currents which occurred at similar waterlevel gradient are averaged and the standard deviation is calculated. This ratio of current : waterlevel of 2009 is shown in Figure 9. This ratio is used during the storm surge of 2017 to calculate the expected currents in Marsdiep, where the gradient is known.

Assumed that the flow velocity values have not changes since 2009, the waterlevel differences between the sea- and landside of the storm of 2017 are taken to determine the velocity in Marsdiep, Figure 10 shows the expected currents in Marsdiep during the storm surge of 11-1-2017 and the waterlevel gradient on which this current is determined.

Due the made assumptions in this method, the simulated flow velocities might deviate from the reference velocities. However, the reference currents gives an good indication of flow velocity over time. As expected, the flow velocity should be maximum at 1/4<sup>th</sup> and 3/4<sup>th</sup> of the storm surge, when the gradients are maximum. The simulated flow velocity should show a similar path as the reference data.

## Appendix 1 – Validation report

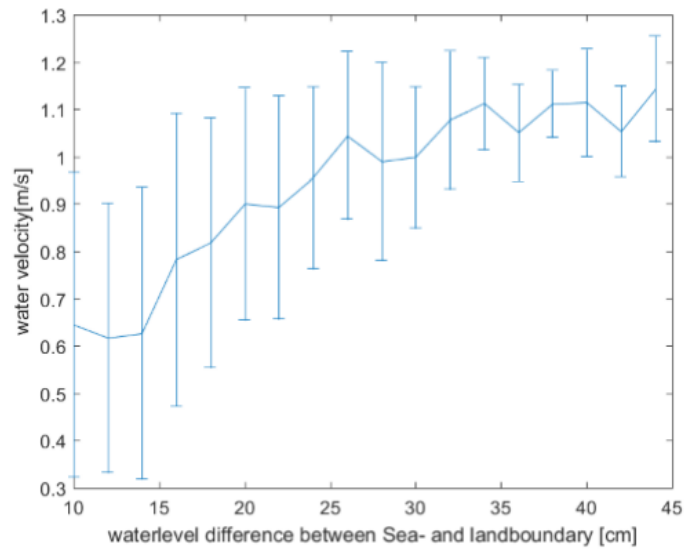


Figure 9 - Currents of 2009 (on id-point 793) compared with waterlevel differences between the sea- and land boundaries of the XBeach model

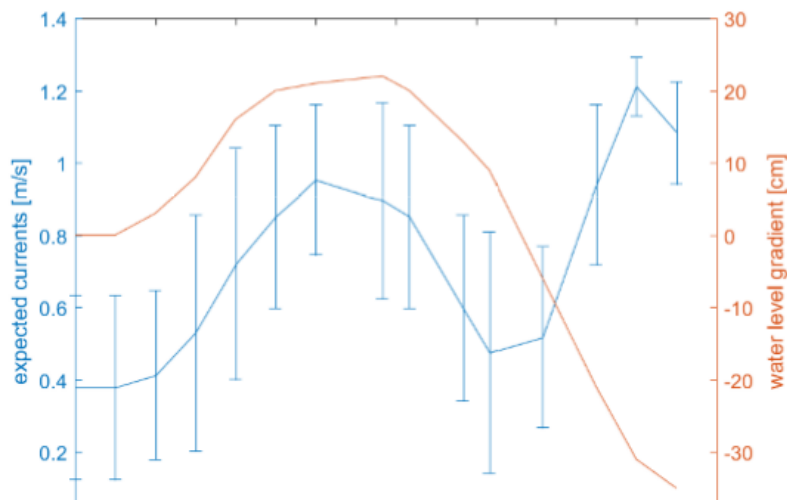


Figure 10 - expected currents (with standard deviation) on id-point 793 in Marsdiep during the simulated storm surge of 2017

### 3.2 Dune (erosion) measurements

To quantitatively calibrate the model, topographic data from dunes located at De Hors (Texel) are available for a day before and after the storm of 11-1-2017. A clear erosion profile on the measured dunes is visible and the maximum sedimentation and erosion of these dunes is known. The simulated storm surge of 11-1-2017 should show a similar erosion pattern with comparable erosion/sedimentation rates. Figure 11 and Figure 12 show an overview of the Hors with the measured dunes with names as they will be called further on. Figure 13 shows the bathymetry of the area with the measured dunes. In section 3.2.1, the western dune field will be analysed. Section 3.2.2 focusses on the middle dune and in section 3.2.3 the eastern dunes are analysed.



Figure 11 - Overview Hors with location of measured dunes



Figure 12 - The three measured dune(field)s on the Hors (located in square of Figure 9)

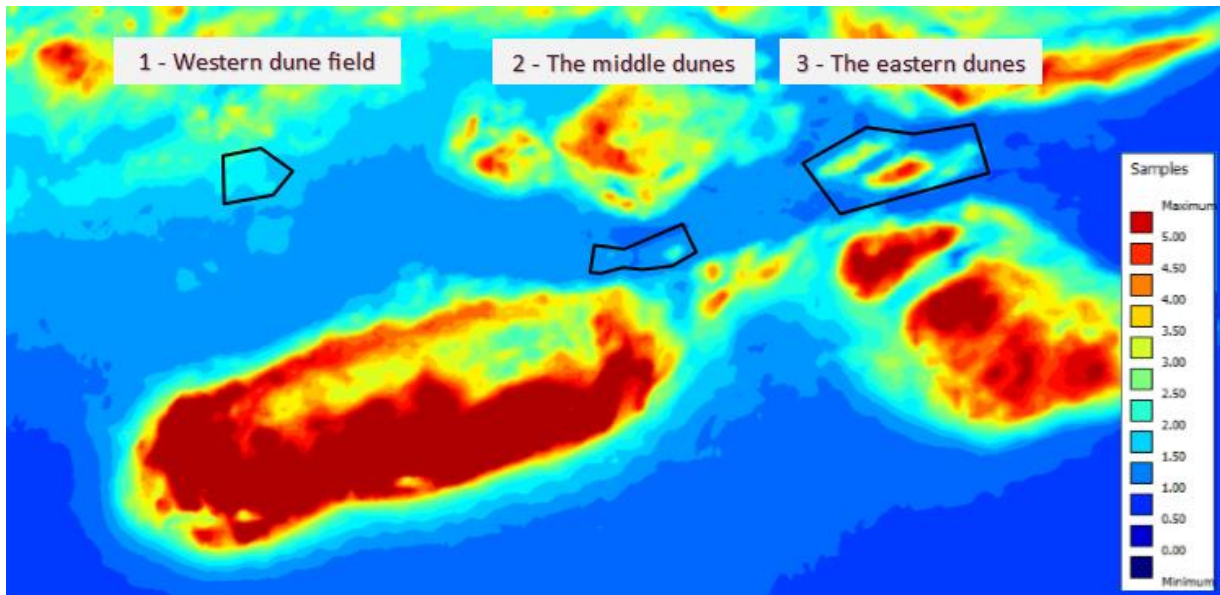


Figure 13 - Overview of bathymetry of three measured dune(field)s on the Hors (located in square of Figure 9) (blue = 0m+NAP, red = 5m +NAP)

### 3.2.1 Western dune field

The western dune field is located in an area with a number of relatively small dunes (max. 3m+NAP). The measurements are taken by walking towards five tops of dunes towards each other (between 2-3m+NAP). The five angles in the measurement are tops of dunes. Figure 14 shows the measurements taken before (11-1) and after (12-1) the storm surge. despite the large gaps in between both datasets, the paths which are followed to gather the measurements are identical. Therefore, when compared the measurements, the level of erosion is realistic. It has to be noted that the gaps are linearly interpolated to fit in the bathymetry. Due to the coarse grid and the gaps in the data, the erosion pattern might be distorted.

Figure 15 shows the bathymetry of the Hors as used, which is similar for both 2012 and 2017 bathymetries because on the Hors, for both bathymetries is the LIDAR data from 2015 used. Figure 16 shows the measured erosion deviated from the samples in Figure 14 (triangular interpolated bathymetry of 12-1 – triangular interpolated bathymetry of 11-1).

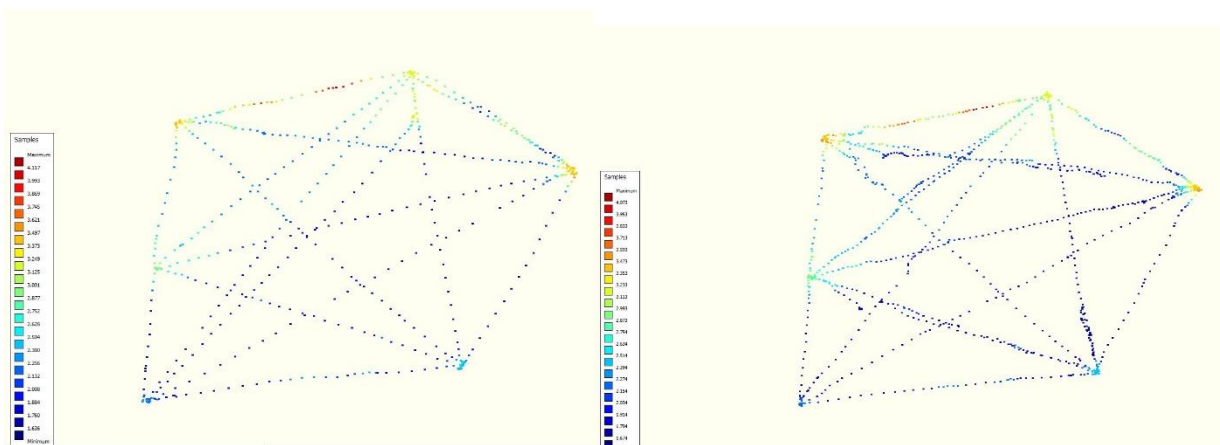


Figure 14A - bedlevel measurements of 11-1-2017

14B – bedlevel measurements of 12-1-2017

# Appendix 1 – Validation report

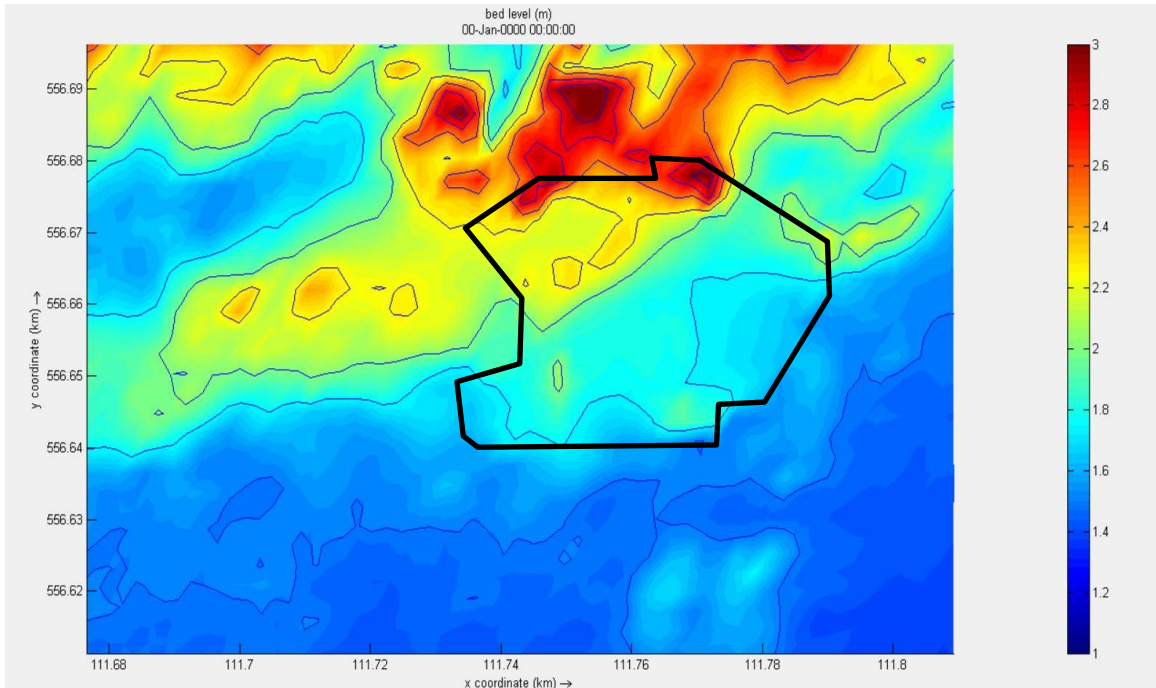


Figure 15 - bathymetry western dunes as used in simulations [m+NAP]

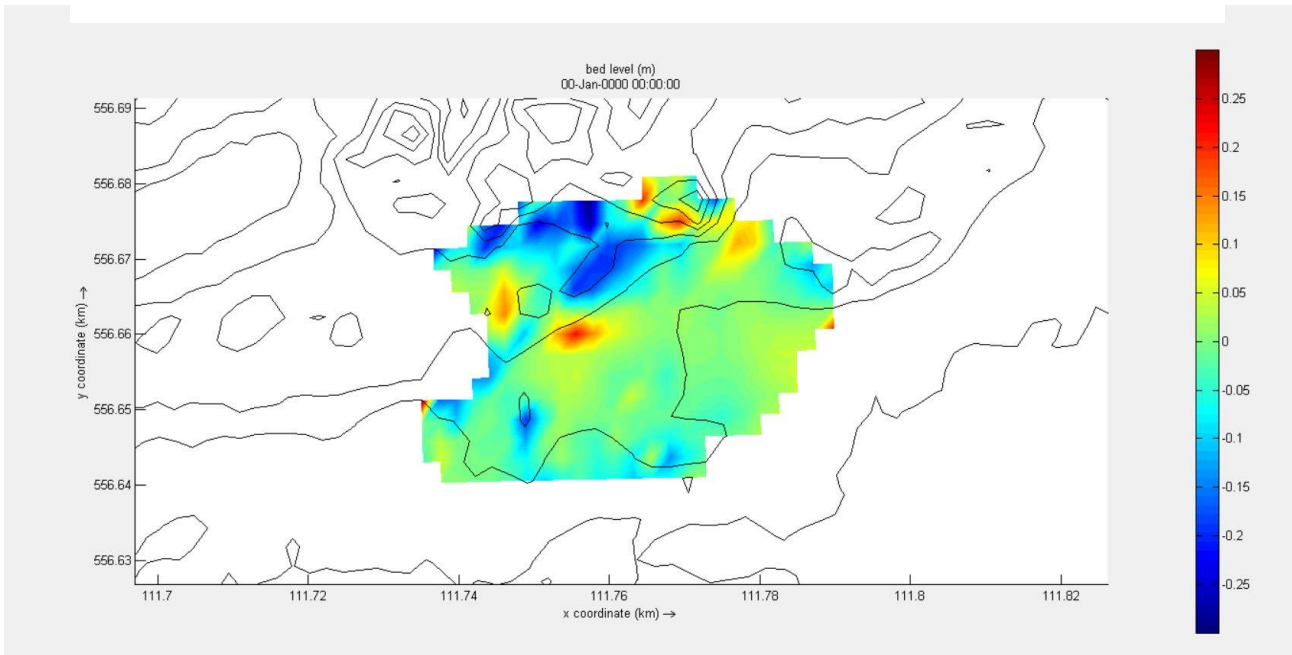


Figure 16 - measured erosion of the western dune field between 11-1 and 12-1 [m]

### 3.2.2 The middle dunes

The middle dune is located in between large dunes which acts as valley where water flows under relatively high velocity (see Figure 12). The top of left dune, which is better visible in Figure 13 is around 1.8m + NAP and the top of the right dune is around 2.8m + NAP. Again, Figure 17 shows the measured depth points (samples) on 11-1 and 12-1. Around the dunes in this area, a bedlevel difference is seen with the 2015 LIDAR data. The bedlevel in the valley in 2015 was respectively 0.2m lower. By only using the surroundings of the dunes, this bedlevel difference is minimized. However, when closely looked at the bathymetry (Figure 18), the boundary between the 2015 LIDAR data and the 2017 measurements is visible.

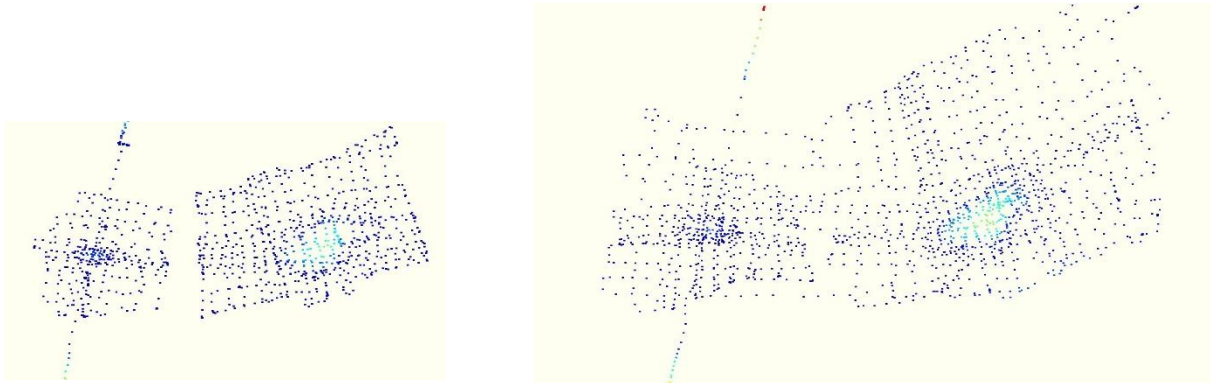


Figure 17 - bedlevel measurements of 11-1-2017

17B – bedlevel measurements of 12-1-2017

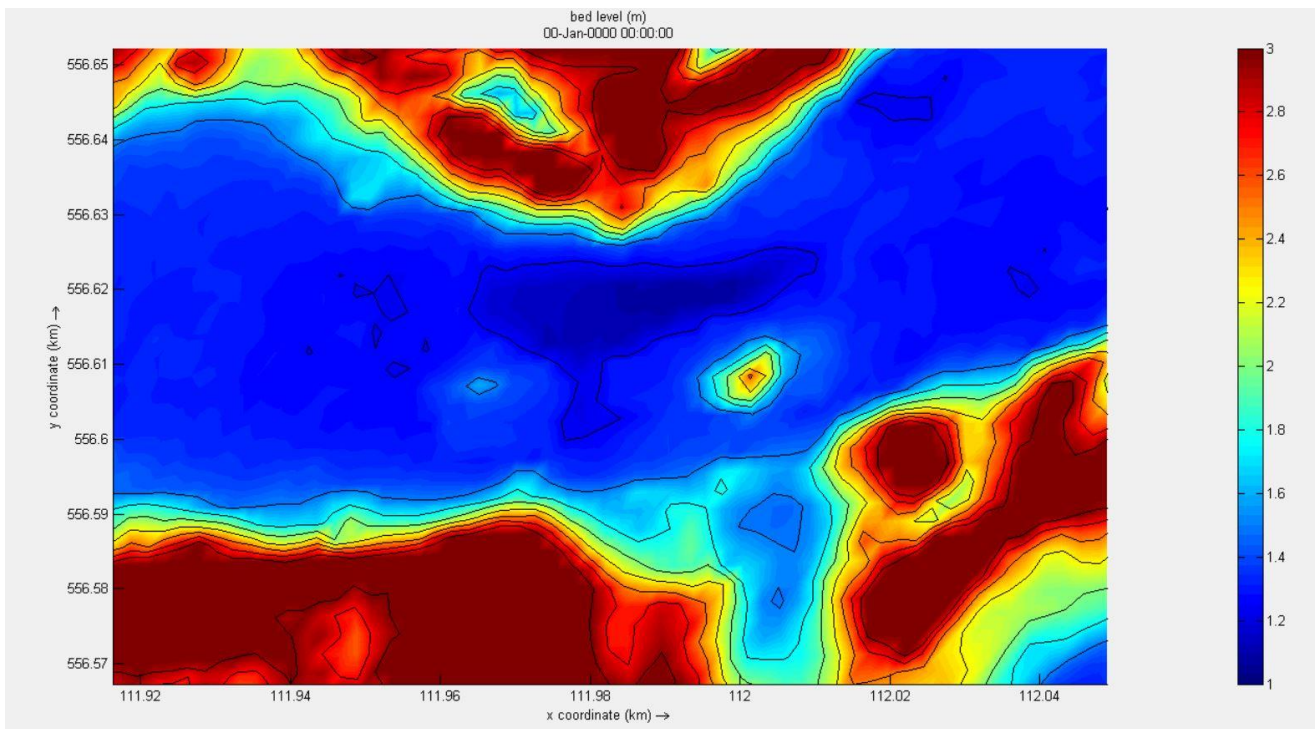


Figure 18 - Bathymetry middle dunes as used in simulations [m+NAP]

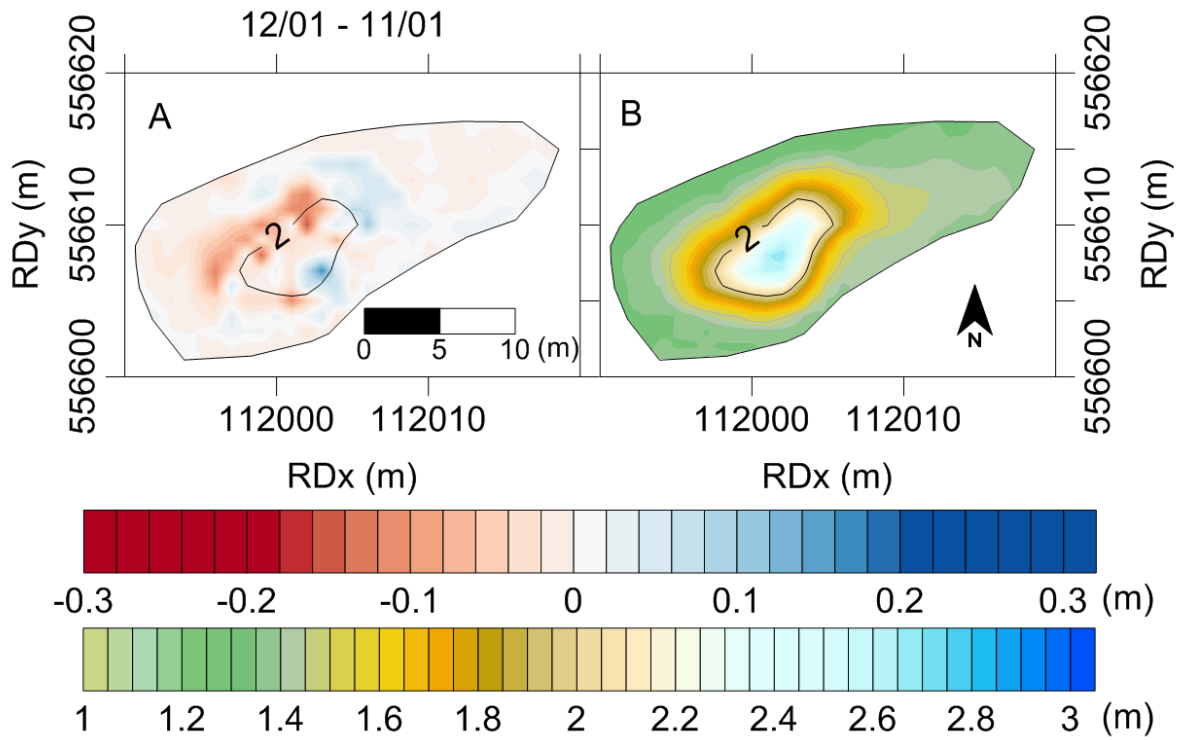


Figure 19 - Refined graph of the measured dune erosion on the eastern located 'middle dune' between 11-1 and 12-1 (made with the samples from Figure 16)

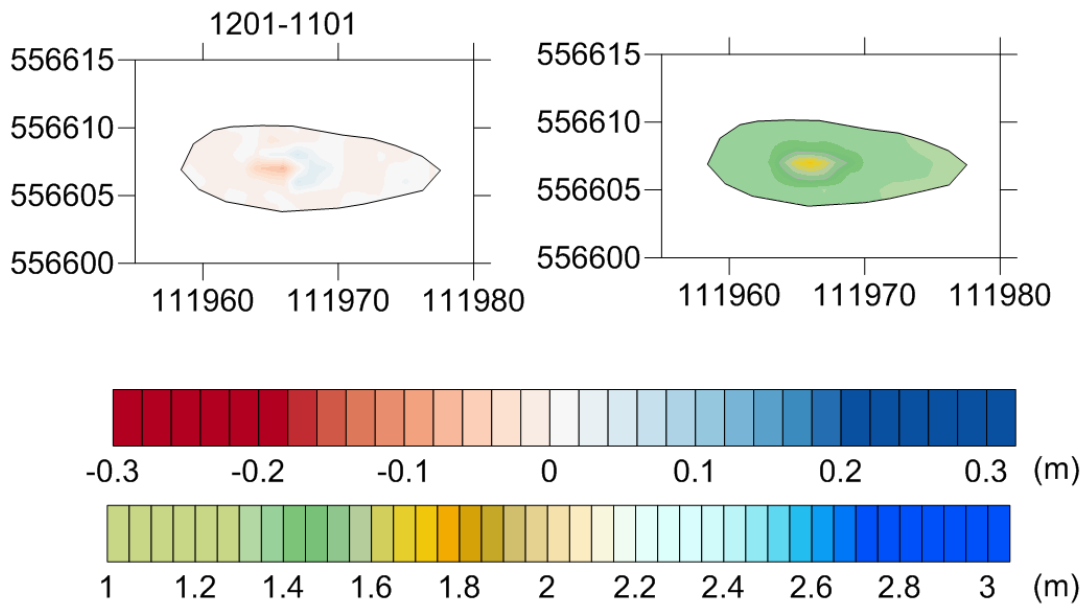


Figure 20 Refined graph of the measured dune erosion on the western located 'middle dune' between 11-1 and 12-1 (made with the samples from Figure 17)

### 3.2.3 The eastern dunes

The middle dune and the eastern dunes are located in the similar valley. Due to the steepness, size and variability of the dune, small deviations from reality are inevitable. Figure 21 shows the bedlevel measurements on 11-1 and 12-1. The 11-1 measurements contain several gaps. The bathymetry of 11&12-1 is constructed with triangular interpolating the measurements, these bathymetries are subtracted from each other and the results contain the erosion/sedimentation in the storm surge (Figure 23). This method has one disadvantage, and that concerns the gaps. For instance, the top of the biggest dune in 11-1 is not measured (Figure 21A), this height is averaged of the surrounding points, which are lower than the actual height. On 12-1, the top of this dune is measured (Figure 21B). When subtracting the bathymetries by each other, it looks like the top is grown in height (Figure 23), which has not happened in reality. In this example, the gap is relatively big and the differences are clearly visible, but this is not for all gaps the same. Therefore, this data is hard to compare to the simulated data. It can be difficult to separate the measurements deviations from real erosion patterns, and results from this dune have to be treated really carefully to conclude an agreement of measured erosion and simulated erosion.

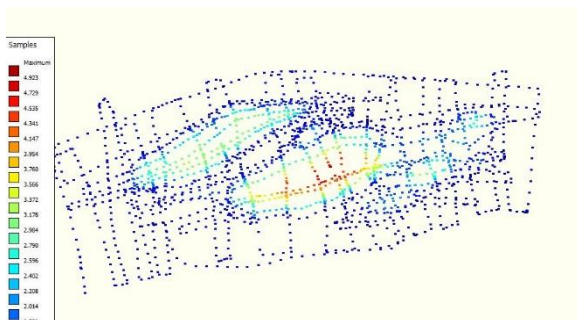
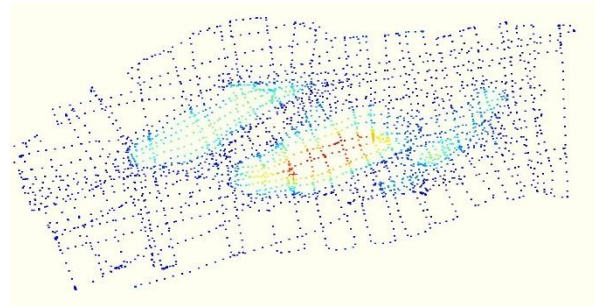


Figure 21A - bedlevel measurements of 11-1-2017



21B – bedlevel measurements of 12-1-2017

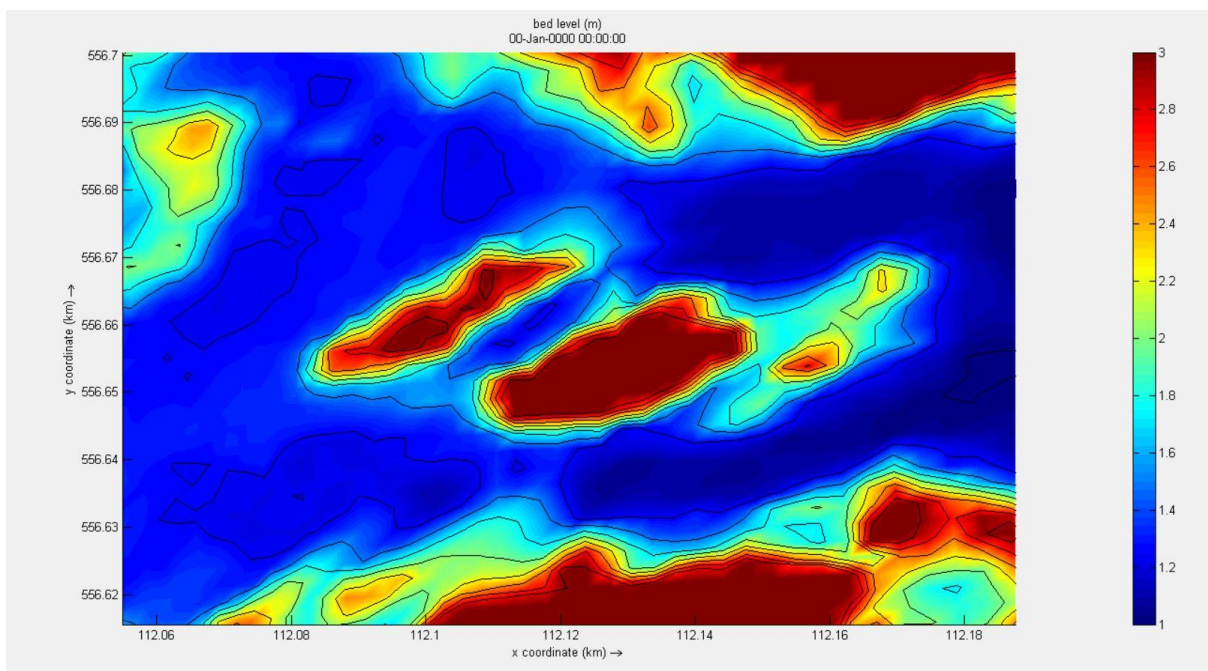


Figure 22 - Bathymetry eastern dunes as used in simulations [m+NAP]

Appendix 1 – Validation report

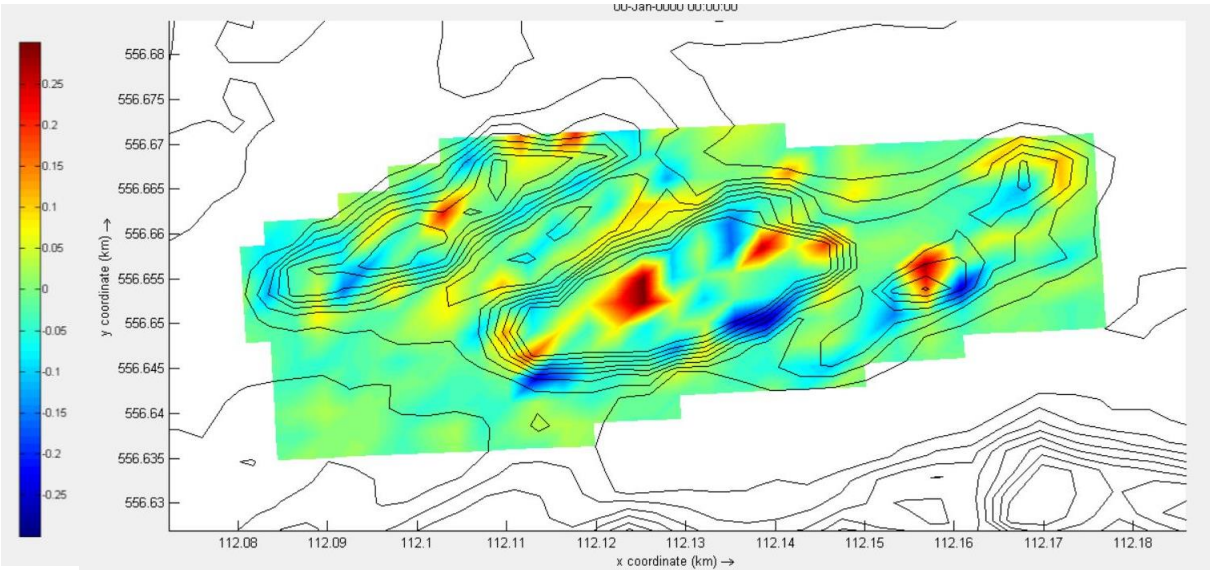


Figure 23 - measured erosion of the eastern dune field between 11-1 and 12-1 [m]

## Chapter 4 – Results

### 4.1 Main results

As explained in the methods, both 2012 and 2017 bathymetries are used during the simulations. It was expected that differences were found in the erosion profile at the west side of the Hors, where the depth was linearly interpolated in the 2017 bathymetry. The waterlevel in the middle of the sea side agrees with the measured data (Figure 24). The oscillation in the simulated waterlevels are the simulated infragravity waves. On the land side, the difference between measured waterlevel and simulated waterlevel differ not only from the measured data, but also from each other. The 2012 bathymetry reaches a higher waterlevel than the 2017 bathymetry. The difference in waterlevel has to be kept in mind when analysing further differences between the 2012 and 2017 bathymetry.

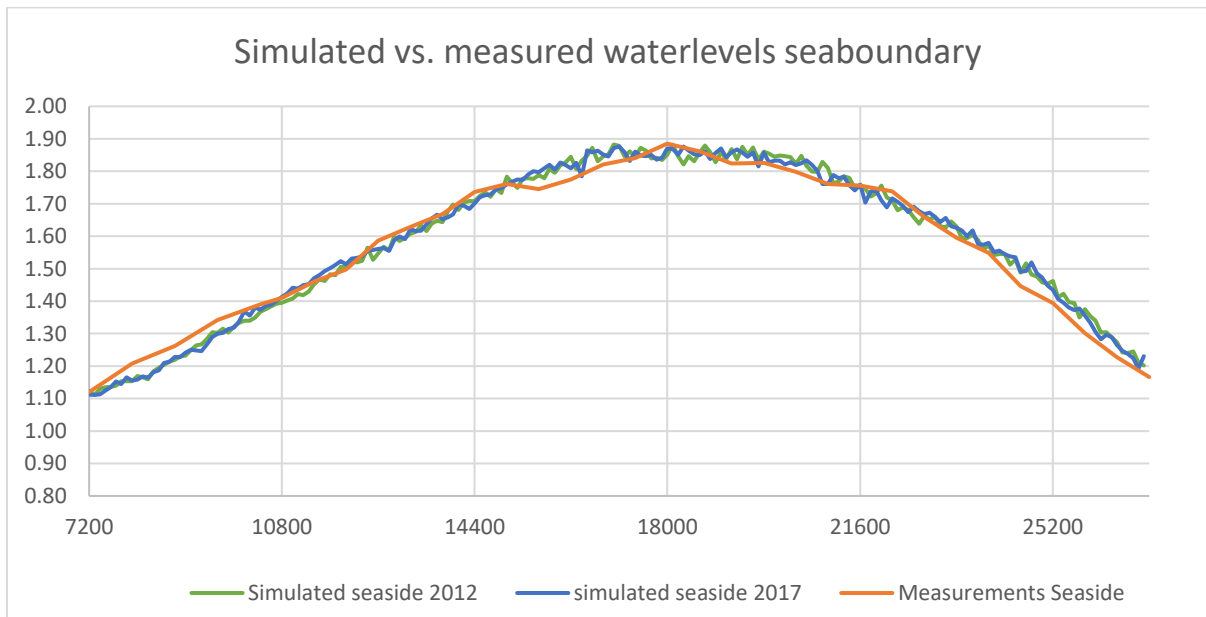


Figure 24 – simulated vs. measured waterlevels at the middle of the seaboundary

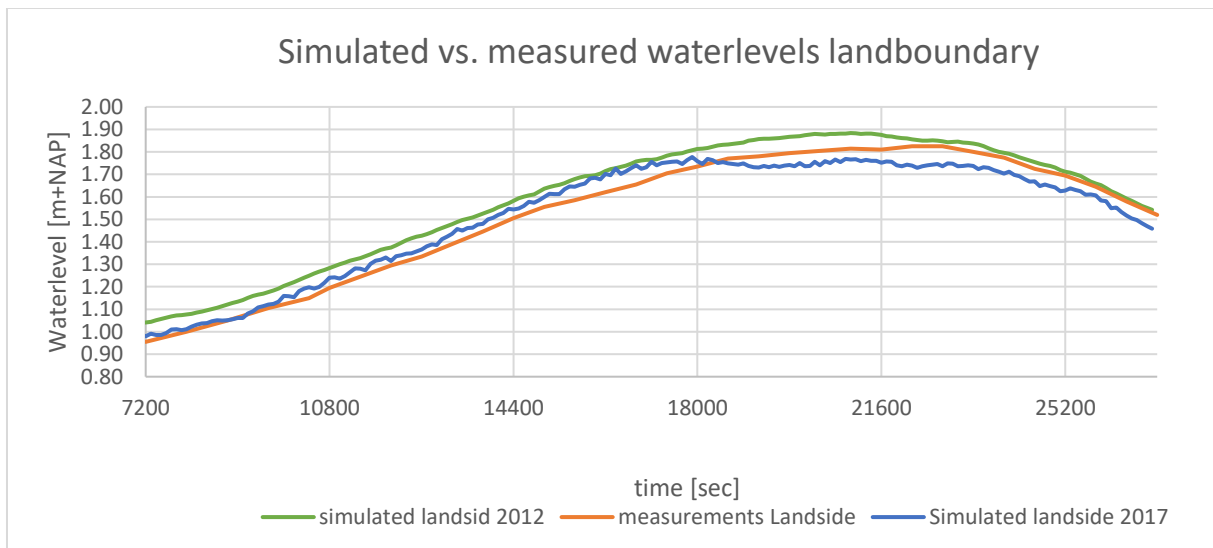


Figure 25 - Simulated vs. measured waterlevels at the middle of the landboundary

### 4.2 TESO current data

Figure 26 show the currents over the Hors during the expected highest currents (at 3 hr into the storm) where the waterlevel difference between sea and landboundary was maximal. Figure 27 shows the same currents as Figure 26, with the magnitude of the currents in the background.

The difference between the 2012 and 2017 bathymetry is located in Marsdiep and Molengat. It is not a surprise that in this area, current value and direction differ from each other. However, the currents on the Hors are comparable for both bathymetries.

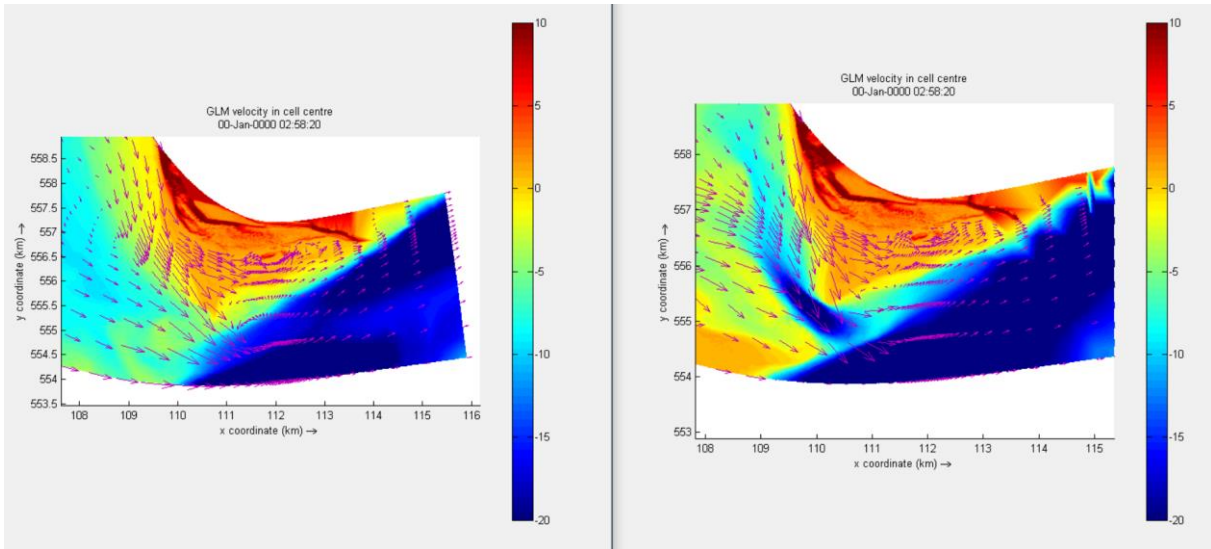


Figure 26 - Currents + direction on expected peak waterlevel of the storm surge (1080sec, 3hr) (with different bathymetry on the back ground. Left = 2017 bathymetry, Right = 2012 bathymetry (boundarylevels in both figures are fixed between -20 and 10, actual heights vary between -43 and + 15m)

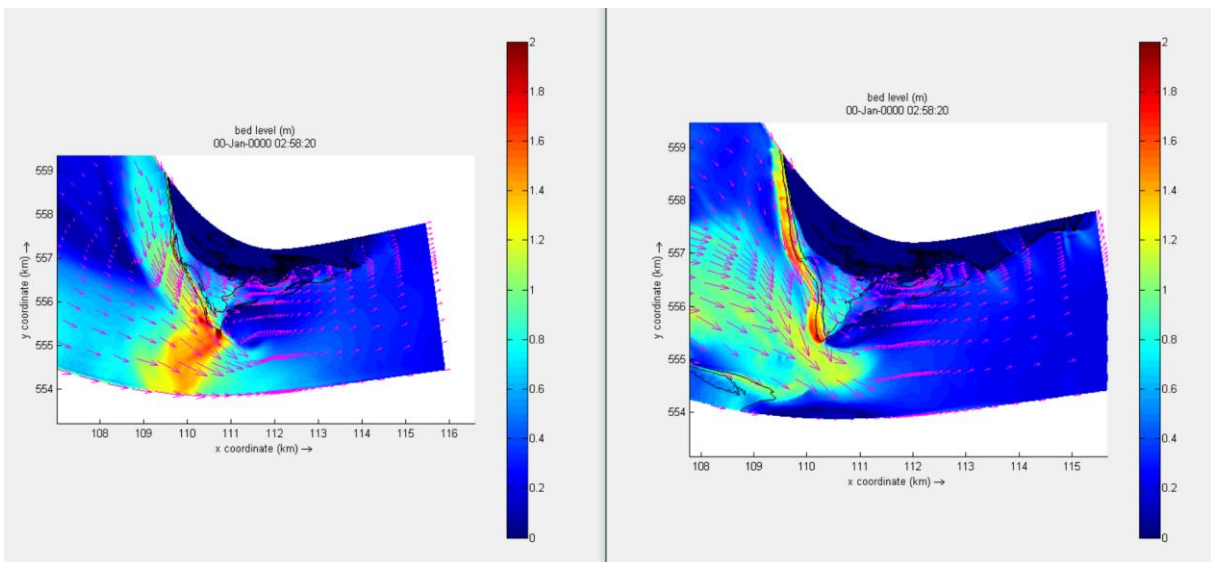


Figure 27 - Currents + direction on peak currents of the storm surge (1080sec, 3hr). Left = 2017 bathymetry, Right = 2012 bathymetry

From the TESO-data of 2009, the expected velocities in Marsdiep over time are known. Figure 29 shows different currents on the TESO-id points. The velocities are taken from the simulation with 2017 bathymetry. They are compared with the 2009 TESO data, as explained in chapter 3.1.

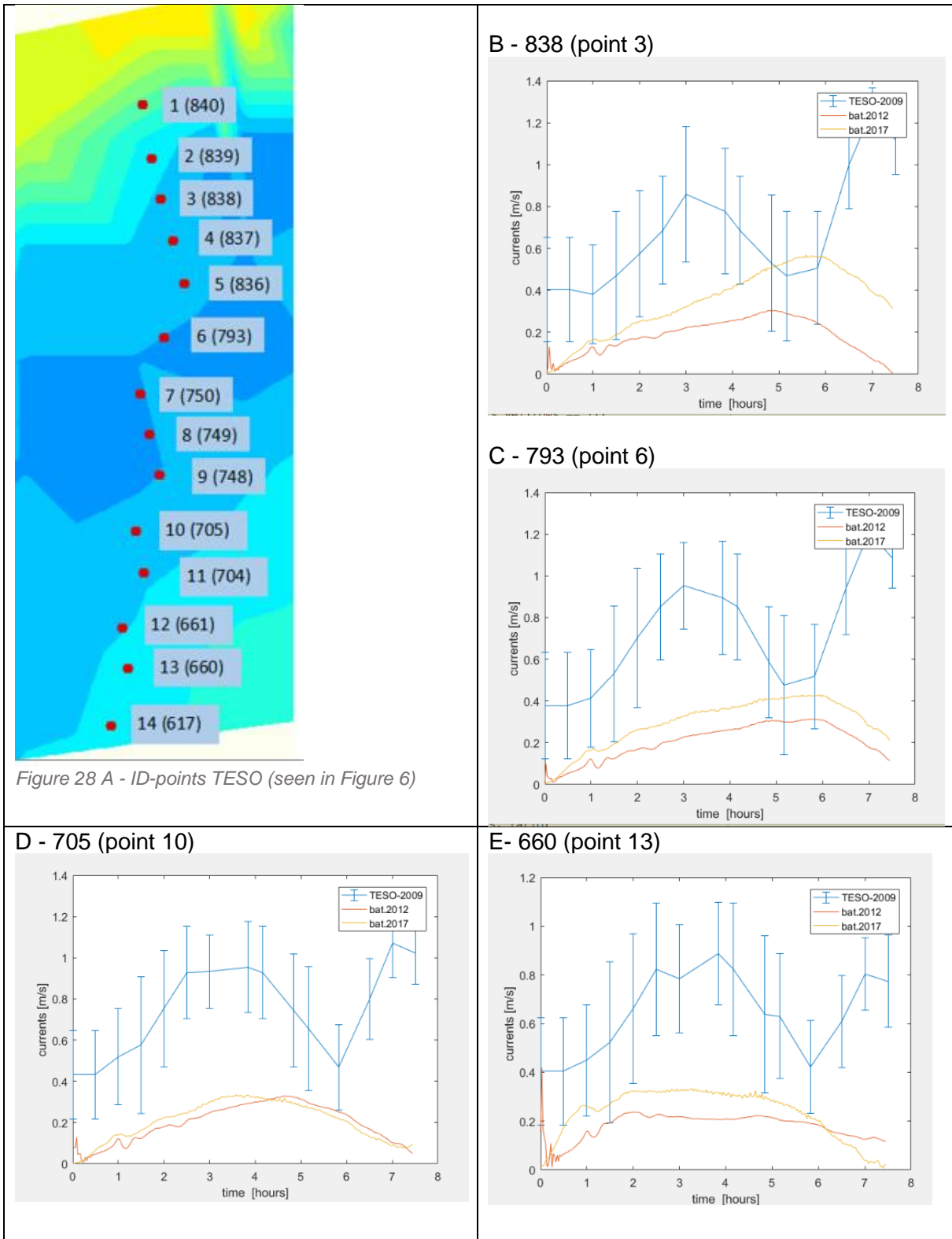
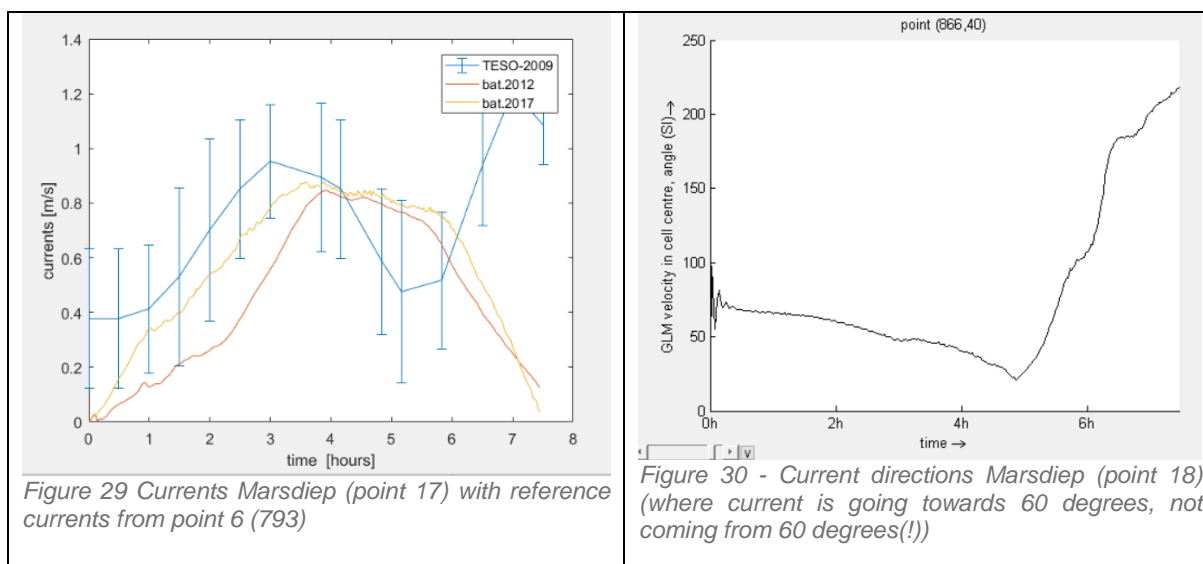


Figure 28 B-E – Simulated currents with the bathymetry of 2012 (red line) and 2017 (orange line) on TESO ID-points compared with the expected currents, based on the waterlevel difference on the boundaries and data of 2009 (blue line)

## Appendix 1 – Validation report



From the results of Figure 28 show an overall underestimation of the currents in Marsdiep. This underestimation is occurring due to the exclusion Marsdiep. The southern inlet of Texel consists of two channels, Marsdiep and Molengat. Marsdiep is considered the main channel which is responsible for most of the flow. The chosen grid only includes Molengat, which decreases the flow dramatically through the most narrow part of the inlet. When the channel gets wider, the flow decreases (flowrate = velocity \* area).

The second deviation concerns the changing tidal current. As said in the introduction, at 1/4<sup>th</sup> of the storm surge, the water velocity (in eastern direction) is biggest. This point is reached around 3.5 hours into the storm. Halfway the storm surge, both water levels are similar and velocities are minimal (around 6 hours of the storm surge). The second half of the storm surge, the water level in the inlet is higher than in the sea and water starts flowing out. This last part is not well defined in the model and this is due to the grid. As can be seen in Figure 4, the sea boundary is wide. From the sea boundary, the grid funnels towards the inlet. This makes that the flow rate in eastern direction is well represented, which can be seen back in the graphs. During the second half of the storm surge, water is coming in from the land boundary. Due to the narrowness and shallowness of this boundary, the amount of incoming water is much lower than the previous half. The current over the Hors is still going in eastern direction, which inserts turbulence, which disturbs the outgoing flow and forces the incoming water to decrease.

However, the water which flows through Marsdiep, has a much better agreement with the expected currents in Marsdiep. Figure 32 shows the currents further into Marsdiep (point 178 in Figure 8) and Figure 33 shows the direction of the current on this location.

Multiple vortexes can be identified near the Hors. Figure 31 shows the angles of currents during the peak of the storm surge. The vortexes are spinning and therefore they can be identified in the points where the colors change with both blue, green, yellow and red (for example on location 112, 555). Testing with multiple tests and different shaped grids kept the vortex in the simulation. It is possible that this vortex occurs in reality. It could be the cause of the decrease in land on the east side of the Hors.

Figure 32 shows the current direction after 6 hours into the storm. A lot of vortexes and fluctuations in directions can be discovered in this figure. It is believed that the strong southwards current is caused by wave breaking. Therefore, the absence of the eastward current is assumed realistic on the Hors.

## Appendix 1 – Validation report

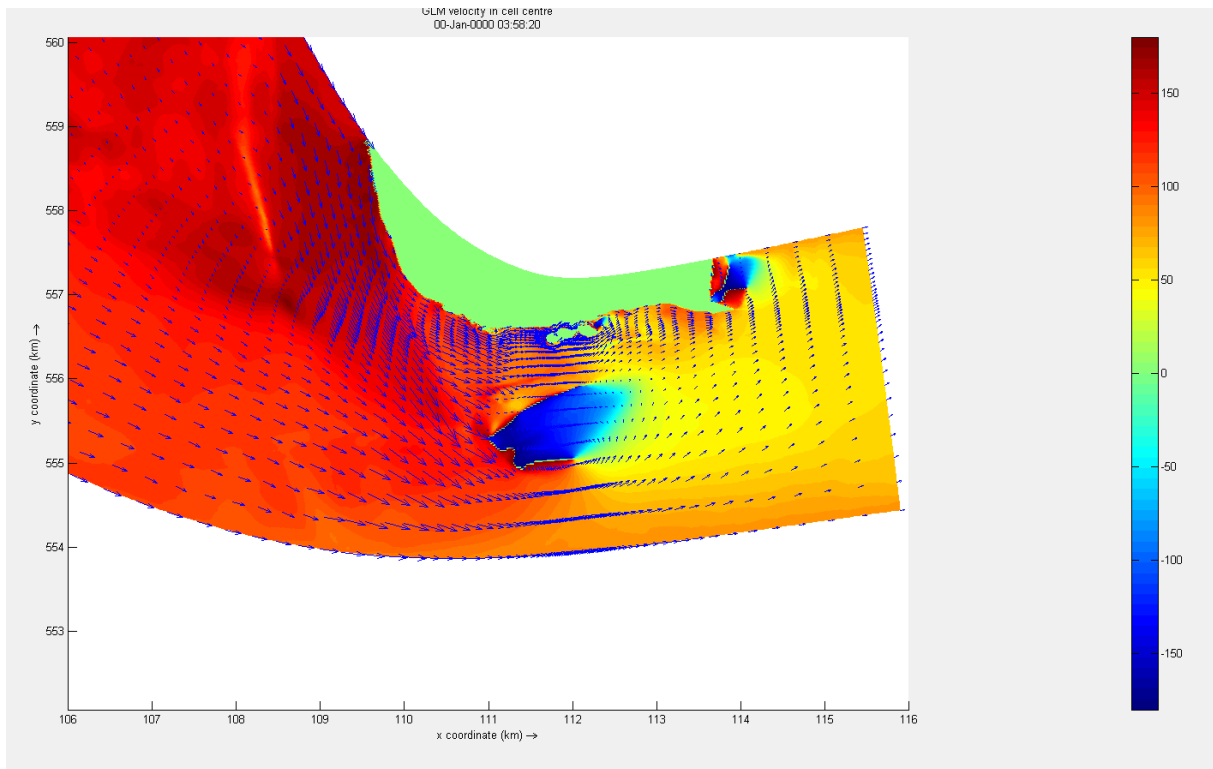


Figure 31 - current direction on the first moment the Hors is completely flooded (on this moment there still is a positive ratio between sea/land boundary)

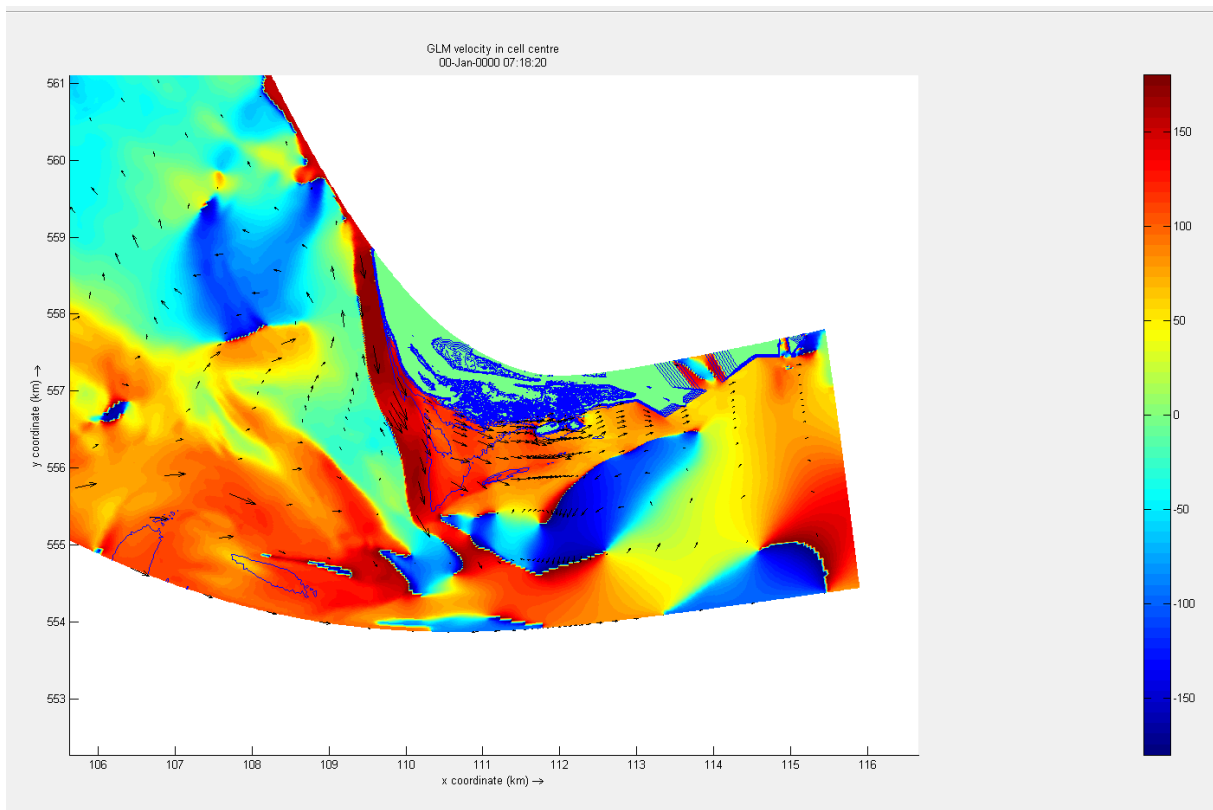


Figure 32 - current direction after 6 hours into the storm surge (with a negative reatio between sea/land boundary)

### 4.3 Dune erosion

#### 4.2.1 Erosion on the outline of the Hors

Figure 33 and 34 shows the overall erosion profiles on the Hors, for both 2017 (left) and 2012 (right) bathymetries. On the north-east side, both the bar in front of the coast and the coastline are eroded up to a meter. Most of this eroded material landed nearby. The south-west part of the outline show in both bathymetries heavy erosion. This eroded material is believed to flow further south and lands after the southern tip of the Hors, or it is taken on the Hors itself, where both bathymetries show a sedimentation of 0.1m. The linearly interpolated gap in bathymetry of the 2017 bathymetry is clearly visible. Apart from that, the erosion profiles are quiet similar.

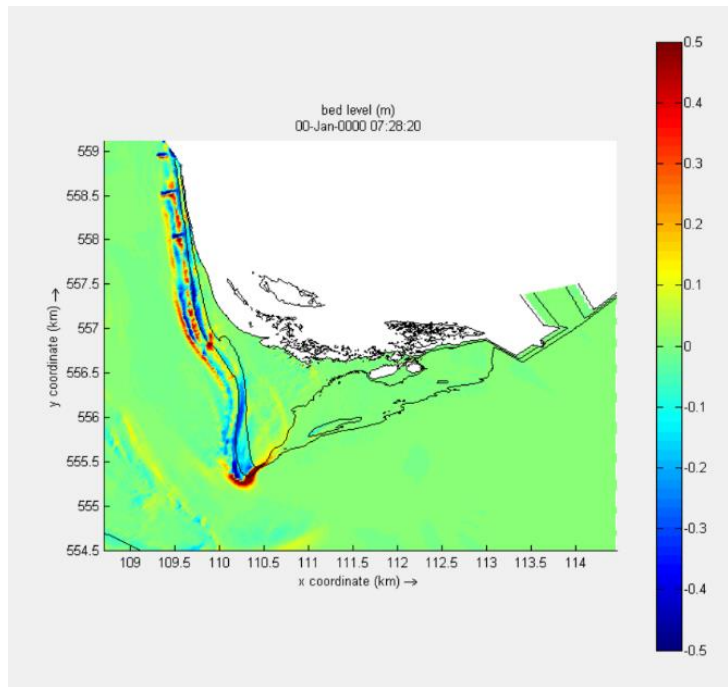


Figure 33 - Overall erosion profiles on the Hors for the 2012 bathymetry [m]

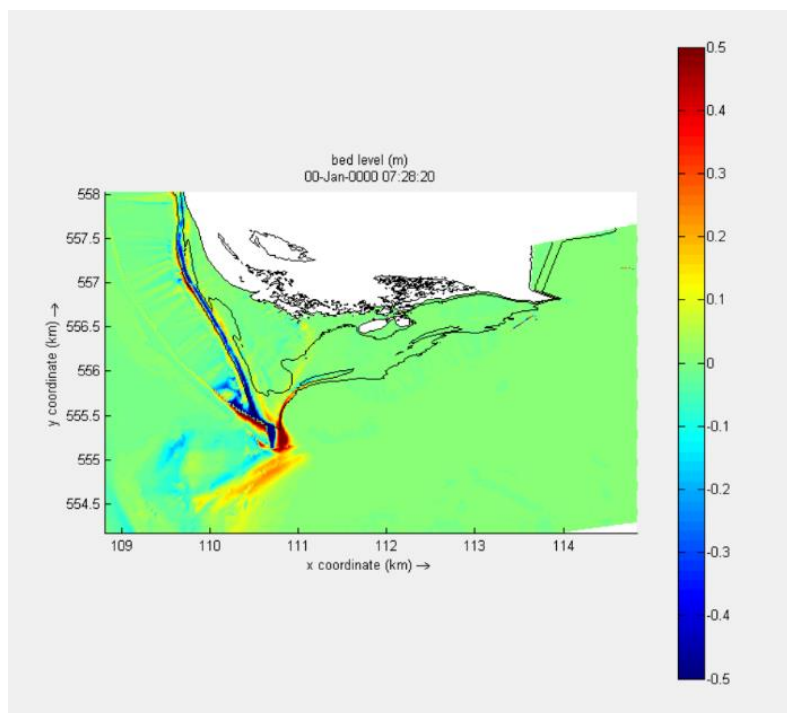


Figure 34 – Overall erosion profiles on the Hors for the 2017 bathymetry [m]

#### 4.2.2 The middle dunes

The erosion/sedimentation in the simulation (Figure 36) is found to be visibly comparable with the measurements (in both erosion/sedimentation levels as patterns (Figure 37)). For the left dune, which has a peak of 1.8m+NAP, the erosion is about 0.05m overestimated, whereas the erosion pattern on top of the dune, with a sedimentation around (0.05m) behind it is shown in both figures. For the right dune, the top is not eroded in the simulation, where erosion occurred in the measurements. Apart from this, both erosion on the north-west side of 0.2m and the sedimentation of 0.07m on the east side of the dune is observed in both the simulated results as in the reference data.

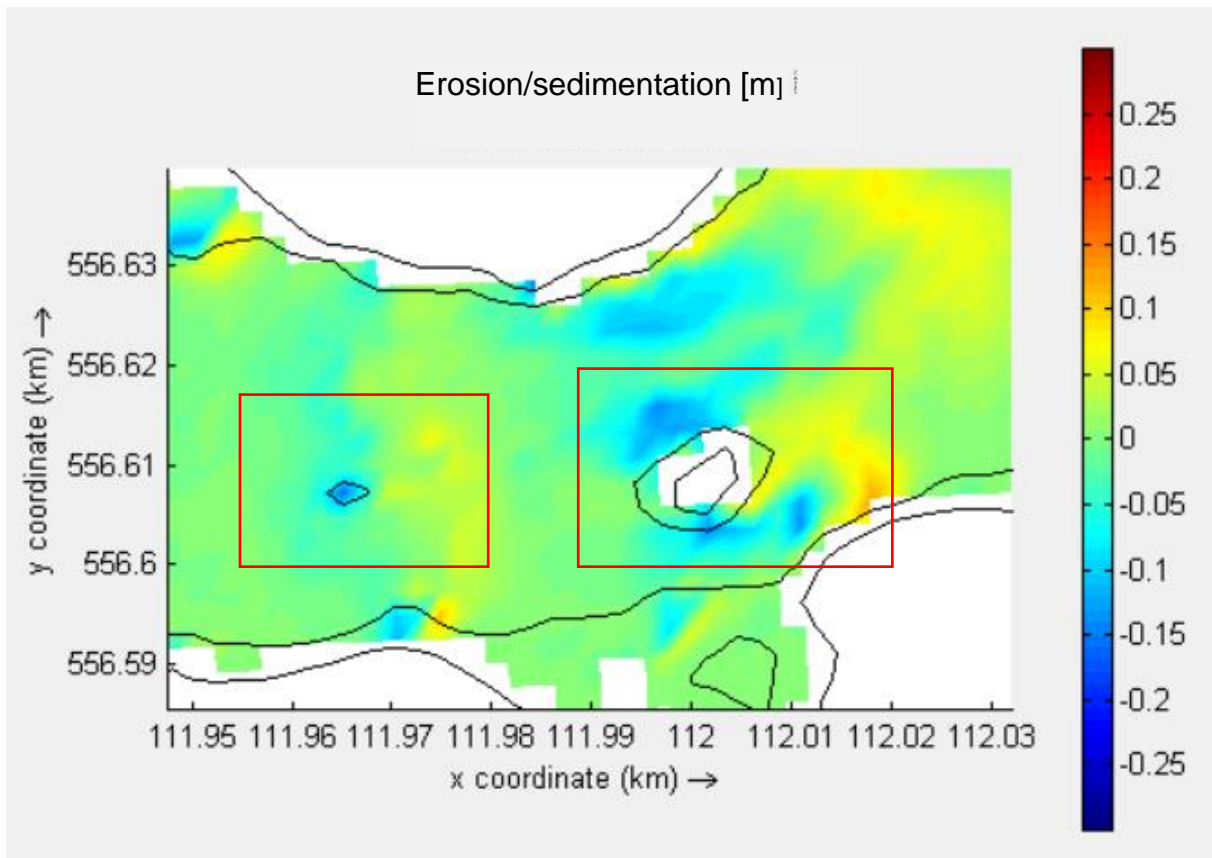


Figure 36 - Simulated erosion/sedimentation of the storm surge of 11-1-2017

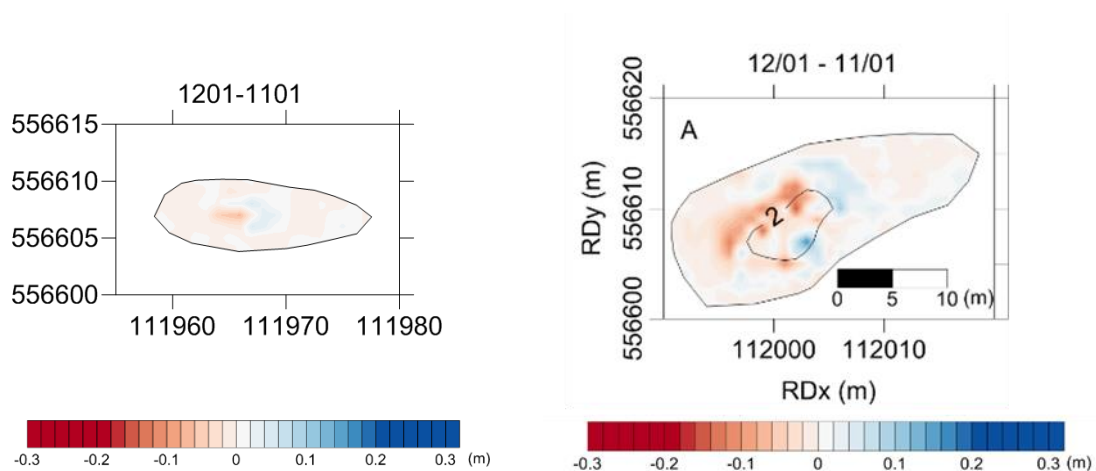


Figure 35 - Measured dune erosion/sedimentation of the middle dunes during the storm surge of 11-1-2017

## Appendix 1 – Validation report

### 4.2.3 Western dune field

Figure 40 and Figure 39 show both the simulated and measured dune erosion of the western dune field during the storm surge of 11-1-2017. The first thing to notice is the lack of erosion in the simulation, where the bed level is over 1.9m+NAP. The small dune in the south-west of the measured area (556.65, 111.75), shows a similar erosion pattern with the measurements. The measured value is lower, however, the erosion on the south-west side of this dune is similar in both results.

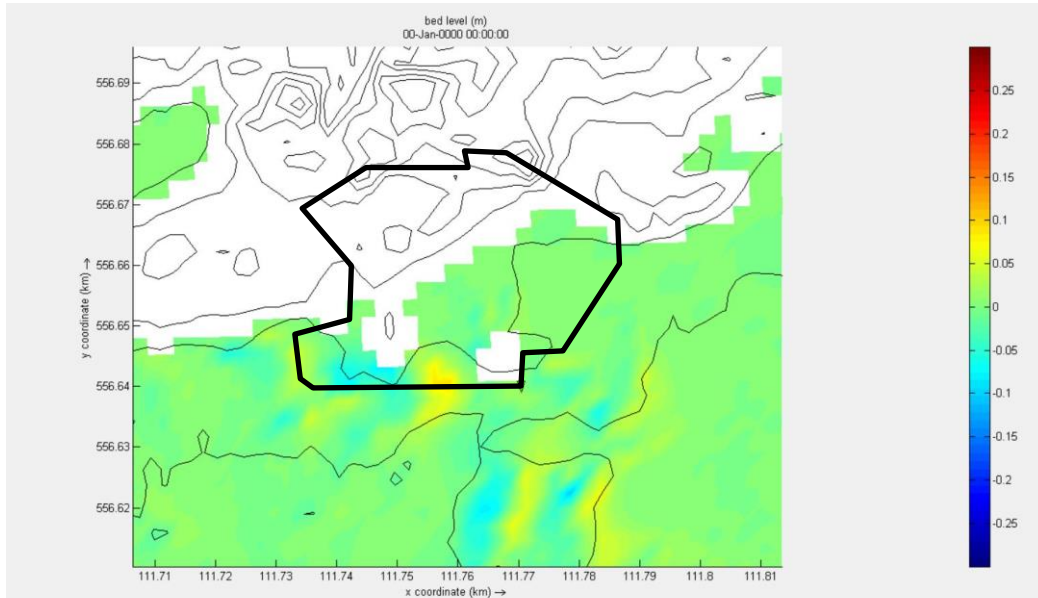


Figure 38 - Simulated erosion/sedimentation of 'the western dunes' after the storm surge of 11-1-2017 with the 2012 bathymetry

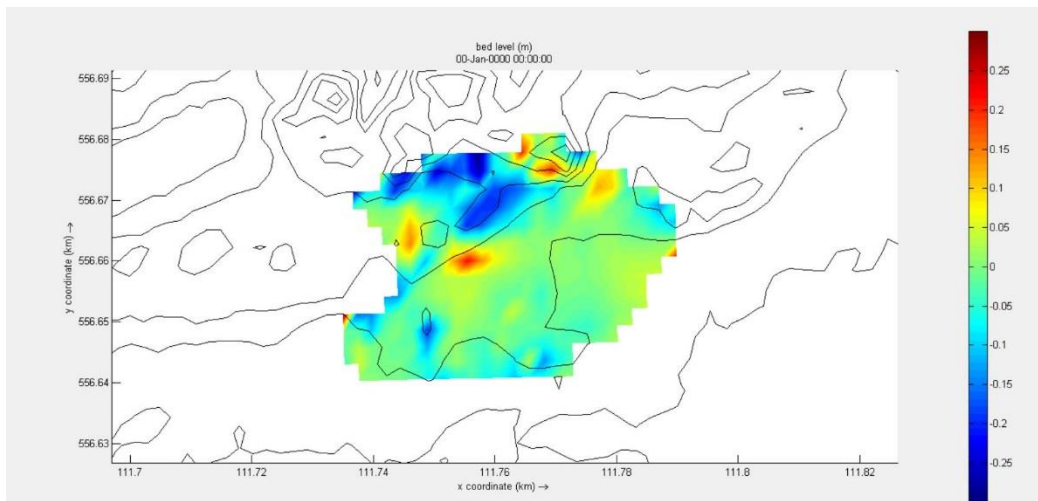


Figure 37 - Measured erosion/sedimentation between 11-1-2017 and 12-1-2017

## Chapter 5 – Discussion

Currents near the landside are low and show deviating directions TESO data. It is believed that due to lack of water from Marsdiep (which isn't modelled), the currents are too low and therefore the water gets turbulent near the boundary, on the location where the id-points are. Tests with a bigger grid show increase of the currents in Marsdiep. Further into the part of Marsdiep which is modelled, better similarities are found. Currents are still lower than the measured values, but again, this is caused by the exclusion of a large part of Marsdiep, which supplies most of the water.

After the peak waterlevel, the waterlevel at the land boundary is higher than the sea boundary and therefore the water should flow from land- to seaboundary. However, this does hardly occur. It is believed this is due to the small length of the land boundary. Not much water comes back into the model at the landside and therefore the effects of the turning are minimal.

Most of the effects of the deviation are believed to be caused in the channels. The currents on the Hors seem to be generated by a combination of the incoming currents and breaking waves. The wave breaking causes a waterlevel set-up on the west side of the Hors. This water flows away over the Hors to Marsdiep. The fact that the currents on Marsdiep are similar on the peak of the storm surge as on the final time step of the storm surge, confirms this theory.

The waterlevel and erosion in the area of the western dunes are underrated. This can be partly due to the input of the 'single\_dir' parameter in XBeach. When this parameter is used, the wave direction is calculated in turns instead of every timestep. This causes less waves in the area of the 'western dunes', because it is in a shadow zone behind the dune row in the middle of the Hors. However, the difference in waterlevel is way too high to be fully caused by this parameter. Simulations with an increase in waterlevels lead to an increase in currents on the Hors, larger currents lead to more erosion and this contradicts with the level of erosion/sedimentation on other dune measurements. For the future research, the erosion pattern might be underestimated, it is possible that erosion occurs higher than the simulation shows. However, the amount of erosion is believed to be comparable, and when looked at the bigger patterns on the main sandflat of the Hors, the patterns are representative.

For the middle dunes, there is consistency between the simulated results and measured data. The only part which can't be explained is the eroded top of the large east dune. It is possible that the waterlevels in the simulated model is underrated (0.2m). This could have the effect that too dunes which are not reached in the simulation, could erode in reality. However, the erosion values are similar, which makes the erosion pattern on the Hors representative.

The differences in dune measurement of the eastern dunes causes disturbances in this measured erosion patterns. From these disturbances it is difficult to compare both erosion/sediment patterns. One dune foot (encircled) seems to be well described in the measurements, and the results show a sedimentation of approximately 0.15m on the dune slope. However, this result is too little to draw conclusions regarding the agreement of measurements and simulation in both hydrodynamical as morphodynamical way. Therefore, this dune measurements won't be further analyzed.

## Chapter 6 – Conclusion

Visually, the simulated storm surge of 11-1-2017 is compared with the measured dune erosion and currents in Marsdiep (TESO data). The TESO data shows deviation however, it is believed that this deviation is due to the limited area which is covered in the grid in both Marsdiep (which would ensure most of the Flowrate and would therefore increase the velocities) and the landboundary relative short and close to the Hors (which makes it difficult for the water to flow back from the Waddensea towards the North sea). However, it is believed that the currents on the Hors are mainly caused by the wave breaking, from which it is believed that the deviating currents in Marsdiep won't affect the erosion pattern on the Hors. After successfully comparing the erosion pattern of measurements with simulated erosion patterns, this statement is confirmed.

It is believed that the wave height on the back of the Hors are underrated, which decreases the erosion values on the Middle-North side of the Hors. However, due to the validated currents and maximum wave height on the Hors, the erosion levels and patterns on the sandflat are considered representative. The erosion patterns on the north-eastern part of the dunes might deviate from reality. However, the level of erosion on this part of the Hors is considered in agreement with the measurement data and therefore the main erosion patterns and values which are visible on the Hors during different storm surges are in agreement with reality.

## Literature

- Bolle, A., Mercelis, P., Roelvink, D., Haerens, P., & Trouw, K. (2011). Application and Validation of XBeach for three different field sites. *Coastal Engineering Proceedings*, 1–13.
- Carrion Aretxabala, B. (2015). Morphological impact of the Sinterklaas storm at Het Zwin: Numerical modelling with XBeach, 75.
- Deltares. (2014). *RGFGRID - User Manual*.
- Deltares. (2015). *Release notes XBeach, version 1.22.4867, codename "Kingsday."*
- Holthuijsen, L. H., Booij, N., & Herbers, T. H. C. (1989). A prediction Model for Stationary, Short-crested Waves in Shallow Water with Ambient Currents. *Coastal Engineering*, 13, 23–54.
- Hoonhout, B. (2015). User manual - XBeach pre- 1.22.4344 documentation. Retrieved July 1, 2017, from <http://XBeach.readthedocs.io/en/latest/>
- Koninklijk Nederlands Meteorologisch Instituut. (2017). Uurgegevens van het weer in Nederland. Retrieved July 1, 2017, from <https://www.knmi.nl/nederland-nu/klimatologie/uurgegevens>
- Nederhoff, K., Elias, E., & Vermaas, T. (2016). Erosie op Ameland Noordwest. Modelstudie: simulaties met Delft3D en XBeach.
- Rijkswaterstaat. (2017). Waterbase Historische waterkwantiteit- en waterkwaliteitsgegevens. Retrieved July 1, 2017, from <http://live.waterbase.nl/waterbase>
- Roelvink, D., Reniers, A., van Dongeren, A., van Thiel de Vries, J., McCall, R., & Lescinski, J. (2009). Modelling storm impacts on beaches, dunes and barrier islands. *Coastal Engineering*, 56(11–12), 1133–1152. <https://doi.org/10.1016/j.coastaleng.2009.08.006>

## Appendix 1 – Xblog

\*\*\*\*\*

Welcome to XBeach

version 1.22.4937

date19-04-2016 22:02:01

URL:http://svn.oss.deltares.nl/repos/XBeach/trunk/

\*\*\*\*\*

Simulation started: YYYYMMDD hh:mm:ss time zone (UTC)  
20170804 17:32:09 +0200

General Input Module

MPI version, running on 7processes

Reading input parameters:

-----  
Physical processes:

XBeach reading fromparams.txt

cyclic =0 (no record found, default value used)  
swave =1 (no record found, default value used)  
single\_dir =1  
lwave =1 (no record found, default value used)  
flow =1 (no record found, default value used)  
sedtrans =1 (no record found, default value used)  
morphology =1 (no record found, default value used)  
avalanching =1 (no record found, default value used)  
nonh =0 (no record found, default value used)  
gwflow =0 (no record found, default value used)  
ships =0 (no record found, default value used)  
vegetation =0 (no record found, default value used)  
setbathy =0 (no record found, default value used)  
viscosity =1 (no record found, default value used)  
advection =1 (no record found, default value used)  
wind =1 (no record found, default value used)

-----  
Grid parameters:

gridform =delft3d  
depfile =finalgrid(2.5x3)2017.dep  
xyfile =finalgrid(2.5x3).grd  
xori =.0000 (no record found, default value  
used)  
yori =.0000 (no record found, default value  
used)  
alfa =.0000 (no record found, default value  
used)  
posdwn =-1.0000  
thetamin =180.0000  
thetamax =340.0000 Warning: value > recommended  
value of180.00  
00  
thetanaut =1  
dtheta will automatically be computed from thetamin and thetamax  
for single\_di  
r = 1  
dtheta\_s =10.0000

## Appendix 1 – Validation report

```
-----  
Model time parameters:  
      CFL =.7000 (no record found, default value  
used)  
      dtset =.0000 (no record found, default value  
used)  
      tstop =27000.0000  
      maxdtfac =50.0000 (no record found, default value  
used)  
-----  
Physical constants:  
      rho =1025.0000 (no record found, default  
value used)  
      g =9.8100 (no record found, default value  
used)  
      depthscale =1.0000 (no record found, default value  
used)  
-----  
Initial conditions:  
      zsinitfile = None specified  
-----  
Wave boundary condition parameters:  
      instat =jons_table  
      bcfile =jons11.txt  
      taper =100.0000 (no record found, default value  
used)  
      nmax =.8000 (no record found, default value  
used)  
      nonhspectrum =0 (no record found, default value used)  
      Hrms =1.0000 (no record found, default value  
used)  
      Tm01 =10.0000 (no record found, default value  
used)  
      Trep =10.0000 (no record found, default value  
used)  
      dir0 =270.0000 (no record found, default value  
used)  
      m =10 (no record found, default value used)  
      lateralwave =neumann (no record found, default value  
used)  
-----  
Wave-spectrum boundary condition parameters:  
      nonhspectrum =0 (no record found, default value used)  
      random =1 (no record found, default value used)  
      fcutoff =.0000 (no record found, default value  
used)  
      trepfac =.0100 (no record found, default value  
used)  
      sprdthr =.0800 (no record found, default value  
used)  
      Tm01switch =0 (no record found, default value used)  
      nspectrumloc =1 (no record found, default value used)  
-----  
Flow boundary condition parameters:  
      front =abs_2d (no record found, default value  
used)
```

## Appendix 1 – Validation report

```
left =wall
right =wall
back =abs_2d (no record found, default value
used)
    ARC =1 (no record found, default value used)
    order =1.0000
    carspan =0 (no record found, default value used)
    freewave =0 (no record found, default value used)
    epsi =-1.0000 (no record found, default value
used)
    tidetype =velocity (no record found, default value
used)
-----
Tide boundary conditions:
    tideloc =2
    paulrevere =land
    zs0file =zs2withsetup11.txt
-----
Discharge boundary conditions:
    disch_loc_file = None specified
    disch_timeseries_file = None specified
    ndischarge =0 (no record found, default value used)
    ntdischarge =0 (no record found, default value used)
    beta =.1000 (no record found, default value
used)
-----
Wave breaking parameters:
    break =roelvink2 (no record found, default
value used)
    gamma =.5500 (no record found, default value
used)
    alpha =1.0000 (no record found, default value
used)
    n =10.0000 (no record found, default value
used)
    gammax =2.0000 (no record found, default value
used)
    delta =.0000 (no record found, default value
used)
    fw =.0000 (no record found, default value
used)
    fwfile = None specified
    fwcutoff =1000.0000 (no record found, default
value used)
    breakerdelay =1 (no record found, default value used)
-----
Roller parameters:
    roller =1 (no record found, default value used)
    rfb =0 (no record found, default value used)
-----
Wave-current interaction parameters:
    wci =0 (no record found, default value used)
    hwci =.1000 (no record found, default value
used)
    hwcimax =100.0000 (no record found, default value
used)
```

## Appendix 1 – Validation report

```

                                cats =10.0000
-----
Flow parameters:
used)          bedfriction =chezy (no record found, default value
used)          bedfriccoef =55.0000 (no record found, default value
used)          nuh =.1000 (no record found, default value
used)          nuhfac =1.0000 (no record found, default value
used)          smag =1 (no record found, default value used)
-----
Coriolis force parameters:
used)          wearth =.0417 (no record found, default value
used)          lat =.0000 (no record found, default value
-----
Wind parameters:
used)          rhoa =1.2500 (no record found, default value
used)          Cd =.0020 (no record found, default value
used)          windfile =wind11.txt
-----
Sediment transport parameters:
default value use
d)            form =vanthiel_vanrijn (no record found,
used)            waveform =vanthiel (no record found, default value
used)            sws =1 (no record found, default value used)
used)            lws =0
used)            BRfac =1.0000 (no record found, default value
used)            facsl =1.6000 (no record found, default value
used)            z0 =.0060 (no record found, default value
used)            smax =-1.0000 (no record found, default value
used)            tsfac =.1000 (no record found, default value
used)            facua =.1000 (no record found, default value
used)            facSk =.1000 (no record found, default value
used)            facAs =.1000 (no record found, default value
used)            turbadv =none (no record found, default value
value used)            turb =bore_averaged (no record found, default
used)            Tbfac =1.0000 (no record found, default value

```

## Appendix 1 – Validation report

Tsmin =.5000 (no record found, default value used)

lwt =0 (no record found, default value used)

betad =1.0000 (no record found, default value used)

sus =1 (no record found, default value used)

bed =1 (no record found, default value used)

bulk =0 (no record found, default value used)

facDc =1.0000 (no record found, default value used)

fallvelred =0 (no record found, default value used)

dilatancy =0 (no record found, default value used)

reposeangle =30.0000 (no record found, default value used)

bdslopeffmag =roelvink\_total (no record found, default value used)

bdslopeffini =none (no record found, default value used)

bdslopeffdir =none (no record found, default value used)

-----

Bed composition parameters:

ngd =1 (no record found, default value used)

nd =3 (no record found, default value used)

por =.4000 (no record found, default value used)

D50 =.0002

D90 =.0003

rhos =2650.0000 (no record found, default value used)

dzg =.1000 (no record found, default value used)

dzg1 =.1000 (no record found, default value used)

dzg2 =.1000 (no record found, default value used)

dzg3 =.1000 (no record found, default value used)

sedcal =1.0000 (no record found, default value used)

ucrcal =1.0000 (no record found, default value used)

-----

Morphology parameters:

morfac =1.0000 (no record found, default value used)

morfacopt =1 (no record found, default value used)

morstart =7200.0000

morstop =27000.0000 (no record found, default value used)

wetslp =.3000 (no record found, default value used)

dryslp =1.0000 (no record found, default value used)

hswitch =.1000 (no record found, default value used)

dzmax =.0500 (no record found, default value used)

## Appendix 1 – Validation report

```
struct =0 (no record found, default value used)
-----
Output variables:
    timings =1 (no record found, default value used)
    tunits = None specified
    tstart =.0000
    tint =100.0000
    tsglobal = None specified
    tintg =100.0000
    tspoints = None specified
    tintp =100.0000 (no record found, default value
used)
    tsmean = None specified
    tintm =7200.0000
    nglobalvar =12
nglobalvar: Will generate global output for variable:zb
nglobalvar: Will generate global output for variable:zs
nglobalvar: Will generate global output for variable:H
nglobalvar: Will generate global output for variable:ue
nglobalvar: Will generate global output for variable:ve
nglobalvar: Will generate global output for variable:thetamean
nglobalvar: Will generate global output for variable:sedero
nglobalvar: Will generate global output for variable:E
nglobalvar: Will generate global output for variable:c
nglobalvar: Will generate global output for variable:ee
nglobalvar: Will generate global output for variable:u
nglobalvar: Will generate global output for variable:v
    npoints =25
    nrugauge =0 (no record found, default value used)
    npointvar =8
Output pointpoint001 xpoint:114405.00    ypoint:554323.00
Output pointpoint002 xpoint:114483.00    ypoint:554583.00
Output pointpoint003 xpoint:114456.00    ypoint:554768.00
Output pointpoint004 xpoint:114554.00    ypoint:555025.00
Output pointpoint005 xpoint:114516.00    ypoint:555213.00
Output pointpoint006 xpoint:114625.00    ypoint:555469.00
Output pointpoint007 xpoint:114580.00    ypoint:555657.00
Output pointpoint008 xpoint:114537.00    ypoint:555845.00
Output pointpoint009 xpoint:114644.00    ypoint:556101.00
Output pointpoint010 xpoint:114738.00    ypoint:556350.00
Output pointpoint011 xpoint:114687.00    ypoint:556544.00
Output pointpoint012 xpoint:114630.00    ypoint:556736.00
Output pointpoint013 xpoint:114588.00    ypoint:556921.00
Output pointpoint014 xpoint:114545.00    ypoint:557168.00
Output pointpoint015 xpoint:108959.00    ypoint:557257.00
Output pointpoint016 xpoint:109215.00    ypoint:556299.00
Output pointpoint017 xpoint:109827.00    ypoint:555328.00
Output pointpoint018 xpoint:111200.00    ypoint:554425.00
Output pointpoint019 xpoint:113068.00    ypoint:555278.00
Output pointpoint020 xpoint:109580.00    ypoint:557086.00
Output pointpoint021 xpoint:109620.00    ypoint:557074.00
Output pointpoint022 xpoint:109685.00    ypoint:557087.00
Output pointpoint023 xpoint:109755.00    ypoint:557100.00
Output pointpoint024 xpoint:110180.00    ypoint:555340.00
Output pointpoint025 xpoint:110336.00    ypoint:555326.00
npointvar: Will generate point output for variable:vmag
```

## Appendix 1 – Validation report

```
npoinvar: Will generate point output for variable:vmagu
npoinvar: Will generate point output for variable:vmagv
npoinvar: Will generate point output for variable:thetamean
npoinvar: Will generate point output for variable:sedero
npoinvar: Will generate point output for variable:H
npoinvar: Will generate point output for variable:zb
npoinvar: Will generate point output for variable:zs
Order of point output variables stored in 'pointvars.idx'
      nrugdepth =1 (no record found, default value used)
      rugdepth =.0000 (no record found, default value used)
      nmeanvar =0 (no record found, default value used)
      outputformat =netcdf (no record found, default value
used)
      outputprecision =double (no record found, default value
used)
      ncfilename = None specified
netcdf output to:xboutput.nc
-----
Output projection:
      projection = None specified
      rotate =1 (no record found, default value used)
-----
Wave numerics parameters:
      scheme =upwind_2 (no record found, default value
used)
      wavint =60.0000 (no record found, default value
used)
      maxerror =.0001 (no record found, default value
used)
      maxiter =500 (no record found, default value
used)
-----
Flow numerics parameters:
      eps =.0050 (no record found, default value
used)
      eps_sd =.5000 (no record found, default value
used)
      umin =.0000 (no record found, default value
used)
      hmin =.2000 (no record found, default value
used)
      secorder =0 (no record found, default value used)
-----
Sediment transport numerics parameters:
      thetanum =1.0000 (no record found, default value
used)
      sourcesink =0 (no record found, default value used)
      cmax =.1000 (no record found, default value
used)
-----
Bed update numerics parameters:
      frac_dz =.7000 (no record found, default value
used)
      nd_var =2 (no record found, default value used)
      split =1.0100 (no record found, default value
used)
```

## Appendix 1 – Validation report

merge =.0100 (no record found, default value used)

-----

MPI parameters:

mpiboundary =auto (no record found, default value used)

-----

Finished reading input parameters

-----

Changing mpiboundary to "x" for stationary wave model

-----

Building Grid and Bathymetry

-----

processor grid:                   1 X                   7

Initializing .....

  readtide: reading tide time series fromzs2withsetup11.txt ...

  readwind: reading wind time series fromwind11.txt ...

-----

Initializing spectral wave boundary conditions

-----

MPI implementation:

Distribution of matrix on processors

| proc | is | lm  | js  | ln |
|------|----|-----|-----|----|
| 0    | 1  | 961 | 1   | 55 |
| 1    | 1  | 961 | 52  | 55 |
| 2    | 1  | 961 | 103 | 55 |
| 3    | 1  | 961 | 154 | 55 |
| 4    | 1  | 961 | 205 | 55 |
| 5    | 1  | 961 | 256 | 55 |
| 6    | 1  | 961 | 307 | 55 |

| proc | left | right | top | bot |   |
|------|------|-------|-----|-----|---|
|      | 0    | T     | F   | T   | T |
|      | 1    | F     | F   | T   | T |
|      | 2    | F     | F   | T   | T |
|      | 3    | F     | F   | T   | T |
|      | 4    | F     | F   | T   | T |
|      | 5    | F     | F   | T   | T |
|      | 6    | F     | T   | T   | T |

-----

-----

computational domains on processors

| proc | icgs | icge | jcgs | jcge | icls | icle | jcls | jcle |
|------|------|------|------|------|------|------|------|------|
| 0    | 1    | 961  | 1    | 53   | 1    | 961  | 1    | 53   |
| 1    | 1    | 961  | 54   | 104  | 1    | 961  | 3    | 53   |
| 2    | 1    | 961  | 105  | 155  | 1    | 961  | 3    | 53   |
| 3    | 1    | 961  | 156  | 206  | 1    | 961  | 3    | 53   |
| 4    | 1    | 961  | 207  | 257  | 1    | 961  | 3    | 53   |
| 5    | 1    | 961  | 258  | 308  | 1    | 961  | 3    | 53   |
| 6    | 1    | 961  | 309  | 361  | 1    | 961  | 3    | 55   |

-----

NetCDF outputformat

Setting up boundary conditions

-----

Calculating spectral wave boundary conditions

-----

## Appendix 1 – Validation report

```
Reading spectrum at location1
  waveparams: Reading from tablejons11.txt ...
Interpreting spectrum at location1
Values calculated from interpolated spectrum:
Hm0      =3.00 m
Trep     =4.57 s
Mean dir  =291.18 degN
Overall Trep from all spectra calculated:4.57 s
  Writing stationary wave energy directional spread
toEs_series00001.bcf ...
Calculating Fourier components
5.1% done
10.1% done
15.1% done
20.1% done
```

## Appendix II - Basic calculations

This report consists of the basic calculations done for wave breaking, the generations of wind waves in a shallow region and the critical velocity for sediment transport. These calculations are shown separately in the next chapters.

### Wave breaking

Using the method of Battjes (Battjes, 1974), the breaker point of a wave can be found, depending on the steepness of the beach, wave height and wave period.

For the parameters, the heighest measurements of the station 'Eierlandse gat' during the storm surge of 11-1-2017 are used.

$H = 5.48\text{m}$  (significant wave height)

$T = 7.5\text{s}$  (significant wave period)

$\beta = 0.688^\circ$

Huge variation of slope angle near the Hors is seen. The chosen beta is a slope is calculated by looking at different lengths of the shoreline between -6meter and 0meter. 500 meter was the average of three measurements .  $6/500 = 0.012$  [-]  $\rightarrow$  angle of  $0.688^\circ$

$$L_{shallow} = T\sqrt{gh}$$

$L_{shallow} = 47\text{m}$  (assumed depth = 4 meters,  $T = 7.5\text{s}$ )

$$\xi = \frac{\tan \beta}{\sqrt{H/L_0}} = 0.035$$

$\xi < 0.5$  = Spilling break

$0.5 < \xi < 3.0$  = plunging waves

$3.0 < \xi$  = surging / collapsing

For spilling waves, a coefficient of  $y = 0.6$  suffices.

$$H(x) = y * h(x)$$

Assumed  $h(x) = 0.5\text{m}$  (on the Hors during the storm of 11-1-2017), a maximum **wave height of 0.3m** can be reached before breaking.

## Appendix II – Basic Calculations

### Wave growth

The method of Bretschneider is able to calculate the significant waveheight and period out of windspeed, waterdepth and fetchlength.

The calculations are done in dimensionless parameters for waveheight (H), wave period (T), waterdepth (d) and fetch length (F) with an given windspeed (u).

$$\tilde{H} = 0.284 \tanh(0.35\tilde{d}^{0.75}) \tanh\left[\frac{0.0125 * \tilde{F}^{0.42}}{\tanh(0.35 \tilde{d}^{0.75})}\right]$$

$$\tilde{T} = 2.4\pi \tanh(0.833\tilde{d}^{0.375}) \tanh\left[\frac{0.077 * \tilde{F}^{0.25}}{\tanh(0.833 \tilde{d}^{0.375})}\right]$$

with:

|  |   |
|--|---|
| $\tilde{H} = \frac{H_{1/3} g}{u^2} \text{ (dimensionless waveheight)}$ $\tilde{d} = \frac{d g}{u^2} \text{ (dimensionless waterdepth)}$ $\tilde{F} = \frac{F g}{u^2} \text{ (dimensionless fetch length)}$ $\tilde{T} = \frac{T_{1/3} g}{u} \text{ (dimensionless wave period)}$ | <p>g = gravitational acceleration [m/s<sup>2</sup>]<br/> u = wind velocity [m/s]<br/> d = water depth [m]<br/> F = fetch length [m]<br/> H<sub>1/3</sub> = significant wave height [m]<br/> T<sub>1/3</sub> = significant wave period [s]</p> |
|--|---|

The fetch length is assumed to be from the westside to the large dune in the east part. This distance is measured with google earth and determined on 1500m.

To know the expected wave influence, the storm characteristics of the storm surge of 11-1-2017 are used for the calculations. To see how different wind/ and fetch parameters result in different wave heights, three calculations are done.

#### Storm surge of 11-1-2017

|                  |      |                  |
|------------------|------|------------------|
| g                | 9.81 | m/s <sup>2</sup> |
| u                | 17   | m/s              |
| d                | 0.5  | m                |
| F                | 1500 | m                |
| H <sub>1/3</sub> | 0.14 | m                |
| T <sub>1/3</sub> | 1.91 | s                |

#### Changed wind velocity (+7 m/s)

|                  |         |                  |
|------------------|---------|------------------|
| g                | 9.81    | m/s <sup>2</sup> |
| u                | 24 (+7) | m/s              |
| d                | 0.5     | m                |
| F                | 1500    | m                |
| H <sub>1/3</sub> | 0.16    | m                |
| T <sub>1/3</sub> | 2.17    | s                |

#### Decreased Fetch length

|   |      |                  |
|---|------|------------------|
| g | 9.81 | m/s <sup>2</sup> |
| u | 17   | m/s              |

## Appendix II – Basic Calculations

|           |             |   |
|-----------|-------------|---|
| d         | 0.5         | m |
| F         | 100 (-1400) | m |
| $H_{1/3}$ | 0.12        | m |
| $T_{1/3}$ | 1.23        | s |

From these calculations, it can be concluded that the wind would not have a significant influence in the wave propagation on the Hors. However, it has to be noted that the used method is proposed for areas with uniform depths with no initial waves. Therefore this calculation can be seen as an indication of the wind affection on the waves on the Hors, but can't exclude other results in a different, more complex, calculation.

## Appendix III – Storm surge analysis

### Introduction

The goal of the research ‘The effects of storm surges on dune systems near inlets’ is gathering more knowledge about the effect of different storm surges affect the hydrodynamics and morphodynamics on the Hors. However, every storm is different and storm parameters including waveheight, waterlevel and waterlevel difference between inner- and outer part of the inlet (gradient) are different for every storm. This report analyses the characteristics of storm surges between 1981 – 2015 to get a better insight in the characteristics and variations of parameters in the storm surges near Den Helder. Results are used to design alternative storm surges of 11-1-2017 (the validation storm) and to get an idea of the reality of these storm surges.

From the website of Rijkswaterstaat ([http://live.waterbase.nl/waterbase\\_wns.cfm?taal=nl](http://live.waterbase.nl/waterbase_wns.cfm?taal=nl), <https://waterinfo.rws.nl/#!/nav/expert/>), several data can be found of several years including: significant wave height, significant wave period, wave direction and waterlevels of several measurementstations. From the wave data, hourly measurements are available. The waterlevels are measured every 10 minutes. From the website of the Royal Netherlands Meteorological Institute (KNMI) data of wind speeds and wind directions of various measurement stations are freely accessible (<https://www.knmi.nl/nederland-nu/klimatologie/uurgegevens>). Figure 1 shows the measurement stations that are used for this analysis.

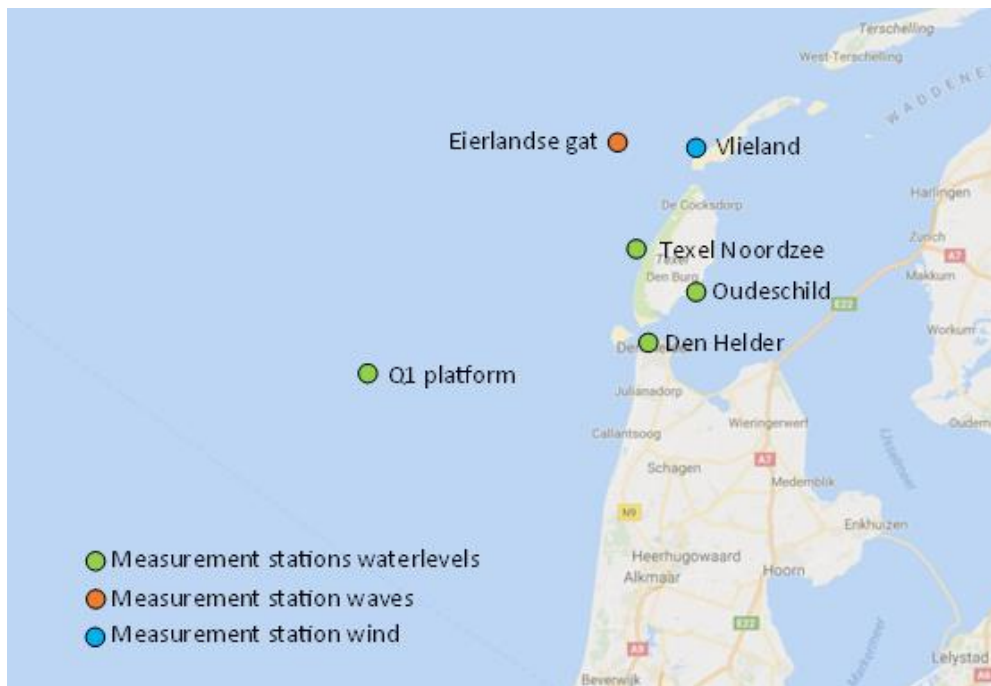


Figure 1 - Location of used measurement stations

The gradient can't be measured with this analysis, because only measurements on the peaks of the storms are available, where the gradient between sea- and landside is minimal.

## Waterlevels + Set up

From the helpdesk from Rijkswaterstaat, a dataset was acquired with peak (and neap) waterlevels at Den Helder, between 1933 and 2015. Other data parameters (wind, waves and waterlevels) were available from 1981 so a complete dataset could be formed between 1985 and 2015 (with a gap between 1990 – 1995). The dataset combines 25 years of storm surge data.

For this research, only storm surges are important that flood the Hors. Peak tides in Den Helder usually reach a waterlevel of 0.9m+NAP. The Hors has a bedlevel around 1.5m +NAP so all peak waterlevels beneath this point could be terminated. This decision decreased the dataset from the initial 37,984 rows, to 230. Table 1 shows an overview of the amount of data sorted per 10cm of peak waterlevel.

*Table 1 - storm characteristics on different waterlevels*

| <b>waterlevelrange<br/>[cm+NAP]</b> | <b>number of peaks<br/>(data points)</b> | <b>mean set-up<br/>[m]</b> | <b>mean wl<br/>[m+NAP]</b> | <b>tide (wl - setup)<br/>[m+NAP]</b> |
|-------------------------------------|--|----------------------------|----------------------------|--------------------------------------|
| <b>150-159</b>                      | 76                                       | 83                         | 154                        | 71                                   |
| <b>160-169</b>                      | 48                                       | 93                         | 163                        | 70                                   |
| <b>170-179</b>                      | 30                                       | 105                        | 174                        | 68                                   |
| <b>180-189</b>                      | 27                                       | 115                        | 184                        | 69                                   |
| <b>190-199</b>                      | 11                                       | 122                        | 192                        | 69                                   |
| <b>200-209</b>                      | 9  | 133                        | 204                        | 70                                   |
| <b>210-219</b>                      | 11                                       | 142                        | 214                        | 71                                   |
| <b>220-229</b>                      | 5  | 153                        | 222                        | 69                                   |
| <b>230-239</b>                      | 4  | 165                        | 235                        | 70                                   |
| <b>240-249</b>                      | 4  | 167                        | 243                        | 76                                   |
| <b>250-259</b>                      | 3  | 191                        | 252                        | 61                                   |
| <b>260-269</b>                      | 0  | 0                          | 0                          | 0                                    |
| <b>270-279</b>                      | 2  | 196                        | 270                        | 74                                   |

The heaviest storm surge in the measured period of time was at 9-11-2007 and reached a waterlevel of 2.71m+NAP. From a chart with the 50 highest waterlevels after 1932 (for Den Helder), this storm surge is the 7<sup>th</sup> highest waterlevel. The list is topped with 3.25m+NAP, which occurred in 1-2-1953.

From table 1, the tidelevel, with a range between 0.61 – 0.74 is quite constant. From this it is concluded that the strength storm surge, as expected, is variable.

## Appendix III – Storm surge analysis

### Wind

To see if there are differences between the different storm surges (based on the waterlevel), other storm parameters are analysed, started with the wind. Table 2 shows the different wind speed + directions with different storm surges.

Table 2 - Wind directions + speed on peaks of different storms (sorted on peak waterlevel Den Helder)

| waterlevel | Wind directions |      |      | Wind speed [m/s] |         |      |
|------------|-----------------|------|------|------------------|---------|------|
|            | min.            | max. | mean | minimal          | maximal | mean |
| 150-159    | 210             | 380  | 289  | 5                | 21      | 14.4 |
| 160-169    | 210             | 370  | 289  | 4                | 22      | 15.5 |
| 170-179    | 220             | 330  | 290  | 4.6              | 20      | 14.6 |
| 180-189    | 230             | 330  | 286  | 7.2              | 21      | 16.5 |
| 190-199    | 270             | 320  | 291  | 9.8              | 20      | 16.0 |
| 200-209    | 250             | 320  | 288  | 13.9             | 23      | 16.9 |
| 210-219    | 250             | 340  | 296  | 13               | 19      | 16.5 |
| 220-229    | 260             | 290  | 276  | 15.9             | 18.5    | 17.1 |
| 230-239    | 280             | 320  | 298  | 17               | 22      | 19.8 |
| 240-249    | 240             | 330  | 283  | 15               | 24      | 19.0 |
| 250-259    | 300             | 320  | 310  | 12.9             | 21      | 18.0 |
| 260-269    | 0               | 0    | 0    | 0                | 0       | 0.0  |
| 270-279    | 310             | 320  | 315  | 17               | 17.5    | 17.3 |

A storm surge from the sea, is originally coming from the sea. It is therefore not a surprise that all winds are coming from the east/north. The mean wind direction is really stable, although the direction angles more towards the north as the waterlevel increases. For the wind speed, the overall change is really small. Higher waterlevels are associated with higher waterlevels, however the range is still too big and the dataset is too small to be conclusive.

### Waves

The wave data had multiple holes in the dataset, so when the waterleveldata + wavedata merged together, the total amount of data points decreased. Therefore, the new amount of datapoints, in combination with minimal, maximal and mean wave characteristics for different waterlevels are shown in Table 3.

Table 3 - wave characteristics

| waterlevel | data points | wave direction [°] |         |      | wave height [cm] |         |      | wave period [s] |         |      |
|------------|-------------|--------------------|---------|------|------------------|---------|------|-----------------|---------|------|
|            |             | minimal            | maximal | mean | minimal          | maximal | mean | minimal         | maximal | mean |
| 150-159    | 42          | 237                | 354     | 297  | 109              | 608     | 383  | 3.5             | 8.1     | 6.5  |
| 160-169    | 32          | 238                | 347     | 296  | 249              | 548     | 411  | 5.4             | 8.2     | 6.7  |
| 170-179    | 16          | 266                | 344     | 299  | 171              | 700     | 412  | 4.2             | 9.2     | 6.6  |
| 180-189    | 11          | 228                | 340     | 289  | 259              | 599     | 411  | 5.6             | 8.0     | 6.6  |
| 190-199    | 4           | 268                | 312     | 293  | 388              | 492     | 433  | 6.6             | 6.9     | 6.7  |
| 200-209    | 4           | 233                | 314     | 289  | 493              | 650     | 537  | 6.9             | 8.3     | 7.5  |
| 210-219    | 6           | 297                | 338     | 311  | 458              | 583     | 514  | 7.0             | 8.6     | 7.7  |
| 220-229    | 1           | 308                | 308     | 308  | 449              | 449     | 449  | 7.0             | 7.0     | 7.0  |
| 230-239    | 2           | 300                | 329     | 315  | 371              | 591     | 481  | 7.1             | 8.2     | 7.6  |
| 240-249    | 3           | 270                | 294     | 285  | 537              | 595     | 557  | 7.2             | 7.6     | 7.4  |
| 250-259    | 2           | 284                | 303     | 294  | 377              | 387     | 382  | 6.8             | 7.0     | 6.9  |
| 260-269    | 0           | 0                  | 0       | 0    | 0                | 0       | 0    | 0.0             | 0.0     | 0.0  |
| 270-279    | 1           | 328                | 328     | 328  | 684              | 684     | 684  | 9.3             | 9.3     | 9.3  |

## Appendix III – Storm surge analysis

The wave direction is, like the wind direction, constantly around 300° no matter the waterlevel. The wave height and wave period show an increase with higher waterlevels. But again, the little amount of data and large range between lowest and highest measured value makes a conclusion difficult.

### Gradients

To get a better understanding of the 'realistic' waterlevel differences on the grid location, and therefore get a better indication of how realistic the proposition of a higher gradient is.

Because the waterlevel differences between the inner- and outer side of the inlet are at their highest at 1/4<sup>th</sup> and 3/4<sup>th</sup> of the storm surge, a different dataset is used for this analysis.

For the whole year of 2009, data of the the waterlevels of the four measurementsstations: Q1, TexelNoordZee, Den Helder and Oudeschild are collected to find gradients as they will occur in the model.

The highest measured waterlevel differences between sea- and landboundary in 2009 was 0.44cm.

Because there is an measurement on every 10 minutes, and a positive peak current occurs every 12 hours, it is assumed that the top 1/72 ratios of all data is the peak ratio. From this assumption, it is found that the peak ratio ranges between 0.3m and 0.44m. It has to be stated that this simple calculation gives merely an indication of the gradients in the grid. Due to the small amount of data (one year) it is possible that higher gradients (during storm surges) are possible.